RISK ASSESSMENT OF FIRE ACCIDENTS IN CHEMICAL AND HYDROCARBON PROCESSING INDUSTRY

by

© Ruochen Yang

A thesis submitted to the

School of Graduate Studies

in partial fulfillment of the requirement for the degree of

Master of Engineering

Faculty of Engineering and Applied Science

Memorial University of Newfoundland

October 2019

St. John's Newfoundland and Labrador

Abstract

Fire disasters are among the most dangerous accidents in the chemical and hydrocarbon processing industry. Fires have been the source of major accidents such as the Piper Alpha disaster (1976), the BP Texas City disaster (2005), the Buncefield oil depot fire (2005), Puerto Rico's fire accident (2009), and the Jaipur fire accident (2009). The catastrophic impact of fire accidents necessitates a detailed understanding of the mechanisms of their occurrence and evolution in a complex engineering system. Detailed understanding will help develop fire prevention and control strategies.

This thesis aims to provide a detailed understanding of fire risk in the hydrocarbon production and processing industry. In order to realize this objective, the work presented in the thesis includes three parts: i) Developing a procedure to study potential fire accident scenarios in an offshore facility with different ignition source locations. This procedure helps to design safety measures. The effectiveness of safety measures is verified using a computational fluid dynamics (CFD) code. This work emphasizes that an FLNG layout must be considered with the utmost care since it is the most effective measure in limiting a potential LNG release and subsequent dispersion effect, and directly influences the fire dynamics and thus limits the potential damage. ii) An integrated probabilistic model for fire accident analysis considering the time-dependent nature of the fire is developed. The developed model captures the dynamics of fire evolution using three distinct techniques Bayesian networks, Petri Nets, and a CFD model. The Bayesian

network captures the logical dependence of fire causation factors. The Petri Net captures the time-dependent evolution of a fire scenario. The CFD model captures the dimension and impact of the fire accident scenario. The results in this work show that a time-dependent probability analysis model is necessary for fire accidents. iii) Whether fire alone can cause a domino effect is demystified in the last work. A solid-flame model is used in a CFD framework to calculate the escalation vector for a domino effect; escalation probability is assessed using a probit model. The results demonstrate that a pool fire alone sometimes may not cause a domino effect in the current industry. It is other factors, such as explosion and hydrocarbon leakage, work together with a pool fire to escalate into a domino event, for example, the results shown in the case study of the Jaipur fire accident.

Keywords: Fire Accident; Fire Risk Assessment; Accident Modelling; Offshore Processing; Process Safety; Floating LNG; Computational Fluid Dynamics; Fire Probability Modelling; Domino Effect; Pool Fire; Probit Model

Acknowledgements

First of all, I would like to express deep appreciation to my supervisor, Dr. Faisal Khan. His motivational feedback, research ideas, and patience have been key to the successful completion of my master's study. His constant support, encouragement, and brilliant supervision have made my life abroad much easier. He brought me to the journey of research two and a half years ago and also has built my confidence to pursue further study in the future.

I want to acknowledge the help of Dr. Depeng Kong, Dr. Ming Yang, Dr. Mohammed Taleb Berrouane, and Mr. Eugenio Turco Neto for their contributions and valuable suggestions for my research.

I am grateful to all my colleagues and friends in C-RISE for their help and support in every aspect these years. It has been my fortune to study and work with these dynamic young researchers.

I would like to remember the sacrifice of my beloved parents. During my time studying abroad, it is they who have encouraged and energized me from thousands of miles away with their inspirational words. Finally, I especially thank Ms. Yaqi Yang for her love, understanding, support, and company. She has become my motivation and strength all these years and throughout this endeavor.

Table of Contents

List of Figures

List of Tables

List of Symbols, Nomenclature and Abbreviations

BN	Bayesian Network
CCF	Common Cause Failure
CDF	Cumulative Probability Distribution
CFD	Computational Fluid Dynamics
CPT	Conditional Probability Table
DBN	Dynamic Bayesian Network
ER	Equivalence Ratio
ETA	Event Tree Analysis
FCV	Flow Control Valve
FLNG	Floating Liquified Natural Gas Facility
LFL	Lower Flammable Limit
LSV	Liquid Level Safety Valve
OOBN	Object-oriented Bayesian Network
PN	Petri Nets
PCV	Pressure Control Valve
RANS	Reynolds-averaged Navier-Stokes
RTE	Radiative Transfer Equation
SPN	Stochastic Petri Nets
ttf	Time to Failure

UFL	Upper Flammable Limit
VCE	Vapour Cloud Explosion

Chapter 1. Introduction

1.1 Overview of fire accidents

Fire is among the most common and devastating accidents in the hydrocarbon production and processing industry. Disastrous fire accidents which have occurred indicate that attention must be paid to the safety area associated with fire accidents. In the Piper Alpha disaster, 167 people were killed [1]. The Piper Alpha is an oil production platform in the North Sea. In July 1988, an explosion occurred on the Piper Alpha platform and caused a serious fire accident which destroyed the whole platform. The total insured loss was about $3.4 billion. This accident is considered as the worst offshore oil disaster in terms of lives lost and industry impact [2]. The Texas City Refinery explosion occurred on March 23, 2005 [3]. A hydrocarbon vapour cloud was ignited, and then an explosion occurred at BP's Texas City refinery in Texas City. In addition, an area estimated at 200,000 square feet of the refinery was badly burned by the subsequent fire that followed the violent explosion. This accident caused 15 workers dead and 180 injuries. The equipment in the refinery was also severely damaged, which caused millions of dollars loss. The Buncefield oil depot fire occurred on December 2005. This disaster was a major fire accident caused by a series of explosions. Followed by the first explosion, a series of further explosions occurred and overwhelmed over twenty tanks in the depot. The fire lasted for two days and caused a huge loss of assets and harm to the environment [4]. In October 2009, a large explosion occurred at

the Caribbean Petroleum Corporation (CAPECO) oil refinery and oil depot in Bayamón, Puerto Rico [5]. Three people were injured in this accident, but fortunately, no fatality was reported. The accident started with an overflowed gasoline storage tank in the tank farm; then, a 107-acre vapour cloud formed quickly over the facility after the fuel aerosolized. The vapour cloud was ignited subsequently in the wastewater treatment area of the facility and led to a huge explosion. Multiple tank fires followed the explosion and burned for nearly 60 hours. Due to the subsequent explosions and fire, 17 of the 48 petroleum storage tanks were damaged significantly.

1.2 Goal of the Research

As discussed in the previous section, fire accidents happened many times in the world in the last few decades. These accidents caused huge damage to human life, assets, and environment. These accidents remind us to pay more attention to it. In order to better understand fire accidents, and then try to mitigate and even avoid it, it is necessary to conduct a risk assessment of it. The goal of this research is to analyze the fire accidents in the chemical and hydrocarbon processing industry and conduct risk assessment, which aims to provide a detailed understanding of fire risk in the hydrocarbon production and processing industry.

1.3 Overview of the fire accident simulation

To assess the risk of the fire accident, the first step is to simulate the fire accident

accurately. In order to simulate the fire accident, several models have been proposed, such as a point-source model, solid-flame model, numerical model, integral model, and zone model [6]. In this section, three famous models, including the point-source model, solid flame model, and numerical model, are discussed below

1.3.1 Point-source models

The point-source model considers that the heat load only originates from a point source, ignoring the shape of the flame [6]. This model is a simplified model; the physical characteristics of the fuel and the distance from the center of the flame to the target equipment are the main factors that affect the heat flux calculated by this model. However, this model usually overestimates the heat flux during application. It is suggested to apply this model in cases when the distance from the center of the flame is 10 radii [6].

1.3.2 Solid flame models

The solid flame model is a classical semi-empirical model that is widely used due to its simple application and accurate results. A solid flame model assumes that the heat flux only originates from the surface of the flame with a specific solid shape [6]. For example, in the case of a pool fire accident, the flame shape is assumed to be cylindrical; in the case of a jet fire, the flame shape is assumed to be a cone. Based on these assumptions, the emitting power is calculated accordingly. Thus, the heat flux caused by a fire accident can be worked out as a function of the surface-emitting power. Other contributing parameters such as the view factor and the atmospheric transmissivity, are also calculated, using

empirical or semi-empirical methods.

1.3.3 Numerical model

Computational Fluid Dynamics (CFD) models, also known as field models, are based on the numerical solution of Reynolds-Average Navier-Stokes equations. Compared with other models such as point-source models or the solid-flame model, a CFD model can provide a more accurate result, although a large computation time may be required [6, 7]. Currently, several CFD models can be used for fire simulation, such as FDS, FLACS, ANSYS FLUENT, AND ANSYS CFX. The principal differences among these models were analyzed and are shown in Table 1-1 [8].

Table 1-1 Comparative analysis of FDS, FLUENT, and CFX [8]

	FDS	ANSYS FLUENT	ANSYS CFX
Discretization method	Finite-volume method: cell-centered method	Finite-volume method: cell-centered method	Finite-volume method: vertex-centered method
Mesh	Rectilinear mesh, all objects need to be represented by cuboids	Various mesh could be selected according to the shape of objects to give higher accuracy than FDS in meshing	Various mesh could be selected according to the shape of objects to give higher accuracy than FDS in meshing
Model	Combustion model using a single step, mixing-controlled chemical reaction which uses three lumped species	Abundant physical models	Abundant physical models

Turbulence Model	For low-speed, thermally driven flow with an emphasis on smoke and heat. Turbulence is treated by Large Eddy Simulation (LES) or Direct Numerical Simulation (DNS)	A wide range of turbulence models can be selected according to different situations including k-ε model, k-w model, LES model	A wide range of turbulence models can be selected according to different situations
Application	Specialty tool developed to study the fire dynamics	Used widely	Used widely

Many previous studies have been conducted using CFD models to simulate and analyze fire accidents. Also, the results by CFD models have been well validated by many studies and experiments.

Hansen et al. [9] used FLACS to develop a CFD model to validate the studies of LNG-vapour dispersion, designing a pool-spread model considering humidity and other effects. In the study conducted by Dadashzadeh et al., an integrated approach for fire and explosion simulation was proposed; the evaporation and dispersion of flammable gas and delayed ignition were simulated using FLACS, while the Fire Dynamics Simulator (FDS) code was used to model the ignition of the rest of the fuel over the liquid pool [10]. Pitblado et al. used PHAST to predict the hazard zone caused by an accident or deliberate attack, and they also developed a range of credible scenarios in this study [11]. Baalisampang et al. conducted a study on fire occurring on a typical FLNG processing facility and its impact on personnel and assets using the FDS code; a water deluge system was used to

mitigate the impact of fire [12]. Also, they identified three credible scenarios and determined the impact of fire on personnel and assets by combining the FDS code and probit method [13]. An inherently safe layout design which highlights the importance of improved layout design and passive control strategies are also proposed by Baalisampang et al. [14]. Van Hees listed many previous validation studies and conducted several simulations to validate the FDS model. The results of these studies show good correspondence between FDS simulation and experiment results [15]. Berg et al. used a CFD model to identify an optimal safety design for an FPSO to quantify the overpressure caused by an explosion and also assessed the risk reduction measures using a quantitative method. The effects of barrier walls, separation gaps, and other influencing factors were discussed in this study [16]. Binbin conducted a comparative analysis of fire simulation using FLUENT and FDS, and found that although Fluent and CFX have more extensive simulation areas and other advantages in terms of meshing, the FDS results have good high consistency with measured results in some situations [17].

In this research, various CFD models are applied in different situations considering data availability, meshing ability, and result post-processing ability. FDS, FLACS, and ANSYS FLUENT are selected as the CFD model in Chapters 2, 3, and 4, respectively.

1.4 Fire accidents in an offshore facility

An FLNG is an offshore facility designed to employ various LNG development

technologies, including gas extraction, gas pre-treatment, natural gas liquefaction, condensate treatment, water treatment, LNG storage, and LNG offloading [18]. Since all these technologies are combined in only one offshore facility, the FLNG has a very congested and complicated layout. This characteristic of the FLNG makes fire accidents occurring in an FLNG can be extremely dangerous; they can cause significant damage to personnel, the structure, and assets [12-14, 19]. Fire accidents that have occurred in offshore facilities with similarly complex and congested areas such as the Piper Alpha disaster[1] and the BP Deepwater Horizon explosion[20] remind us to focus on the area of fire accidents occurring in an offshore facility such as an FLNG.

In this research, a typical FLNG is used for case studies to explore fire risk in Chapters 2 and 3.

1.5 Domino effect caused by fire accidents

The domino effect is responsible for a number of severe accidents in the chemical and process industry [21-23].

Compared with stand-alone accidents, domino effects are more likely to cause huge damage to personnel assets, humans, and the environment. As shown in previous research, the frequency of the domino effect has increased in the chemical and process industries in the last few decades [24, 25]. These accidents caused by a domino effect, such as the BP Deepwater Horizon explosion[20], the Buncefield oil depot fire[4], the CAPECO explosion and fire accident [5], and Jaipur's fire

accident [26] have indicated the domino effect's huge damage to society and focused people's attention on accidents caused by the domino effect. Among all kinds of accident scenarios, the pool fire is often blamed as one of the primary accidents that trigger a domino event[27-32].

There are several previous studies that focused on the domino effect caused by pool fires. Khan and Abbasi conducted a series of studies on the domino effect, in which the pool fire is one of the principal accident scenarios that can escalate into a domino effect [24, 25, 33-35]. In one of these studies, Khan and Abbasi considered two failure modes failure of the equipment due to high-pressure build-up and equipment rupture due to material failure, to be the main failure modes of a vessel exposed to fire. They also derived a series of analytical formulas to calculate the escalation probability of a domino effect in cases of fire accidents [25]. The computational fluid dynamics (CFD) model was used by Jujuly et al. to simulate an LNG pool fire, and the effect on the adjacent equipment was analyzed. In this study, the authors found wind speed can affect the pool fire significantly and may cause a domino effect [28]. Landucci et al. studied the damage probability of equipment in domino events triggered by the fire. They proposed a simplified model to estimate the vessel time to failure (ttf) in the case of thermal radiation [30]. Furthermore, a series of probit models have been proposed by Cozzani et al. to analyze the escalation probability of a domino effect caused by various accident scenarios, which provides a simplified method for probabilistic assessment [21, 31]. In several studies by Khakzad et al., the dynamic Bayesian network (DBN)

and the probit method proposed by Cozzani et al. were used to analyze the propagation sequence of a domino effect, which considered the time-dependent feature of the domino effect [27, 29, 36].

1.6 Research Gap and Objectives of the Research

A review of the literature on previous work shows that although many works have been conducted in the area of fire accidents, there are still some research gaps that need to be explored. For example, research on the effectiveness of the safety measures for fire accident is rare. Given different fire accident scenarios, different safety measures may have different performance. In the hydrocarbon production and processing industry, various fire scenarios need to be identified, and safety measures selection also needs to be assessed. The second challenge lies in assessing the fire probability considering its time-dependent feature. Considering the fire accident is a process, this feature needs to be identified in the risk assessment of fire accidents. The third question with respect to whether or not the pool fire alone will cause a domino effect. In the previous studies, the pool fire is usually blamed to be one of the main causes of the domino effect. In order to solve the problems mentioned above, the thesis includes three specific areas that are reflected in three major works.

The first objective is to assess the safety measures for fire accidents in the hydrocarbon production and processing industry, especially in an offshore facility. The effectiveness to prevent fires and mitigate their impact of safety measures in different fire accident scenarios will be analyzed.

The second research objective aims to propose an integrated probabilistic model for fire accident analysis considering the time-dependent nature of the fire. Many previous works assessed fire accident likelihood; however, most of these studies considered fire probability as spatially distributed, ignoring the time dependence of the fire accident scenario. This study proposes a robust and practical model to analyze fire accident probability in a congested and complex processing area, considering its time-dependent feature.

The third objective is to demystify whether fire alone can cause a domino effect. As mentioned before, a pool fire is usually blamed as one of the reasons that cause a domino effect. Also, this study applies simulation to explore which factors contribute to the domino effect caused by pool fires.

1.7 Contribution and Novelty of the Research

In this thesis, three works have been conducted to realize the three objectives described above.

The first work proposes a procedure to study potential fire accident scenarios in an offshore facility. In this work, accident scenarios with different ignition source locations are analyzed. The effect of different ignition source locations is also studied using potential scenarios in this research. In addition, safety measures include firewalls and fire suppression systems are analyzed. The ranges of safety measures of these fires are also studied to determine their effectiveness to prevent fires and mitigate their impact. The uniqueness of this study is the integration of

release, dispersion, and fire modeling scenarios, simplifying the fire analysis and increasing its effectiveness from the offshore process system design and analysis perspectives.

The second work is to propose an integrated probabilistic model for fire accident analysis considering the time-dependent nature of the fire. Many previous works assessed fire accident likelihood; however, most of these studies considered fire probability as spatially distributed, ignoring the time dependence of the fire accident scenario. This study proposes a robust and practical model to analyze fire accident probability in a congested and complex processing area, considering its time-dependent feature. The novelty of this work is that the model integrates a conditional probability approach – the Bayesian network (BN) - with a time-dependent scenario evolution approach, Stochastic Petri Nets (SPN), and the computational fluid dynamics (CFD) serves as an accurate technique to incorporate all on-site variables.

The third work is to demystify whether fire alone can cause a domino effect. As mentioned before, a pool fire is usually blamed as one of the reasons that cause a domino effect. This study applies simulation to explore which factors contribute to the domino effect caused by pool fires. In addition, case studies based on real accidents are conducted to assess the escalation probability of the domino effect caused by pool fires in current industries.

1.8 Thesis Structure

This thesis is written in manuscript format. It includes two manuscripts submitted to peer-reviewed journals, and one manuscript is ready to be submitted and published. The manuscript in chapter 2 is submitted to the Ocean Engineering journal; the manuscript in chapter 3 is submitted to the Fire Safety Journal; the manuscript in chapter 4 is going to be submitted to a peer-reviewed journal and published. The outline of each chapter is explained below:

Chapter 1 is a brief introduction to the possible scenarios caused by fire risks and several models that can be used to simulate the fire risk. The research objectives of the research are mentioned in this section.

Chapter 2 is based on the first objective. A numerical model, FDS, which is a commercial software designed specifically for fire modeling, is applied to simulate the fire accident. This study presents a rigorous procedure to study potential accident scenarios in an offshore facility. Fourteen scenarios with different ignition source locations are explored. In addition, the ranges of safety measures are also studied to determine their effectiveness to prevent fires and mitigate their impact. This work provides a simple and efficient way to analyze the impact of key design parameters.

Chapter 3 is based on the second objective. For this study, an integrated model is proposed to assess the probability of fire accidents considering their time-dependent features. The proposed model integrates a conditional probability approach – the Bayesian network (BN) - with a time-dependent scenario evolution

approach, Stochastic Petri Nets (SPN). In addition, the CFD tool is used to estimate the time-dependent scenario consequences. The outcome of the model is fire probability as a function of time and location caused by a specific leak rate and leak duration.

Chapter 4 is based on the third objective. In this investigation, the possibility that pool fires alone cause a domino effect is explored. Two models, a solid-flame model and a numerical model, are applied to simulate the heat load caused by pool fires. A probit model is used to assess the escalation probability of the domino effect caused by pool fires. Several potentially influencing factors that have effects on pool fire results are explored in a sensitivity study. In addition, two case studies based on real accidents are conducted to analyze the pool fire's impact on the current industry.

Chapter 5 summarizes the results of the research. Based on the conclusion of the work in chapters 2, 3, and 4, it provides several potential research scopes in this area for future work.

Chapter 2. A Numerical Fire Simulation Approach for Effectiveness Analysis of Fire Safety Measures in Floating Liquefied Natural Gas Facilities[1]

Co-authorship statement

A version of this manuscript has been accepted for publication in the Journal of Ocean Engineering in 2018. Author Ruochen Yang has conducted this study under the direct supervision of Faisal Khan. Ruochen Yang has developed the model and conducted test runs under the guidance of author Faisal Khan. Authors Faisal Khan and Ming Yang helped test the model results and verified the developed model. Authors Depeng Kong and Changhang Xu helped conduct the application. All co-authors reviewed and provided feedback on the manuscript. Ruochen Yang revised the manuscript based on the co-authors' feedback and during the peer review process.

Abstract

The fire remains a serious threat to a floating liquefied natural gas facility. It is of greater concern, given the remote locations and limited accessibility of emergency

[1] Yang, R., Khan, F., Yang, M., Kong, D., & Xu, C. (2018). A numerical fire simulation approach for effectiveness analysis of fire safety measures in floating liquefied natural gas facilities. Ocean Engineering, 157, 219-233.

services. This study aims to present a rigorous procedure to study potential accident scenarios in an offshore (floating processing) facility with different ignition source locations and verify the effectiveness of safety measures using computational fluid dynamics code. The uniqueness of the present study is the integration of release, dispersion, and fire modeling scenarios, simplifying the fire analysis and increasing its effectiveness from the offshore process system design and analysis perspectives. The first step of the procedure is to identify the range of potential release scenarios and their strength of dispersion in confined and semi-confined spaces. Subsequently, potential fire scenarios are analyzed considering the influence of the location. Computational fluid dynamics models are used to analyze these three steps of the scenarios. The application of the procedure is demonstrated on an offshore facility by analyzing 14 credible scenarios. The ranges of safety measures of these fires are also studied to determine their effectiveness to prevent fires and mitigate their impact. This study provides a simple and efficient way to analyze the impact of key design parameters. In this study, the transition from fire to explosion is not considered and all the environmental factors are assumed to be constants in the simulation.

2.1 Introduction

Global energy demand is continuously rising. Natural gas is one of the cleanest sources of energy, and its demand is sharply rising. Because of the growing demand, many oil companies are currently increasing their investment in floating liquefied natural gas (FLNG) facilities such as Floating Storage and Regasification Units (LNG FSRU) and Floating Production Storage and Offloading (LNG FPSO). With the development of shipbuilding and offshore industries, the concept of the FLNG was recently proposed[37]. An FLNG facility uses various types of technologies developed for conventional land-based LNG, offshore oil and gas, and marine transport industries[38]. An FLNG facility can implement gas extraction, gas pre-treatment, natural gas liquefaction, condensate treatment, water treatment, LNG storage, LNG offloading and combined technologies in one offshore facility, which creates a congested and complicated layout[18].

Fire and explosion accidents such as the Piper Alpha disaster[1], the BP Texas City disaster[3], the BP Deepwater Horizon explosion[20], the Cleveland explosion[39] and Buncefield oil depot fire[4] have demonstrated the importance of safety in oil and gas operations. In a typical onshore oil refinery or chemical plant, hazardous facilities are usually separated from other parts of the plant. However, on an FLNG, facilities have to be arranged in a congested layout. While this layout brings economic and environmental benefits[40], it has a higher fire risk compared to a conventional natural gas processing unit[41]. In addition, offshore and remote operations usually have limited infrastructure and resources

support. All these make it more challenging to assure fire safety in offshore facilities.

Fire accidents caused by flammable hydrocarbons' leakage have been well studied by many researchers[9, 10, 42-51]. The overpressure resulting from a flammable gas explosion is not significant in open areas, while places with confined layouts are dangerous[10]. Luketa-Hanlin[46] studied the behaviour of LNG spills and pool formations on water and discussed the modeling of LNG spills, taking combustion events such as pool fires and vapour cloud fires into consideration. Fay constructed a model to predict the dynamics of spills from LNG and oil tankers. The pool fire area, duration, and heat release rate were determined using this model[47]. Jet fires, explosions, and flash fires occurring on the topside of LNG-FPSOs were analyzed considering different leakage hole sizes. It can be concluded that even though the LNG is safe enough under ALARP criteria, there is a need to select independent protection layers to meet a higher standard[48]. Sun validated the CFD model of fire radiation by comparing the simulation results and experimental data, followed by a hazard analysis of an LNG Satellite station. The distance between dike walls and AVV banks was suggested to be enlarged by the author[49]. Hissong described the key factors used to model an LNG spill on the water; the results from pool fires on land were compared with the results of pool fires on water[50].

Using computational fluid dynamics (CFD) tools to model the consequences of fire accidents and conduct an analysis has been well validated by many studies and

experiments. Dadashzadeh et al. proposed an integrated approach for fire and explosion simulation; FLACS was used to simulate the evaporation and dispersion of flammable gas and delayed ignition, while the Fire Dynamics Simulator (FDS) code was used to model the ignition of the rest of the fuel over the liquid pool[10]. Baalisampang et al. used the FDS code to study fire occurring on a typical FLNG processing facility and its impact on personnel and assets. In his study, a water deluge system was applied to mitigate the impact of fire[12]. In another study conducted by Baalisampang et al., three credible scenarios were identified, and the impact of fire on personnel and assets was determined by combining the FDS code and probit method[13]. Baalisampang et al. also proposed a method to determine an inherently safe layout design and highlight the importance of improved layout design and passive control strategies[14]. In the study conducted by Hansen et al. [9], FLACS was used to develop a CFD model to validate the studies of LNG-vapour dispersion; humidity and other effects were considered in this study to design a pool- spread model. PHAST was used by Pitblado et al. to predict the hazard zone caused by an accident or deliberate attack; a range of credible scenarios was developed in this study[11]. Berg et al. identified an optimal safety design for an FPSO by using a CFD model to quantify the overpressure an explosion can cause and also assessed the risk reduction measures using a quantitative method. The effects of barrier walls, separation gaps, and other influencing factors were discussed in this study[16]. Van Hees listed many previous validation studies and also conducted several simulations to validate the

FDS model. The results of these studies show good correspondence between FDS simulation and experiment results[15]. Binbin conducted a comparative analysis by fire simulation using FLUENT and FDS, and found that although Fluent and CFX have more extensive simulation areas and other advantages in terms of meshing, the result of FDS has high consistency with measured results in some situations[17]. Table 1-1 shows the main differences of FDS, FLUENT and CFX. In this study the fire analysis is mainly based on the FDS code- a specialty CFD tool developed to study fire dynamics.

Many previous studies have explored natural gas fire accidents[9, 11, 12, 46, 47, 50, 52] with a focus on leakage parameters such as the leakage point, leakage probability, release rate and environmental parameters such as wind speed and direction. However, these studies ignore the impact of the location of the ignition source. In this study, the influence of the effect of the ignition source location is mainly considered.

The objective of this study is to present a rigorous procedure to study potential accident scenarios in an offshore floating processing facility with different ignition source locations and verify the effectiveness of safety measures based on the consequences of potential FLNG fire accident scenarios. The scenarios with different ignition source locations are modeled using the FDS code under the assumption that all the environmental factors are constants in the simulation. Another unique aspect of the present study is consideration of a fire's impact using areas of influence and temperature distribution. Safety measures (firewalls and fire

suppression systems) are analyzed for their effectiveness in mitigating the effect of fire. A limitation of this study is that it does not consider the transition from fire to an explosion during the simulation.

2.2 Proposed Methodology

This study focuses on the simulation of fires caused by ignition sources located in different places on an FLNG and the verification of the effectiveness of safety measures. It incorporates the release and dispersion modeling of an LNG for the development of various credible scenarios and employs CFD simulations for each scenario to analyze the fire's impact on the FLNG to determine the most dangerous scenario. This is followed by the implementation of safety measures such as a firewall and automatic fire suppression system to mitigate the fire's impact on human beings, adjacent assets, and structures. Figure 2-1 demonstrates the procedure of this study.

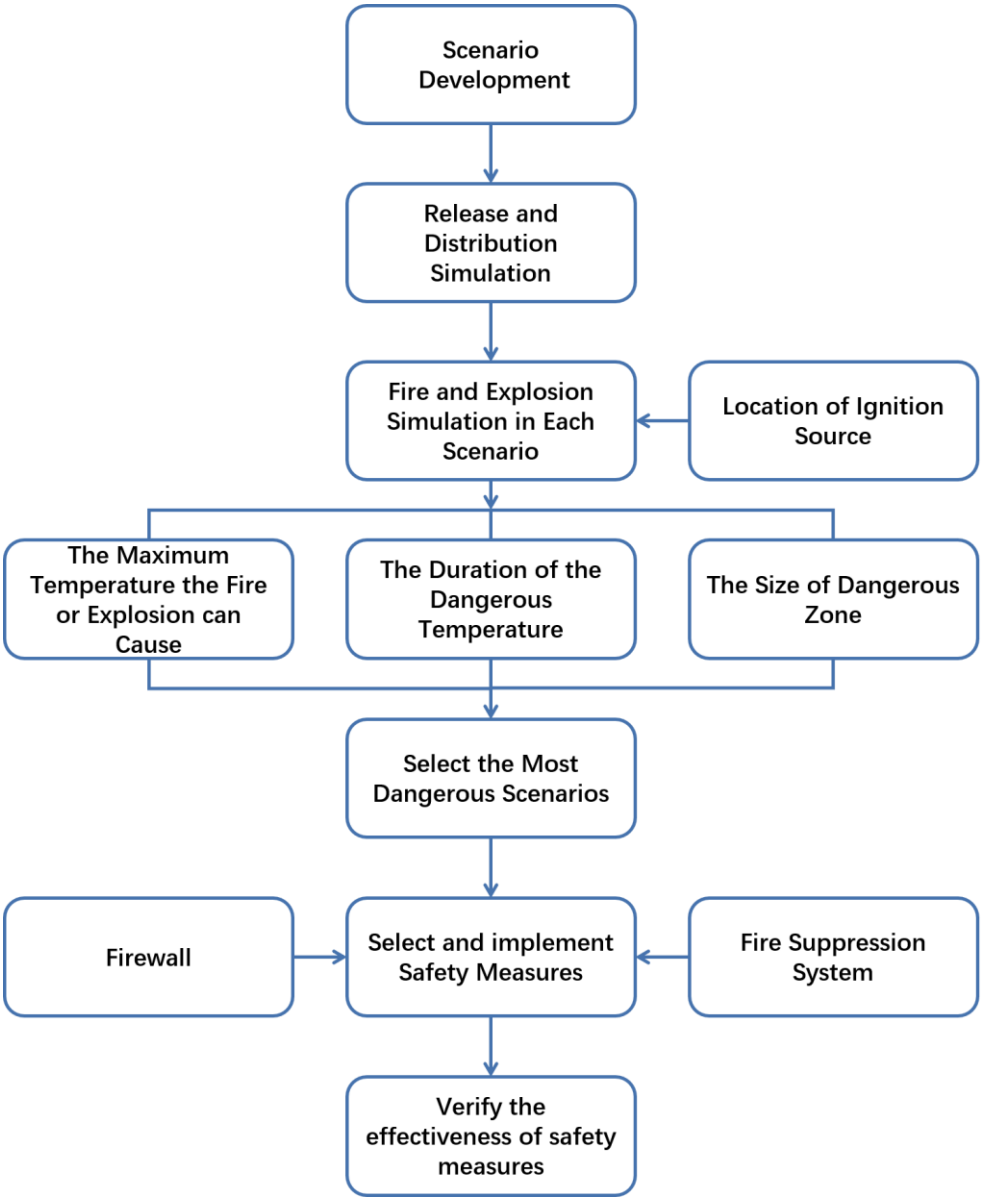

Figure 2-1 The Flow Chart of the present Study

2.2.1 Step 1: Scenario Development

When developing a credible scenario, many parameters which could contribute to a fire must be considered, such as miscellaneous parameters (pressure, temperature and humidity), fuel parameters (chemical and physical properties), leak parameters (rate, location, duration and direction), wind parameters (speed and direction) and so on. In order to study the impact of locations of ignition sources

on safety measure design, all the parameters except the location of the ignition source remain unchanged in all scenarios developed in this study. The users of this approach may choose other parameters that are not limited to those used in this study.

2.2.2 Step 2: Fuel Release and Dispersion Analysis

Fire occurs when the concentration of gas fuel reaches the combustion limit[53]. It is considered that the combustion limit of natural gas is 5 – 15%[54]. The release and dispersion simulations are conducted using the FDS model in this study to determine the distribution of the concentration of gas fuel so that the size of the fuel vapour cloud can be calculated to develop credible scenarios.

LNG released from a tank can vaporize quickly due to the ambient temperature. LNG vaporization occurs in two ways[43]: (1) heat transfer from the ambient temperature when no fuel is ignited; (2) heat transfer from the fire occurring in the surrounding area when natural gas is ignited. Natural gas is a combustible hydrocarbon gas mixture, formed primarily of methane, ethane, propane, butane, pentane, and sometimes a small percentage of carbon dioxide, nitrogen, hydrogen sulfide, or helium[50]. In this study, it is assumed that natural gas is mainly composed of methane.

In FDS, Lagrangian particles are used to represent objects that cannot be resolved on the numerical grid[55]. Liquid droplets are the most common example. In this study, the liquid fuel is LNG and needs to be represented by Lagrangian particles. A sprinkler is used to represent the fuel release from a hole in the tank in this study.

In this FDS simulation, a mixture of gas species such as air is simplified as a lumped species, which is considered to transport and react together. Therefore, only one transport equation needs to be solved for this "lumped species". The transport equation for both lumped species and a single species utilized by FDS is shown in Equation (2.1)[56].

$$\frac{\partial \rho}{\partial t}(\rho Z_\alpha) + \nabla\cdot(\rho Z_\alpha \boldsymbol{u}) = \nabla\cdot(\rho D_\alpha \nabla Z_\alpha) + \dot{m}'''_\alpha + \dot{m}'''_{b,\alpha} \tag{2.1}$$

where: ρ is the mass density, t is the time, **u** is the velocity vector, Z_α is the mass fraction of lumped species α, D_α is the diffusivity of species α, $\dot{m}'''_\alpha$ is the mass production rate per unit volume of species α by chemical reactions, and $\dot{m}'''_{b,\alpha}$ is the mass production rate per unit volume of species α by evaporating droplets/particles.

2.2.3 Step 3: Fire Consequence Analysis

Eliminating the existence of ignition sources can prevent a fire. However, there are many types of ignition sources that cannot be completely identified and eliminated[53]. Thus, it is necessary to investigate how ignition sources would affect the potential consequences of FLNG fire accidents.

This study focuses on the impact of an ignition source's location on the consequences caused by fire. All parameters except the location of the ignition source remain unchanged to find the most dangerous scenarios caused by different ignition sources' location. Considering the results of the release and dispersion model, various credible scenarios can be developed.

The FDS code is used to conduct simulations of various credible scenarios. FDS is a computational fluid dynamics (CFD) model of fire-driven fluid flow, developed by the National Institute of Standards and Technology (NIST). FDS has been validated by NIST and also by a large number of studies and experiments[57-59]. To decrease the computational cost, most combustion models in FDS use a single step, the mixing-controlled, infinitely fast chemical reaction of lumped species. Each reaction using a simple chemistry model is assumed to be of the form as in Equation (2.2)[55].

$$\mathrm{C_X}H_Y O_Z N_V + V_{O_2} O_2 \rightarrow V_{CO_2} CO_2 + V_{H_2O} H_2O + V_{CO}\mathrm{CO} + \mathrm{V_S} Soot + V_{N_2} N_2 \quad (2.2)$$

Temperature and the concentration of fuel gas caused by the leakage and combustion in various scenarios are extracted from the simulation to conduct a detailed fire analysis. The thermal radiation model used in FDS is defined by Equation (2.3) and (2.4)[56].

$$\dot{q}_r''' \equiv -\nabla . \dot{q}_r''(x) = k(x)[U(x) - 4\pi I_b(x)]; \quad (2.3)$$

$$\mathrm{U(x)} = \int_{4\pi} I(x, s')\, \mathrm{d}s' \quad (2.4)$$

where $k(x)$ is the absorption coefficient, $I_b(x)$ is the source term;

$I(x, s')$ is the solution of the radiation transport equation (RTE) for a non-scattering gray gas and is explained in Equation (2.5).

$$\mathrm{s}.\nabla I(x, s) = k(x)[I_b(x) - I(x, s)] \quad (2.5)$$

To validate the FDS code, a set of simulations with known conditions reported in the literature was conducted. The results obtained were compared with the results

reported in the literature. They showed good agreement. This partially validates the FDS code.

According to the previous studies[12, 60], at 538℃, the yield strength of steel will be reduced to approximately 60% of its normal value, which does not have the ability to support the steel structure's function, according to the American Institute for Steel Construction (AISC)[61]. In this study, a temperature higher than 538℃ is defined as dangerous, while the area that the dangerous temperature caused by a fire can reach is defined as the dangerous zone.

In the current study, the fire's impact on adjacent assets and structures is evaluated through these aspects: the maximum temperature the fire can cause, the duration of the dangerous temperature and the size of the dangerous zone.

2.2.4 Step 4: Safety Measure Design and Effectiveness Analysis

Considering the serious impact of fire on adjacent assets and structures, some safety measures, including active and passive measures, are used to mitigate this impact. Apart from applying active safer designs, passive measures, including protective equipment, cannot be ignored, due to the chemical properties of flammable hydrogen. The term passive measures refers to designs that could mitigate the impact of accidents. Among these safety measures, firewalls, water deluge systems, and carbon dioxide fire suppression systems are considered effective methods to mitigate the impact of fire.

In this section, the simulations are conducted using the FDS code after applying safety measures. Three evaluation aspects are used to analyze the impact of fire:

the maximum temperature the fire can cause, the duration of the dangerous temperature and the size of the dangerous zone. The results from the FDS simulation are used to compare with the results from the simulation without applying any safety measure, to study the effect that safety measures would have on the fire.

2.2.4.1 Firewall

In traditional onshore chemical plants, each module is separately located at an adequate distance. However, in offshore facilities, due to their compact layouts, firewalls are typically used to implement segregation[62]. In this study, the firewall is installed around the leakage tank to prevent the spread of fuel and fire.

2.2.4.2 Fire Suppression System

An auto fire suppression system is an effective way to provide protection against fire. In the current study, in order to effectively mitigate the impact of fire on adjacent assets and structures, a carbon dioxide fire suppression system, as well as a water deluge system, is installed on an FLNG facility.

A carbon dioxide fire suppression system is also a reliable way to mitigate the impact of fire. Carbon dioxide is a colourless, odourless, electrically non-conductive, and easily available gas that is highly efficient as a fire suppression agent. While a water spray could reduce the temperature by water evaporation, carbon dioxide can be used to reduce the flammable gas concentration and thus smother fires. This method to extinguish a fire is called Clean Agent Fire Suppression by the National Fire Protection Association[63]. In this study, the

carbon dioxide fire suppression system is installed according to the NFPA 2001.

2.3 Application of the Methodology

2.3.1 Step 1: Scenario Development

The geometry of the target offshore structure is an FLNG processing facility, shown in Figure 2-2. The information for the target offshore structure is extracted from a typical FLNG processing facility. The target structure model is comprised of a life module, central control room and helicopter deck, process and utility modules, hull and ship systems, a turret and fluid transmission control rotary joint and mooring and riser systems. Among them, the processing unit is considered one of the most hazardous areas and needs more attention[41]. In this study, liquid fuel is assumed to be released from a tank in the process and utility modules, considering its higher risk.

The simulation volume is set as 72m*80m*36m and the grid cell is 0.5m*0.5m*0.5m. The total number of grid cells in each scenario is 1658880. Figure 2-3 shows the simulation area in the target structure. According to Ichard et al., a finer, as well as a coarse grid cell, have been used in sensitivity studies to guarantee that the grid solution is independent of the cell size[51]. A coarse mesh with 964800 cells and a fine mesh with 1878750 cells were selected. Figure 2-4 shows good correspondence between the simulation results of temperature changes over time in certain slice files with different meshes. The simulation period of 60 seconds is considered for each scenario. Higher simulation duration may be considered; however, in the present study, simulation results did not make

much difference. Therefore, this scenario is restricted to a first-minute simulation. In the current study, the ambient pressure is set to be atmospheric pressure and the ambient temperature is set to be 5 degrees Celsius, considering cold region operating conditions. Wind speed is assumed to be 3m/s and the wind comes from the +X axis, while the atmospheric stability class is D, which is a credible scenario, according to Pitblado et al. [42]. For release factors, the leakage point is assumed to be on the tank in the process and utility modules. LNG is released at the speed of 10m/s due to the inner pressure of the tank and considering the high wind zone offshore. According to Pitblado et al.'s study, the maximum credible hole caused by accidental operational events is 750mm[42]. The release rate of LNG can be calculated using 10m/s and 750mm as the release velocity and hole size. Instead of treating release as instantaneous or at a constant rate, as in most studies, the release rate in this study is treated as a time-varying value. The release starts at 0s, gradually reaches the specified rate at 3 seconds and then remains constant. From 57s, the release rate decreases gradually and finally stops.

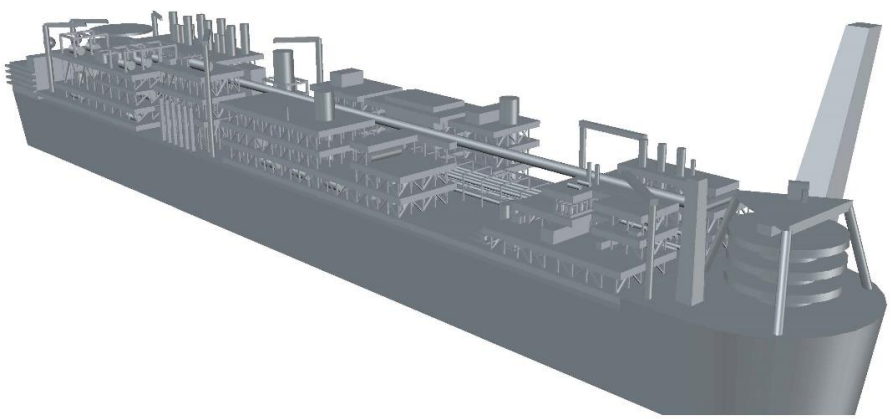

Figure 2-2 The FLNG Structure

Figure 2-3 The simulation area

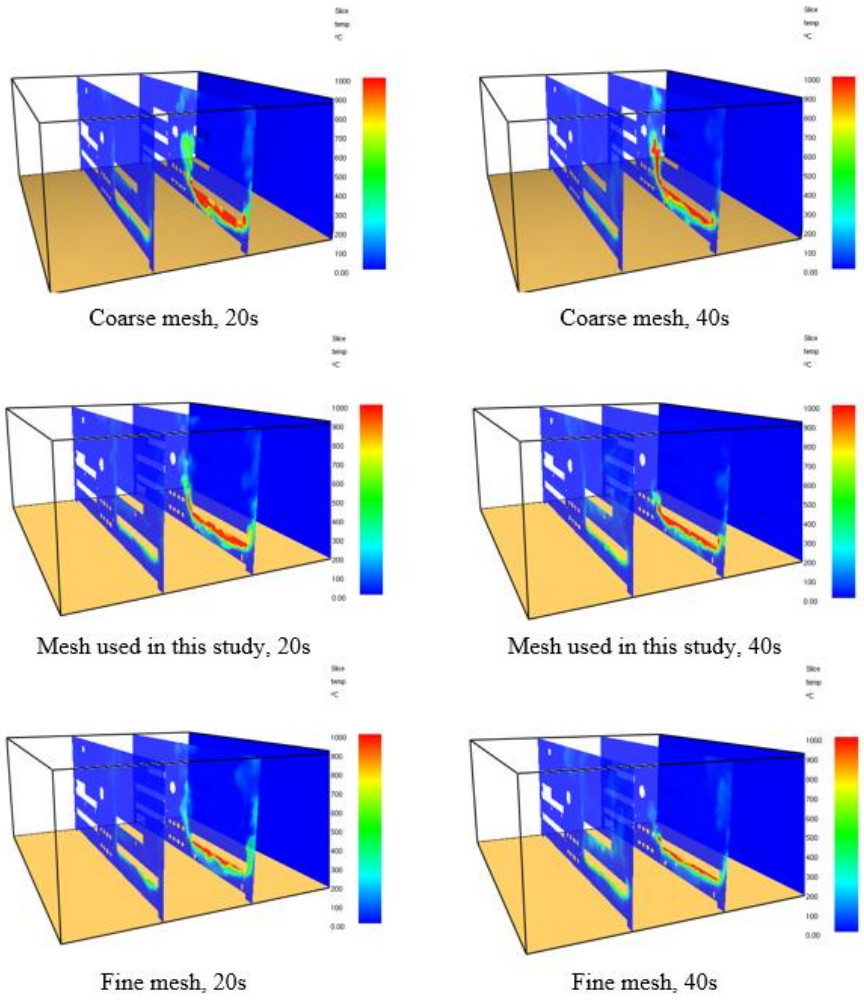

Figure 2-4 Sensitivity study result

2.3.2 Step 2: Release and Dispersion Simulation

In the dispersion simulation, the ambient pressure is set to be atmospheric pressure and the ambient temperature is set to be 5 degrees Celsius (considering cold region operating conditions). The wind speed is 3m/s, and the wind comes from the +X axis. Ten planes are selected and evenly distributed on an X axis to show the concentration of gas fuel. Based on the results of the simulation, LNG vaporizes quickly after release from the tank, due to conditions in the surrounding

environment. With wind action, natural gas disperses quickly and in approximately 20 seconds, natural gas covers most of the entire simulation area. In actual offshore operation, the release rate and leakage point may change, and environmental factors such as wind speed and temperature might cause natural gas to vaporize and disperse at an even higher speed. Figure 2-5 shows an example of the results using the FDS code.

(a) 10s

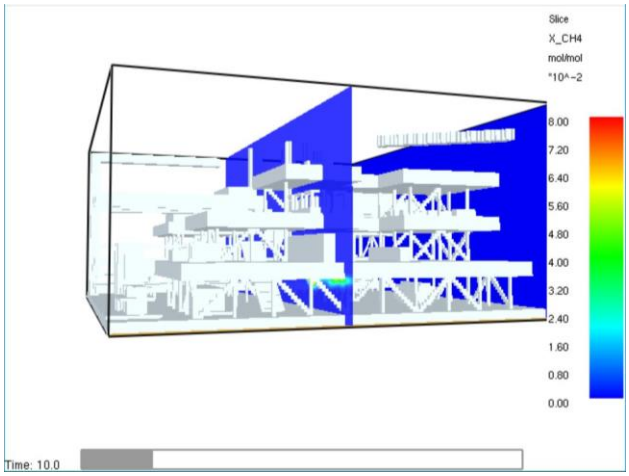

(b) 30s

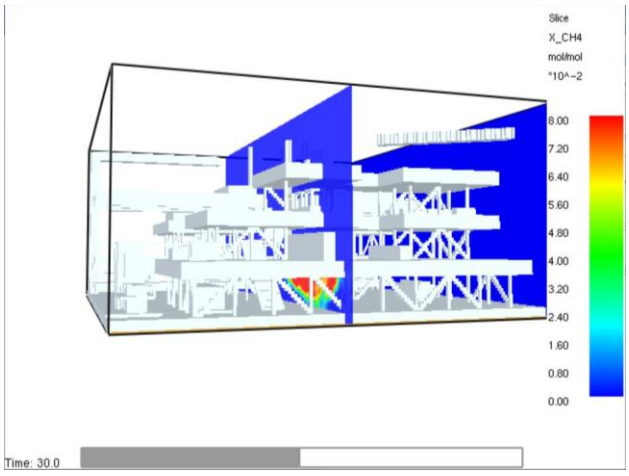

(c) 50s

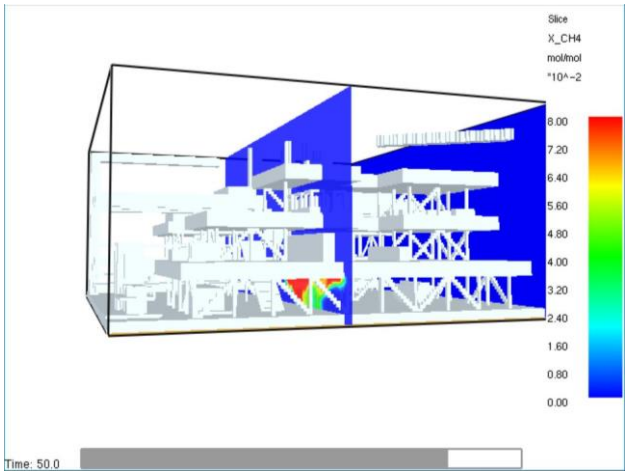

Figure 2-5 An Example of Slice File of Concentration at Different Times

2.3.3 Step 3: Fire Simulation and Analysis

The area where the concentration of gas fuel within the flammable limit is selected as a credible fire scenario, based on the results of the release and dispersion simulation. A total of fourteen different accident scenarios with different locations of the ignition source in the process and utility module are developed in this study. While only one scenario is developed on the second deck because of the lower likelihood that the gas fuel can disperse to the second deck according to the result from dispersion and release result, 13 ignition locations are evenly developed throughout the first deck. The FDS code is used to conduct a fire simulation for each scenario. Table 2-1 describes the 14 credible scenarios with different locations. Figure 2-6 shows the location of the ignition source.

Table 2-1 The Location of the Ignition Sources

	X(m)	Y(m)	Z(m)
Scenario 1	11	10	4
Scenario 2	11	22	4
Scenario 3	11	34	4

Scenario 4	23	10	4
Scenario 5	23	22	4
Scenario 6	23	34	4
Scenario 7	35	10	4
Scenario 8	35	22	4
Scenario 9	35	34	4
Scenario 10	47	10	4
Scenario 11	47	22	4
Scenario 12	59	10	4
Scenario 13	59	22	4
Scenario 14	23	22	12

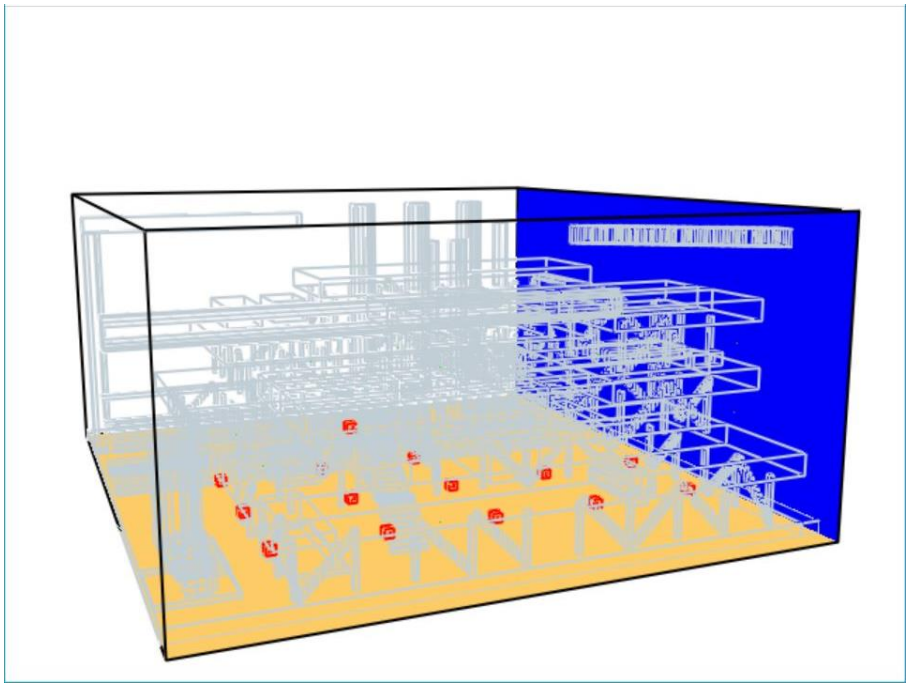

Figure 2-6 The Locations of the Ignition Source

In this section, the FDS code is used to conduct fire simulation for 14 credible scenarios.

In order to obtain precise data at a specific point in the simulation, 66 thermocouples are set in the target structure. These 66 thermocouples are distributed evenly over the target structure and can record the temperature of the

monitoring points changing over time. Figure 2-7 indicates the location of 66 thermocouples. Additionally, 10 slices are selected and placed evenly on the X-axis to show the concentration of gas fuel and temperature change over time in Smokeview. Figure 2-8 indicates the location of 10 slices.

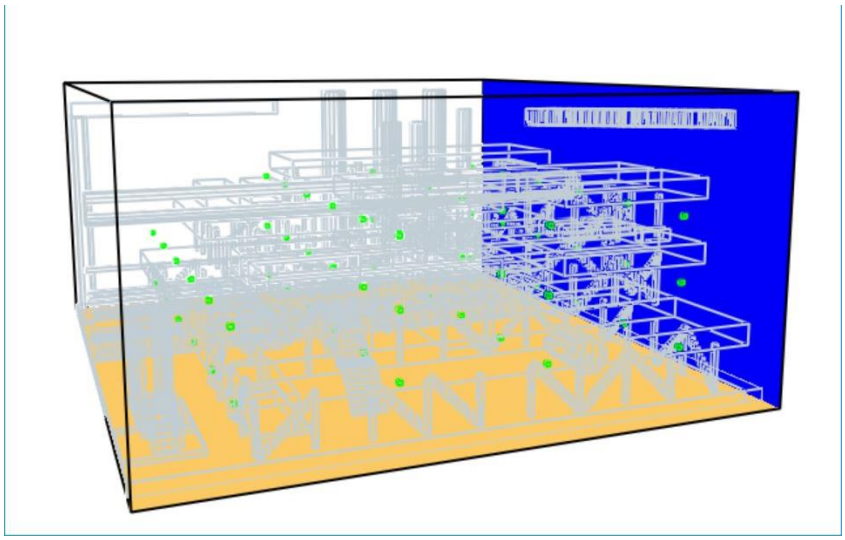

Figure 2-7 The Location of 66 Thermocouples

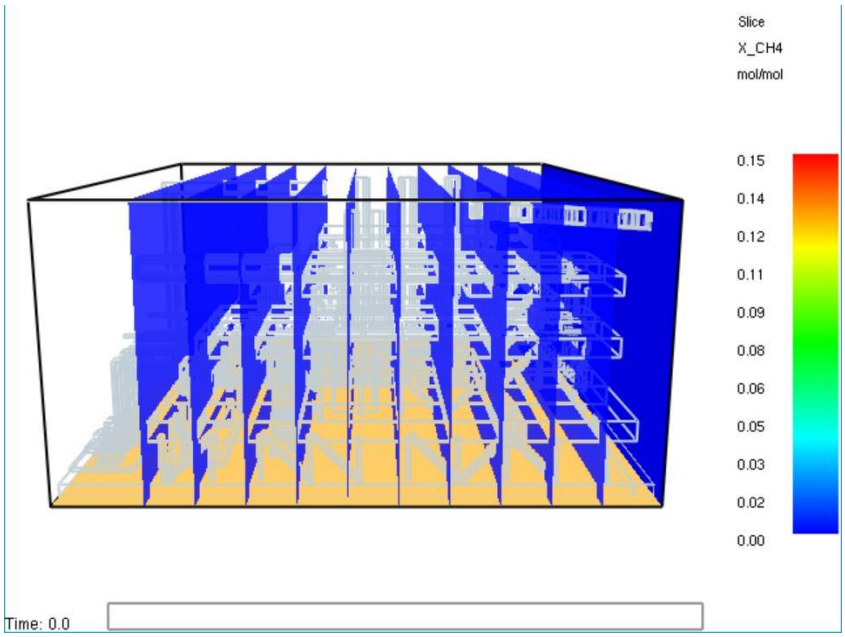

Figure 2-8 The Location of 10 Slices.

In scenario 2, with the wind action, the fuel gas disperses rapidly and is exposed to the ignition source. At about 21s, the vapour gas is ignited when the fuel gas reaches the flammable limit and the temperature reaches the ignition temperature. Due to the existence of confined geometry around the ignition source in scenario 2, the fire occurs, and the temperature rises rapidly after the fuel vapour is ignited. The flame rapidly returns to the leakage point and ignites all the fuel released from the vessel. The spill fire then forms until the leak stops. In this scenario, the longest time of all 14 scenarios is needed to ignite the vapour cloud, so the flame has the shortest duration and the period of the damage to the adjacent assets and structure is short. However, the highest maximum temperature of all 14 scenarios is found in scenario 2, which will be analyzed in detail in the next section. Figure 2-9 shows the contours of the fire change over time for scenario 2 in Smokeview. Six monitoring points are selected as examples of temperature change over time for scenario 2, as shown in Figure 2-10. Note that for most monitoring points, the temperature reaches a peak after the 30s, indicating a very high rate of temperature rise, giving less time for safe mustering.

(a) 24.7s

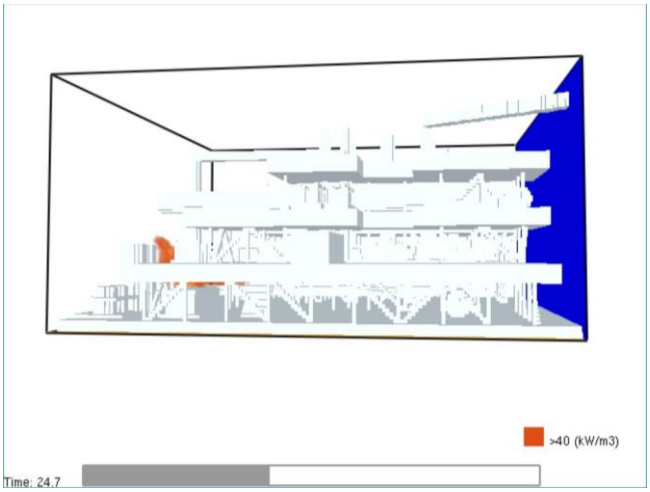

(b) 34.5s

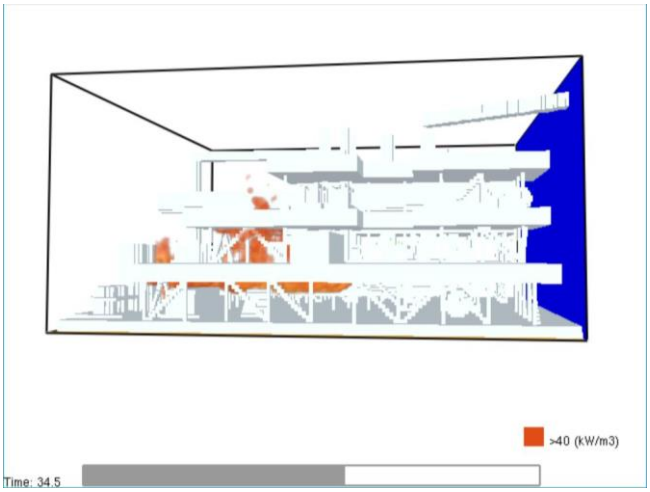

(c) 50.0s

Figure 2-9 The Contours of the Fire Over Time for Scenario 2

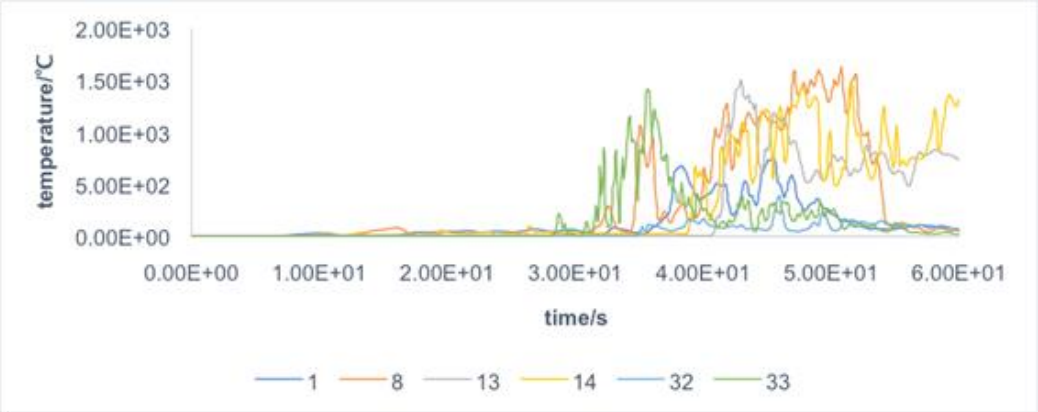

Figure 2-10 Temperatures Recorded at 6 Monitoring Points

Figure 2-11 shows the maximum temperature that a fire could cause in each scenario. According to the result, Scenario 2 has the highest temperature while Scenario 6 has the lowest. Apparently, the highest temperatures of Scenarios 3, 6, 9 and 14 have different degrees of reduction, which indicates that due to the existence of some structures between the location of the ignition source and the leakage point, the gas fuel may not spread far and thus the fire will not cause as serious a result as others within the simulation period.

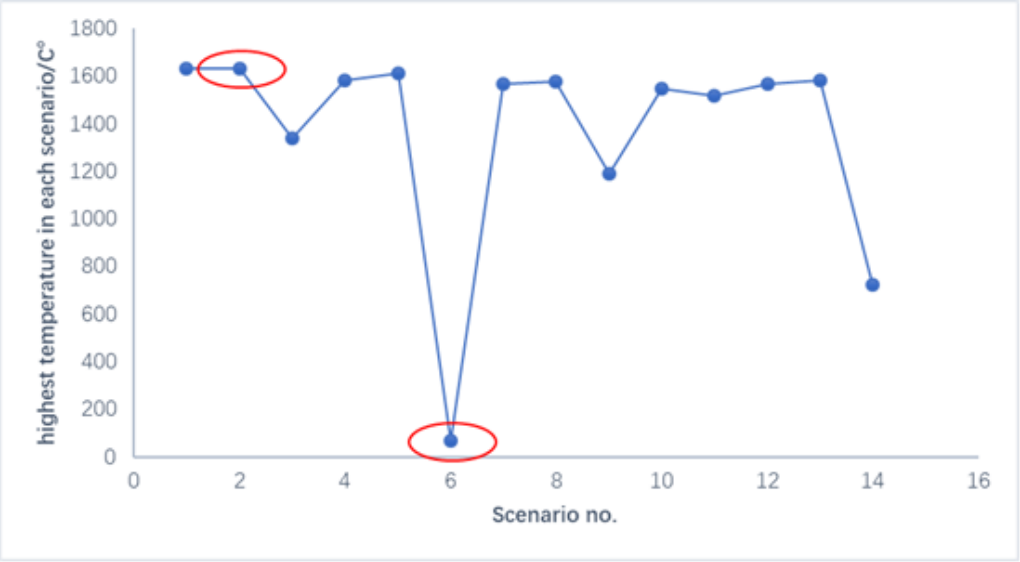

Figure 2-11 The Maximum Temperature in Each Scenario

As shown in Figure 2-12, some thermocouples are selected in Scenario 11 to indicate the difference between 538℃ and the temperature recorded at some monitoring points. This is highlighted in Figure 2-12, which shows the period of dangerous temperature rise. The duration of the dangerous temperature caused by a fire is monitored by measuring points and plotted in Figure 2-11. Analysis of the results of all credible scenarios shows that scenario 11 has the maximum time duration of a dangerous temperature, while scenario 6 has the minimal time duration of a dangerous temperature. It can be concluded that due to the close distance and a scarcity of other structures between the location of the ignition source and the leakage point in Scenario 11, the fire could occur more easily than in other scenarios, so a fire caused by a close ignition source could last for a long time.

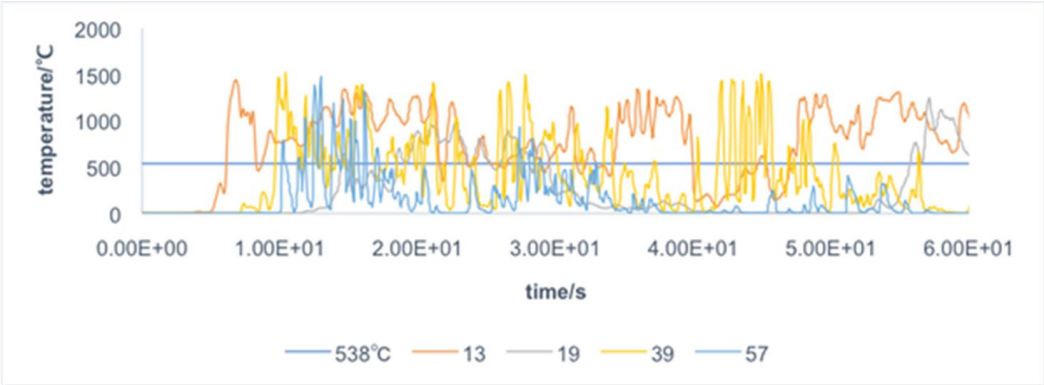

Figure 2-12 Temperatures Recorded in Some Monitoring Points in Scenario 11

The size of the dangerous zone can be shown using a slice file that is perpendicular to the Z-axis. Figure 2-13 shows the slice file of the temperature in scenario 13. Of all credible scenarios, scenario 2 can cause the largest dangerous zone. A long period before ignition gives gas fuel the opportunity to disperse further, which leads to it being the largest dangerous zone.

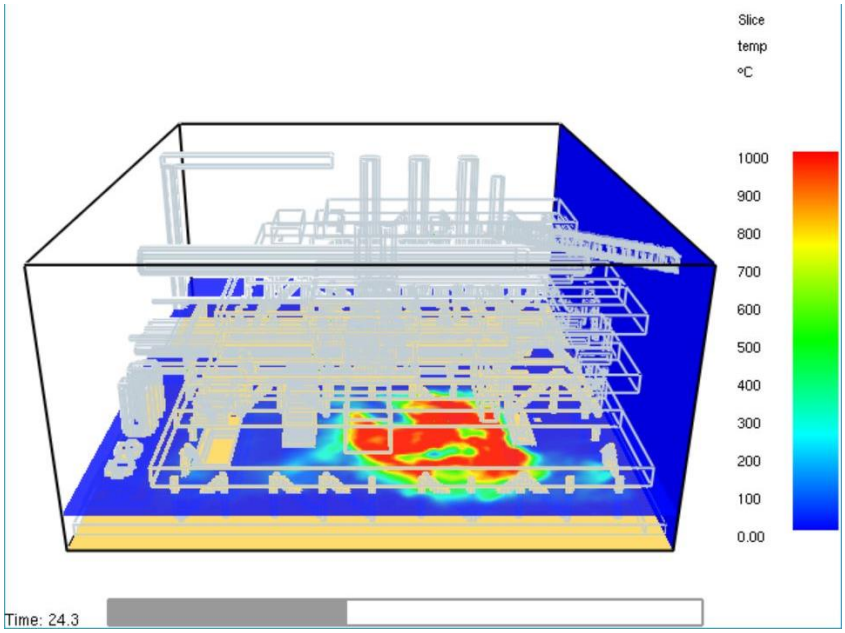

Figure 2-13 Slice File of Temperatures in Scenario 13

For the leakage occurring in a specific tank, the location of the ignition source affects the result of the fire. To sum up, based on the fire analysis of all credible scenarios in this case, considering the aforementioned three aspects that measure the impact of fire, Scenarios 2, 11 and 13 are considered the three most dangerous scenarios overall in terms of thermal effect.

Considering the confined layout of an FLNG, transition from fire to explosion may possibly occur. In this study, FLACS, a CFD software used extensively for explosion modelling, was used to simulate a possible explosion occurring under the same conditions. Since this study mainly focuses on the fire's effect on an offshore facility, the explosion simulation result is presented briefly. The ignition location is selected based on the release and dispersion simulation results achieved through FLACS. Figure 2-14 shows the pressure caused by the explosion changing over time in the FLACS simulation. According to the results, ignition occurred at about 30s. Overpressure caused by the explosion is not high enough to cause damage to assets in this case and thus, thermal radiation is considered to be the main impact in this study.

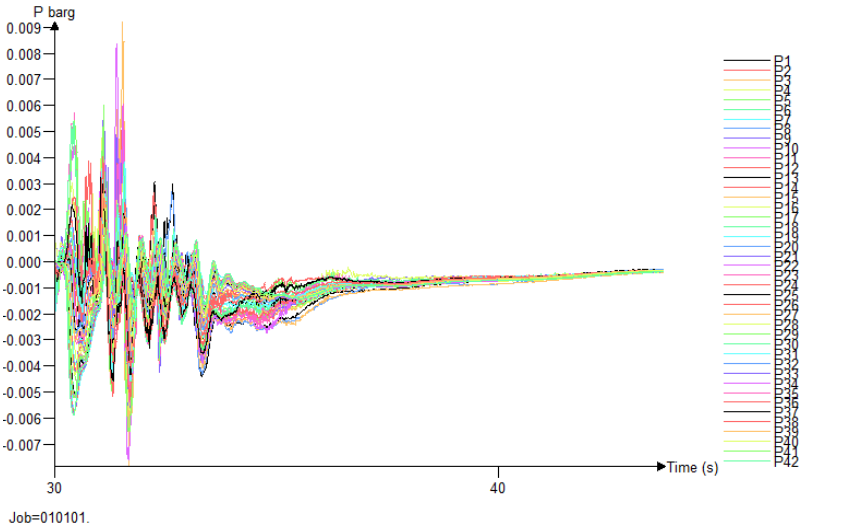

Figure 2-14 Pressure changes over time in FLACS simulation

2.3.4 Step 4: Fire Suppression Simulation and Analysis

In this section, a firewall and an auto fire suppression system are installed in the FLNG facility and then a CFD simulation is conducted with the same parameters as are used in the previous sections.

The deluge system is simulated using the FDS code with Lagrangian particles. Sprinkler heads with a 12 m^2 coverage area is installed and the distance between the sprinkler heads is set to be 4.5 m, according to the NFPA 13 standard [64]. When the sprinkler heads are exposed to fire and the temperature around them reaches 60 degrees Celsius, they will be activated automatically[12].

Figure 2-15 shows the maximum temperature at which the fire can reach the target structure in the absence of any safety measures and the maximum temperature at which the fire can reach the target structure under the protection of a firewall and

fire suppression system in the three most dangerous scenarios. Obviously, due to the existence of a firewall and fire suppression system, the maximum temperature of all scenarios is decreased in varying degrees. In Scenario 2, the firewall is very helpful because it can prevent the spreading of fuel and the fire. Since Scenario 2 has the longest distance from the leakage point to the ignition source, preventing the spreading of fuel can highly decrease the opportunity for natural gas to meet the ignition source and thus highly decrease the impact of a fire. However, in the other two scenarios, the fire suppression system plays a more vital role in mitigating the effects of the fire in terms of maximum temperature the fire can cause. In Scenarios 11 and 13, the distances between the leakage points and ignition sources are very short so the natural gas is still very likely to meet the ignition sources, in spite of the existence of a firewall. Therefore, the fire suppression system can be a more effective way to mitigate the impact of fire in this case.

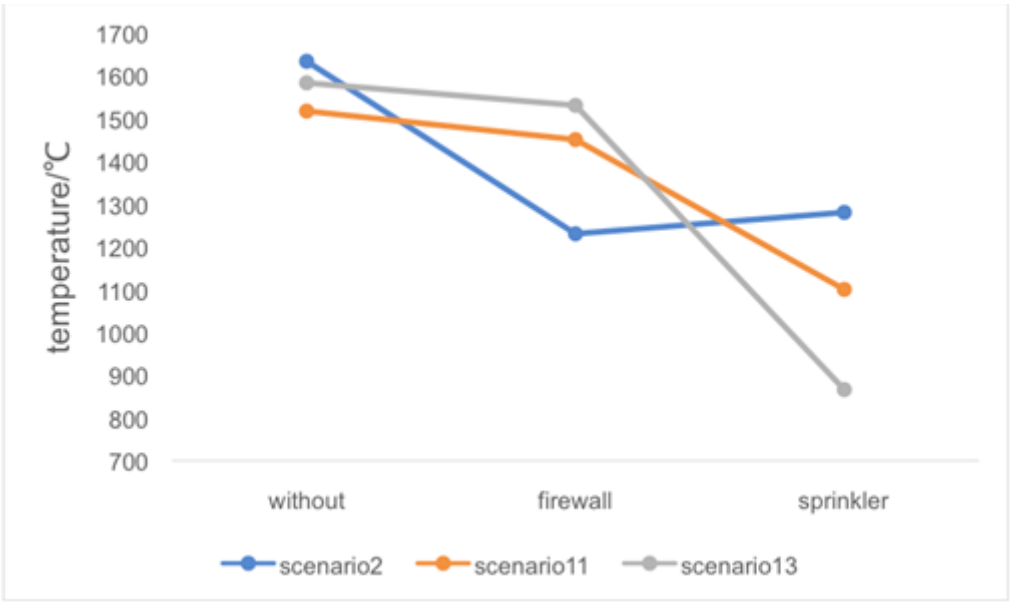

Figure 2-15 Maximum Temperature the Fire Caused Before and After Application of Safety Measures

The following figures take Scenarios 2 and 13 as examples to show the effectiveness of safety measures.

In Figures 2-16 and 2-17, 4 monitoring points are selected to show the temperature changes over time in Scenarios 2 and 13. In each scenario, the figures show the results both before and after the application of safety measures. In this section, the dangerous temperature line is set to show the difference between the dangerous temperature and the temperature caused by fire. The part that exceeds the dangerous temperature has been highlighted in the figures; thus, the duration of a dangerous temperature can be explicitly demonstrated.

According to the results shown in Figures 2-16 and 2-17, both the firewall and the fire suppression system can effectively mitigate the impact of fire on varying degrees in terms of the duration of a dangerous temperature. For scenario 2, the firewall plays a more vital role than the fire suppression system. Compared to the scenario without applying safety measures, it is obvious that in scenario 2, ignition is delayed at some specific monitoring points such as points 13 and 39 due to the existence of a firewall. For scenario 13, the firewall is ineffective to delay ignition because of the short distance between the leakage point and ignition source. However, the FLNG avoids a more serious impact of fire with the help of the fire suppression system.

In Figure 2-18 and 2-19, slice files are used to show the temperature of the cross-section perpendicular to the Z-axis and the slice plane and the largest size of the dangerous zone is recorded in each scenario. In scenario 2, the firewall is not very useful to prevent the spreading of fire, but it effectively reduces the high temperature. The insignificant opportunity for natural gas to meet the ignition gas contributes to this result. A small amount of natural gas meeting an ignition source brings a comparatively low temperature, but the firewall cannot effectively reduce the size of a fire when the fire has already started. In scenario 13, due to the existence of a firewall, the spread of fuel gas and flames is highly suppressed. Therefore, the high temperature mainly concentrates within the firewall and for this reason, the dangerous zone can be reduced. However, the area within the firewall has a comparatively higher temperature. Although a fire suppression system cannot influence the spread of fuel gas and flames, it can reduce the size of a dangerous zone by reducing the overall temperature in the FLNG. The results in this section further demonstrate that for different scenarios, the effectiveness of the safety measure varies.

In summary, both firewalls and auto fire suppression systems can effectively mitigate the impact of fire in terms of the maximum temperature the fire can cause, the duration of the dangerous temperature and the size of the dangerous zone. However, for different scenarios, these two safety measures have different effectiveness. For a scenario in which the ignition source is far from the leakage point, the firewall can effectively prevent the spread of natural gas and thus reduce

its opportunity to meet the ignition source. For a scenario in which the ignition source is close to the leakage point, such as in Scenarios 11 and 13, the firewall cannot delay the occurrence of fire but it can limit most of the fire to inside the firewall, and thus effectively reduce the size of the dangerous area. However, introducing a firewall will increase the confinement of the FLNG layout. This may increase the chance of an explosion. An auto fire suppression system can reduce the flammable gas concentration and reduce the heat through vaporization and thus effectively mitigate the impact of a fire.

(a) Without Safety Measures

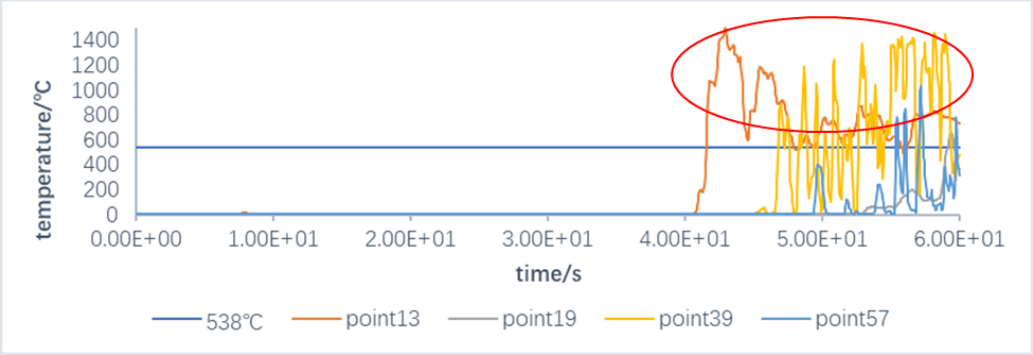

(b) Firewall

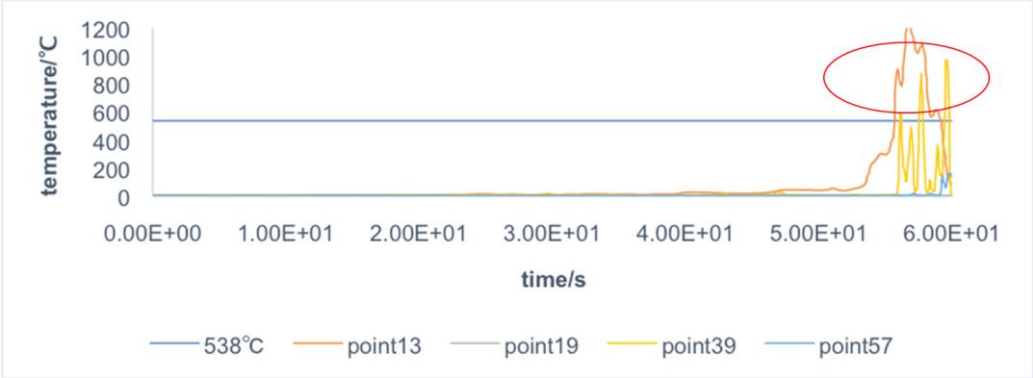

(c) Fire Suppression System

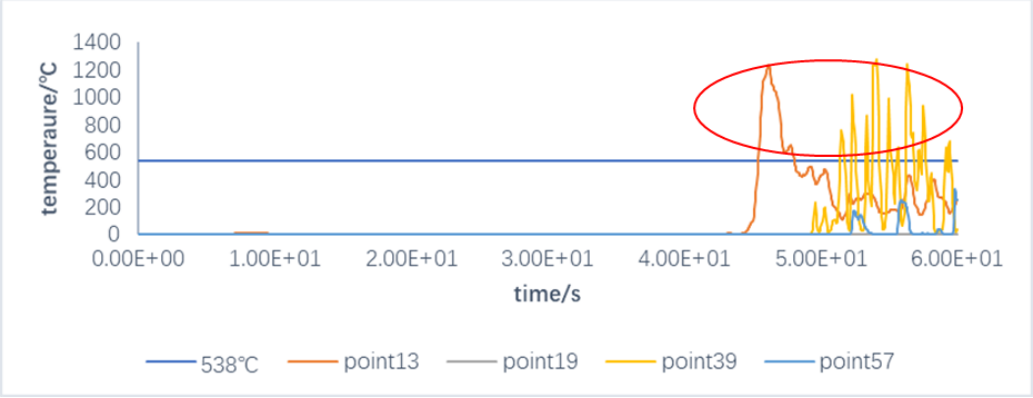

Figure 2-16 Temperatures Recorded at Some Monitoring Points Before and After Application of Safety Measures in Scenario 2

(a) Without Safety Measures

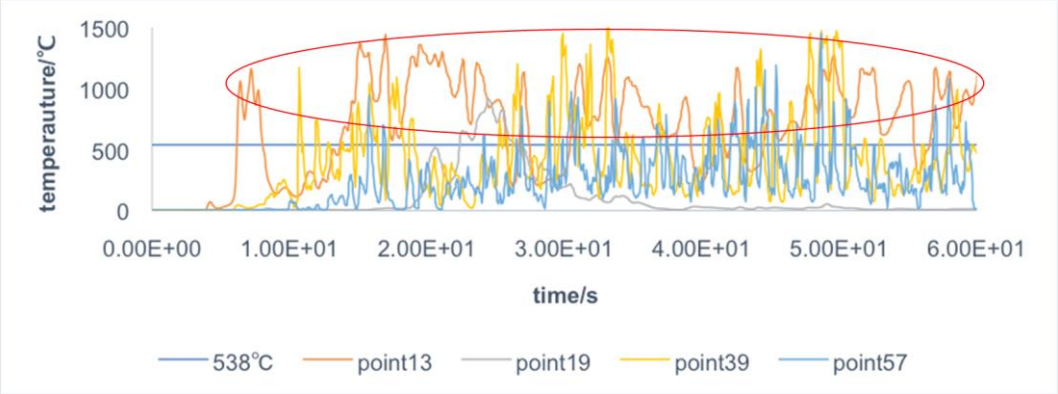

(b) Firewall

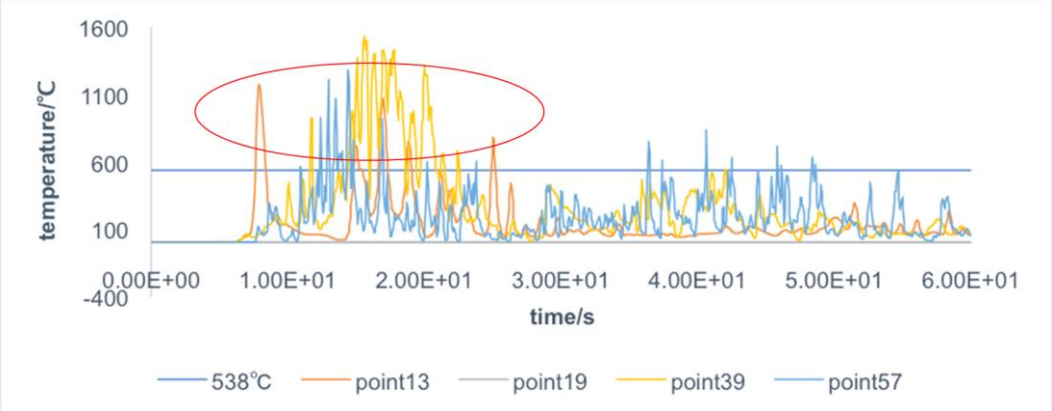

(c) Fire Suppression System

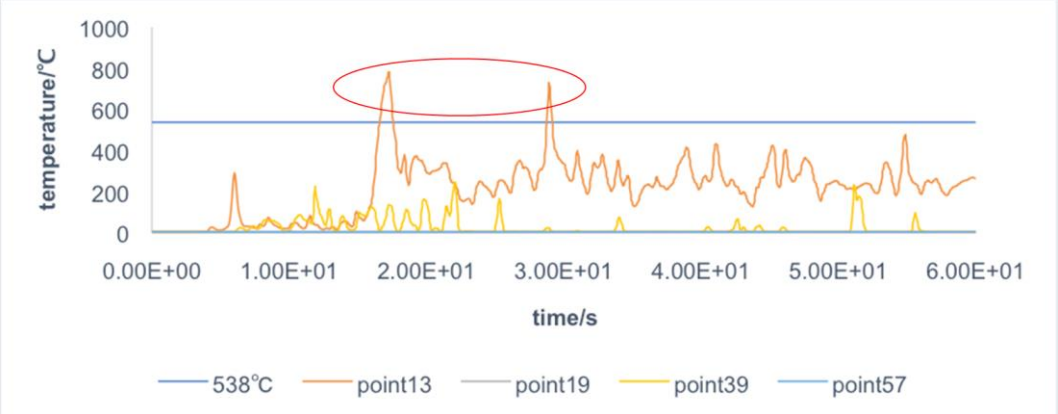

Figure 2-17 Temperature Recorded at Some Monitoring Points Before and After Application of Safety Measures in Scenario 13

(a) Without Safety Measures

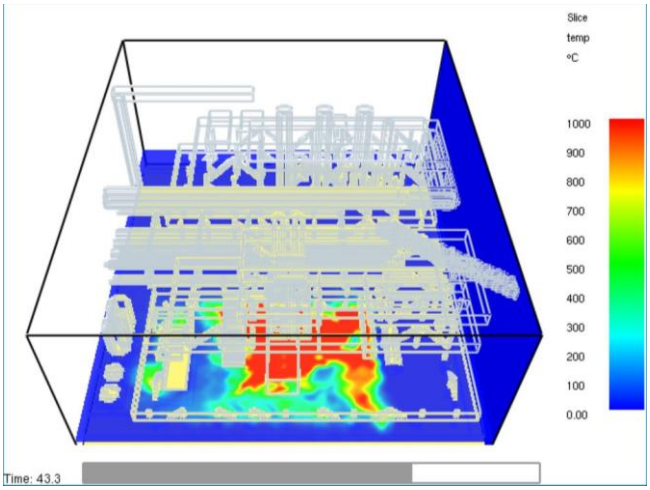

(b) Firewall

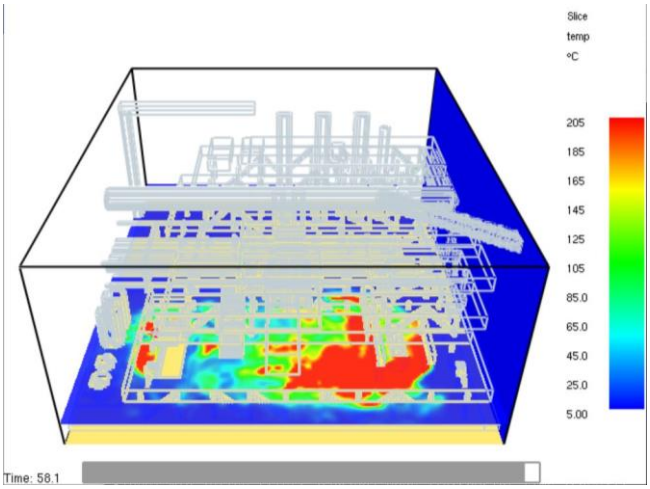

(c) Fire Suppression System

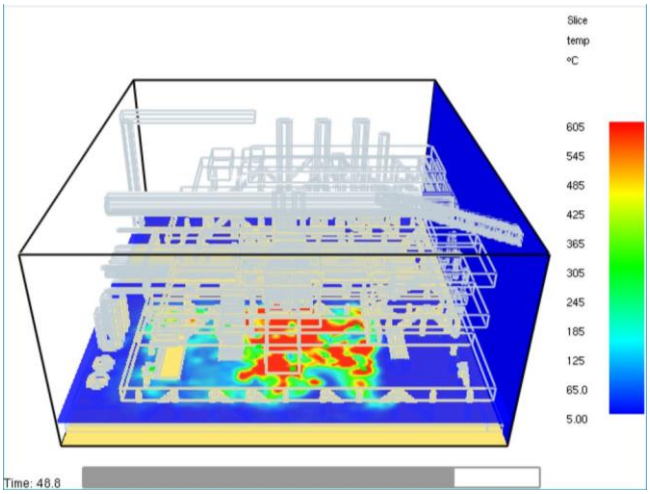

Figure 2-18 Slice File of Temperatures in Scenario 2

(a) Without Safety Measures

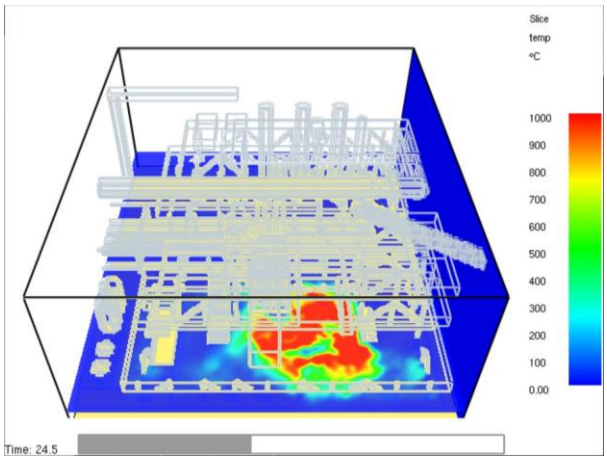

(b) Firewall

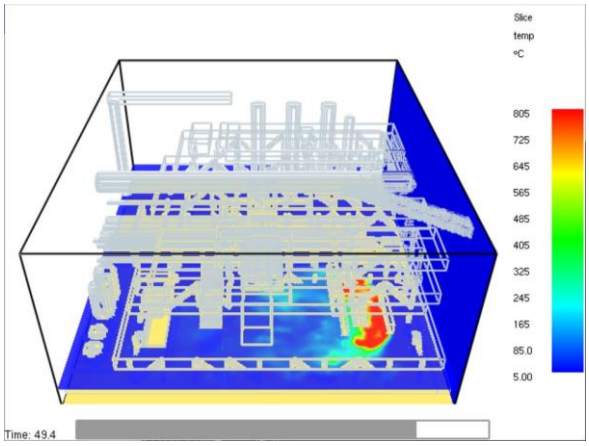

(c) Fire Suppression System

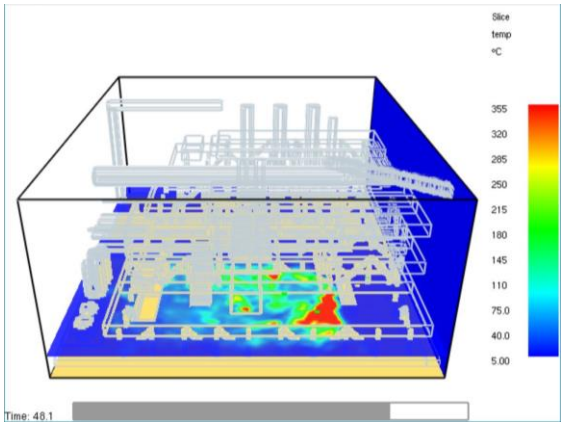

Figure 2-19 Slice File of Temperatures in Scenario 13

2.4 Conclusions

This paper proposes a procedure for analyzing the effectiveness of safety measures in reducing the impact of fire caused by an LNG release in an FLNG facility, considering the impact of the ignition source location.

The fire simulations are conducted for credible scenarios with different ignition source locations and the results extracted to determine the most dangerous scenarios. In this study, three aspects are considered to model the impact of accident scenarios. They are the maximum temperature the fire can cause, the duration of the dangerous temperature and the size of the dangerous zone. The results of the study confirm that the release of LNG is a serious threat to personnel on board and the assets. The relatively small differences in ignition source locations can increase the effect of the consequences of a fire.

To mitigate the impact of fire, a firewall and fire suppression system are selected and implemented. FDS is used as a tool to analyze the impact of each scenario with different ignition source locations after applying safety measures. Comparing the results before and after applying safety measures, it can be concluded that safety measures such as firewalls and auto fire suppression help to limit the impact of fire; however, the threat still remains significant. Using the proper layout to isolate the danger is identified as most effective in terms of limiting the impact of potential accidents.

This study emphasizes that an FLNG layout must be considered with the utmost

care. This step is the most effective measure in limiting a potential LNG release and subsequent dispersion effect, and directly influences the fire dynamics and thus limits the potential damage.

The scope of this study is limited to fire safety analysis through a numerical simulation approach. The transition from fire to an explosion will be studied in future work. The proposed approach will be further validated through a control experiment (field) data reported in the literature.

Chapter 3. A Time-Dependent Probabilistic Model for Fire Accident Analysis[1]

Co-authorship statement

A version of this manuscript has been submitted for publication in the Fire Safety Journal. Author Ruochen Yang conducted this study under the direct supervision of Faisal Khan. Faisal Khan provided the principal topic of this study, and Ruochen Yang developed the model, conducted the case study simulation, analyzed the simulation results, proposed the system optimization method and analyzed its effectiveness. Author Faisal Khan has reviewed the simulation results, provided feedback on model results and verified the developed model. Mohammed Taleb-Berrouane reviewed the manuscript and helped with the paper's composition. Author Depeng Kong helped conduct the application. All co-authors reviewed and provided feedback on the manuscript. Ruochen Yang revised the manuscript based on the co-authors' feedback and during the peer review process.

Abstract

Fire is among the most common and devastating accidents in the hydrocarbon production and processing industry. Many efforts have been dedicated to assessing fire accident likelihood; however, most of these studies considered fire probability

[1] Yang, R., Khan, F., Taleb-Berrouane, M., & Kong, D. A Time-Dependent Probabilistic Model for Fire Accident Analysis. Submitted to Fire Safety Journal

as spatially distributed, ignoring the time dependence of the fire accident scenario. In this study, a robust and practical model is proposed to analyze fire accident probability in a congested and complex processing area. This model integrates a conditional probability approach – the Bayesian network (BN) - with a time-dependent scenario evolution approach, Stochastic Petri Nets (SPN). The computational fluid dynamics (CFD) tool is used to estimate the time-dependent scenario consequences. The outcome of the model is fire probability as a function of time and location caused by a specific leak rate and leak duration. A case study of fire probability analysis in a Floating Liquified Natural Gas facility (FLNG) is presented. This study demonstrates the importance of the temporal dependency of the fire scenario and the proposed model can serve as the required tool for time-dependent fire probability analysis, further safety measures' application and system optimization.

3.1 Introduction

Fire accidents caused by hydrocarbon leakage are extremely hazardous in hydrocarbon processing and handling facilities. Moreover, due to the complex and congested layout of oil and gas facilities, a fire has a high damage potential for humans and assets [65]. Fire and explosion accidents which occurred in the last decades such as the Piper Alpha disaster[66], Buncefield oil depot fire accident [4], the BP Texas City disaster [3], the BP Deepwater Horizon explosion [20] and the Cleveland explosion [39] have already highlighted the importance of focusing on fire and explosion accidents.

Numerous studies have been conducted to analyze the fire accidents caused by hydrocarbon leakage. A series of studies conducted by Baalisampang et al. used a Fire Dynamics Simulator (FDS) code to model fire accidents occurring on a typical floating liquified natural gas processing facility (FLNG) and their effects on personnel and assets. In these studies, the effectiveness of a water deluge system's ability to mitigate the fire impact was verified, and the Probit method was combined with a Computational Fluid Dynamics (CFD) code to determine the fire's effects. According to the results, improved layout design and passive control strategies are necessary, and inherently safe layout design is then determined [12-14]. Yang et al. used FDS to simulate the hydrocarbon leakage and fire accidents caused by ignition sources at different locations. The fires' impacts on structures and humans on the topside were assessed, and the effectiveness of safety measures was analyzed in this study [8]. The method of BORA-Release proposed by Aven et al. analyzed the ability of safety barriers to prevent hydrocarbon leakage, as well as other influencing factors, such as the platform's technical conditions, human

factors and operational and organizational risks affecting barrier performance [67].

To assess the risk of a fire accident, it is important to accurately determine its occurrence probability. In the current oil and gas industry, the following methods are commonly used to analyze the likelihood of a fire accident [68]:

- Historical accident frequency data
- Fault tree analysis
- Theoretical modelling
- Event tree analysis (ETA)
- Human reliability analysis
- Expert judgement
- Bayesian analysis

In the study conducted by Paik et al., the fire probability is calculated by Equation (3.1) [69]. In this study, the leak frequency is calculated by combining historical data and simulation, considering the leak amount, while the ignition probability is obtained with historical data.

$$\text{Fire frequency} = \text{leak frequency} \times \text{ignition probability} \tag{3.1}$$

In the research by Lee et al., two types of LNG supply systems are assessed in terms of their fire accident risk. The fire probability is assessed using an ETA [70]. The failure probability of each safety barrier is estimated from historical data, while the ignition probability after leakage is determined by Equation (3.2) [71].

$$P = 0.017m^{0.74} \tag{3.2}$$

where m is the mass flow rate of the gaseous fuel, kg/s.

Zhu et al. explored several studies on ignition probability given a leakage accident. Some previous studies and reports proposed methods to calculate the ignition

probability based on mass flow rate [68]. For example, Cox et al. proposed a simplified equation for continuous instead of instantaneous releases, while coefficients a and b are estimated for different scenarios, as shown in Equation (3.3) [72]. In addition, Equation (3.4) is used to estimate the ignition probabilty for gas release with delayed ignition [73].

$$P = am^b \tag{3.3}$$

where m is the mass flow rate, kg/s.

$$P = (e^{-4.16}m^{0.642}) \times (e^{-2.995}m^{0.38}) \tag{3.4}$$

where m is the mass flow rate, kg/s.

Wang et al. used the Dynamic Bayesian Network (DBN) to predict the occurrence probability of fire on an offshore platform considering the effects of the human factor. In this study, the fire probability is considered to be the combination of the probability of an ignition source and hydrocarbon leakage. The other factors may be explained by the conditional probability table (CPT) but are not mentioned in the text. The results showed that the hot surfaces of equipment, waste gas, torch flames, and static sparks contribute the most to fire and explosion in oil and gas processing units [74]. Bilal et al. analyzed the risk of fire and explosion accidents in the pipelines using BN and Bow tie [75]. The theory of fuzzy sets is applied to consider the uncertainty due to impression. This work provides good view of the accident and calculate the occurrence probability. However, the dynamics feature of the accident is ignored in this work.

A fire accident can be viewed as a process in which the time dependency is an

essential feature. However, most of the studies mentioned above have considered fire probability as spatially distributed, ignoring the time dependence of the fire accident scenario. Techniques such as DBN are good at modeling the relationships among variables using CPT [76-78], and these tools have the ability to simulate time-dependent feature to some extent. For example, they can capture the probability in different time slices; however, they fail to capture the feature between time intervals. The SPN model enables capturing the time-dependent feature [79]; however, its ability to capture causal relationships between variables is not as strong as that of BN, especially the ability to capture the conditional relationships. In a fire modeling, BN can be used to model leakage probability as it provides an outcome of a complex interaction of parameters, while ignition probability is a time-dependent and random process, which is best modeled by SPN. Therefore, the integration of SPN and BN provides a robust method to capture the causal relationship between variables and time-dependent features. In addition, the CFD model serves as an accurate technique to incorporate all on-site variables and is also a good tool for viewing the value of a variable of interest over time in transient modeling. Taking the time dependence and factor dependence of the fire accident scenario into consideration through the combination of BN, SPN and CFD models, the present paper proposes a robust and practical model to analyze the fire accident probability in a congested and complex processing area, such as an offshore vessel, as a time-dependent process, which is lacking in the currently existing models. The present study aims to overcome existing models' shortcomings as described above by proposing a time-dependent probabilistic model for fire accident analysis.

An FLNG is an offshore facility designed to employ various LNG development technologies, including gas extraction, gas pre-treatment, natural gas liquefaction, condensate treatment, water treatment, LNG storage, and LNG offloading [18]. The FLNG is very congested with complex layouts. Because of its limited area, the FLNG has a substantial risk of fire accidents. The previous work by Yang et al. demonstrates how the fire accident can damage the structure and humans on the topside [8]. Therefore, it is necessary to determine the fire accident probability in the congested and complex processing area in an FLNG. To demonstrate the application of the proposed methodology, the probability assessment of a fire accident occurring in an FLNG is conducted as a case study in this research.

3.2 Proposed Methodology

Three core factors that cause a fire accident are hydrocarbon leakage, the concentration being within the flammable limit and ignition. These three elements need to coexist to cause a fire. Thus, the fire probability can be represented by Equation (3.5).

$$\mathrm{P(f)} = \mathrm{P(I, L, C)} \tag{3.1}$$

where,

$\mathrm{P(I, L, C)}$ is the probability that all three causation factors, including hydrocarbon leakage, the concentration being within the flammable limit, and ignition, occur simultaneously.

Based on the conditional probability theory [80], the fire occurrence probability equation can be further developed and defined in Equation (3.6).

$$\mathrm{P(f)} = \mathrm{P(I, L, C)} = \mathrm{P(L)} \times \mathrm{P(C|L)} \times \mathrm{P(I|L, C)} \tag{3.2}$$

where,

$P(L)$ is the occurrence probability of a hydrocarbon leakage;

$P(C|L)$ is the probability of the concentration being within the flammable limits, given a hydrocarbon leakage;

$P(I|L,C)$ is the ignition probability given a hydrocarbon leakage as well as the concentration being within flammable limits.

In this study, Equation (3.2) is used to calculate the occurrence probability of a hydrocarbon fire accident. Three terms in Equation (3.2) are modeled using advanced methods. The occurrence probability of a hydrocarbon leakage, $P(L)$, is modeled using the BN model, the probability of the concentration being within the flammable limits given a hydrocarbon leakage, $P(C|L)$, is obtained through applying CFD simulation, and the ignition probability, given a hydrocarbon leakage as well as the concentration being within flammable limits, $P(I|L,C)$, is modeled through the leakage duration simulation using SPN, with the assumption that an ignition source always exists. As shown in Figure 3-1, the proposed methodology in this study comprises five main steps: i) assessment of the leakage probability using a BN model, ii) assessment of the ignition probability using an SPN model, iii) assessment of the flammable vapour cloud probability using a CFD model, iv) probability assessment of a fire accident and v) optimization of system configuration to minimize fire scenario probability. Detailed steps of the simulation section are presented in Section 3.2.1-3.2.4.

The assumptions made in the proposed methodology include: (1) the proposed

methodology considers conditional probability theory, comprised of three factors, as the cause of the fire accident; (2) probability of a hydrocarbon leakage is calculated by BN, considering that all its non-descendant variables in the network are conditionally independent; (3) probability of ignition is calculated using PN and Monte Carlo simulation, considering variables following lognormal distribution; (4) the parameters and assumptions made in the case study are listed in the case study section.

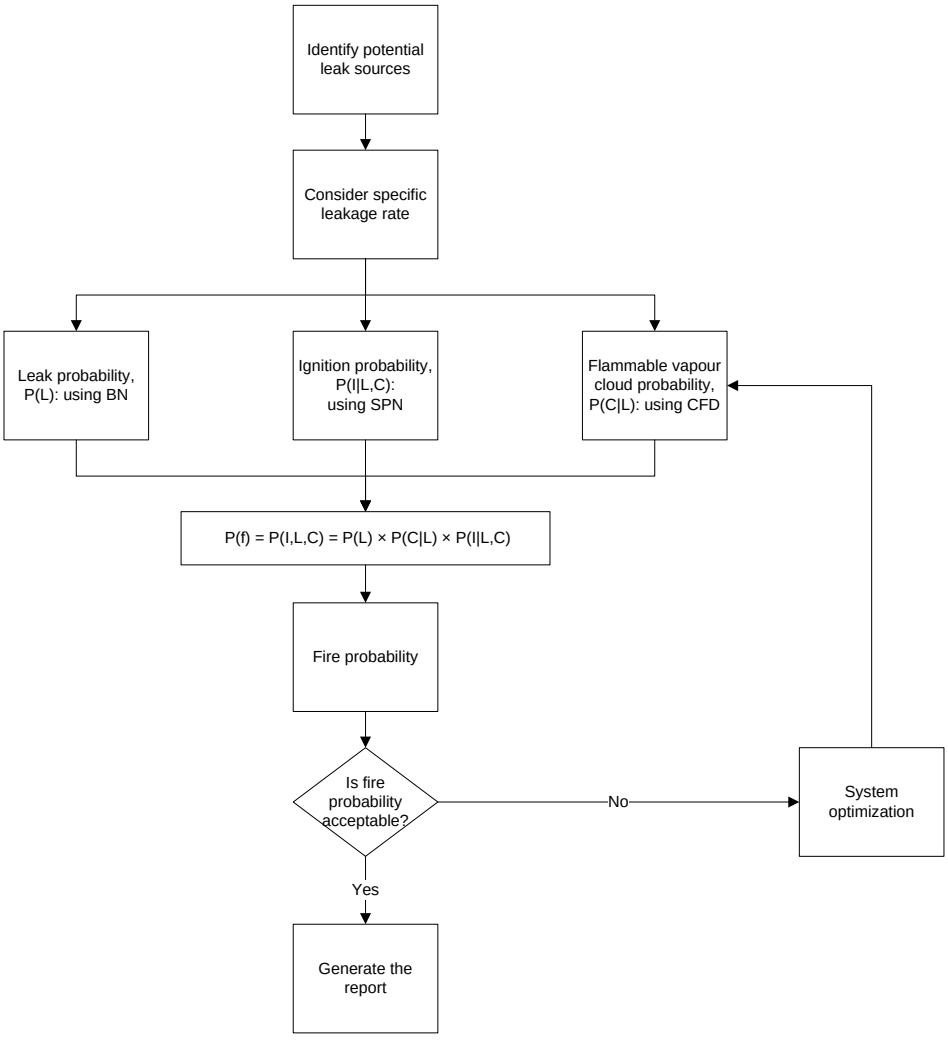

Figure 3-1 Flow chart of the proposed methodology.

3.2.1 Assessment of leakage probability

A leak is a starting point of a fire accident scenario. The leak sources and the probability of hydrocarbon leakage, $P(L)$, are modeled and determined using the BN model.

BN, also called a belief network, is a powerful tool for probabilistic modeling having uncertainty, using a directed acyclic graph and CPTs. In a BN, nodes represent variables, and directed arcs are used to represent the causal relationships between the variables [81]. Probabilistic analysis using BN is based on the conditional relationships among variables and d-separation. The joint probability distribution P of the random variables in some sets, $V = \{X_1, X_2, X_3 \ldots X_n\}$, can be represented in Equation (3.3) [82].

$$P = \prod_{i=1}^{n} P\left(X_i \middle| Pa(X_i)\right) \tag{3.3}$$

where $Pa(X_i)$ represents the parent of the variable X_i.

The object-oriented Bayesian network (OOBN) simplifies the graphical interface of complex BN structures [83]. It provides a concise way to present the framework of the BN using sub-networks. In addition to the usual nodes in a typical BN, instance nodes are used in the OOBN to represent the sub-networks. This allows a hierarchical structure for better understanding [84]. In the proposed model, OOBN is applied when the typical BN model is too complex to clearly represent the present model.

3.2.2 Assessment of ignition probability

As described in the methodology section, the ignition probability, given a hydrocarbon leak as well as the concentration being within flammable limits,

$P(I|L, C)$, is modeled through a leakage duration simulation using SPN, with the assumption that an ignition source always exists. Given that the concentration is within flammable limits, the ignition probability is related to the leakage scenario with specific parameters. By determining a specific leakage scenario, the corresponding ignition probability can be determined.

In a hydrocarbon leakage scenario, leak rate and duration are two important parameters. While a leak rate can be easily modeled using analytical and empirical methods, the duration of a leak remains challenging to model. The ignition probability increases with the duration of a leak. Many previous works assume this value in their release and dispersion simulations[8, 12]; however, this value needs to be accurately determined, considering its significant influence on the probability assessment of the fire accident. In this step, the leak duration is modeled and analyzed using SPN, due to its ability to perform process modeling and time-dependent probability modeling.

Petri nets, which were developed in the early 1960s by Carl Adam Petri, are widely used in representing the workflow process. A PN is a directed graph, in which the place is used to represent a certain state of the system, and the transition between two places is used to represent the state change from one place to another. To conduct the probability analysis, the traditional Petri net needs to be extended; firing rates of a transition are necessary. The SPN can overcome this limitation by introducing λ as the firing rate associated with transitions [85].

In this step, the initial state is defined as the leakage occurrence, and the final state is defined as the stopped leakage. In reality, the release can be stopped either by the control system or by the exhaustion of inventory. Thus, the release duration is

less than or equal to the time of the depletion of relevant inventory. In the present study, it is recommended to consider the maximum duration of release, to be on the conservative side. Therefore, this effect is analyzed in the case study by considering several leak inspection and maintenance parameters. Two principal factors that contribute to the leakage duration, the time to detect the hydrocarbon gas and the time to determine the leak point, are considered and assumed to follow a probability distribution over time. Accordingly, the probability distribution of the leakage duration can be obtained by measuring the time duration from the initial state to the final state using Monte-Carlo simulation, and then the ignition probability can be determined.

3.2.3 Assessment of flammable vapour cloud probability

This step focuses on hydrocarbon dispersion, which leads to the formation of a flammable cloud. The flammable cloud is the region that has hydrocarbon within flammable limits. The flammable cloud is the reactive area and thus controls the probability of a fire accident. In this study, FLACS is used to model the hydrocarbon release and dispersion consequences. FLACS, which relies on turbulence models based on Reynolds-averaged Navier-Stokes (RANS) equations, is an advanced CFD simulation software specially designed for dispersion, fire and explosion modeling. It has been tested and validated using the field and experimental data in previous studies and has proven to be a reliable tool for modeling gas dispersion [86, 87]. Using a 3-D Cartesian grid, the mass, momentum, turbulent kinetic energy, mass-fraction of fuel and mixture-fraction are solved using a finite volume method in FLACS. To better represent complex geometries on a coarse grid, FLACS uses a distributed porosity concept for small

objects, which need to be represented by a sub-grid [88]. Therefore, sub-grid objects, which may be ignored by other CFD software, can contribute to the simulation results in the FLACS.

The leakage duration with different occurrence probabilities obtained in the previous step is used as a simulation parameter in this step. The vapour cloud caused by the hydrocarbon leakage with a specific leakage duration can be obtained, and therefore, the flammable area can be determined through CFD modeling. As a result, the flammable cloud volume, V_i, over time and the net volume of the simulation area, V_w, are extracted. These two values are used to calculate the probability of the concentration being within the flammable limits, given a hydrocarbon leakage $P(C|L)$. In the current study, the probability of the concentration being within the flammable limits given a hydrocarbon leakage $P(C|L)$ is calculated using V_i/V_w, which is a time-dependent value, with the change of the flammable cloud volume over time, V_i. This ratio accounts for the fact that when the cloud in the entire area is within the flammable limit, the probability of the concentration being within the flammable limits given a hydrocarbon leakage is equal to one, while, when no cloud is within the flammable limit, the probability is equal to zero.

3.2.4 System configuration optimization to minimize fire probability

Given the fire accident probability of a system, a system can be optimized to reduce the fire occurrence probability and therefore, the fire accident risk. In the oil and gas industry, system optimizations such as fire protection system

installation, layout optimization, and leak detection system improvement can be applied according to the specific conditions. The results obtained from the new system are compared to the probability from the original system. The optimal design can then be determined using the proposed approach.

3.3 Case study

In this study, the probability of a fire accident occurring in an FLNG is modeled as a case study using the proposed methodology.

An FLNG is comprised of a life module, central control room, processing unit, hull and ship systems, a turret and fluid transmission control rotary joint and mooring and riser systems. Among them, the processing unit is considered to be the most hazardous area [41]. In this study, the proposed approach is applied to assess the probability of fire occurrence in the processing unit of an FLNG.

3.3.1 Assessment of leakage probability

Considering the essential conditions of a fire existing in the processing unit of an FLNG, the hydrocarbon leakage is analyzed in this section using BN. Table 3-1 shows the probability of each basic node according to OREDA [89] and the studies by Wang et al. and Yang et al. [90, 91]. Given the failure rate of the component in OREDA, the failure probability is calculated by assuming that every component follows a constant failure rate within 15 years. Also, probabilities of other nodes are obtained directly from the studies by Wang et al. and Yang et al.. The relationships among events are represented in the form of CPTs, which are determined based on expert knowledge of the subject (Experts in this study include Dr. Faisal Khan, who is the Canada Research Chair (Tier I) of Offshore Safety and Risk Engineering, Dr. Mohammed Taleb-Berrouane, who works in safety and risk

area for many years). In this study, BNs are developed using Hugin Software version 8.6 (http://www.hugin.com) [92]. Detailed BNs are presented in Figures 3-2 to 3-8.

Table 3-1 Probability of basic nodes [89-91]

Basic Node	State	Probability
Process equipment leakage		
Failure of LSV	yes	0.0032
Failure of FCV	yes	0.0885
Excessive flow	yes	0.0064
High pressure	yes	0.0060
Failure of the pressure relief valve	yes	0.1088
Failure of PCV	yes	0.0885
Junction leakage		
Faulty installation	yes	0.0045
Corrosion		
Condition induced factors	yes	0.01
Corrosive fluid	yes	0.0149
High surface conductivity	yes	0.1
Coating damaged	yes	0.0077
Welding defects	yes	0.01
Aging	yes	0.0024
Poor corrosion management	yes	0.02
External damage		
External weather	yes	0.002
Object collision	yes	0.0001
Damage of insulation coating	yes	0.062
Delayed maintenance	yes	0.0017
Equipment displacement		
Loose junction bolts	yes	0.1263
Seismic activity	yes	0.02
Excessive vibration	yes	0.1383

For the probability assessment of a hydrocarbon leakage, the OOBN is applied in this study, with its ability to divide the system into sub-networks. Figures 3-2 presents the overall OOBN framework of the hydrocarbon leakage in the studied

area. A leak can be expected to occur in the process equipment, at the junction or on the pipeline, and any one of those scenarios has the potential to cause a fire accident. In the network, this fact is indicated by the arrows from the nodes of these scenarios to the node of hydrocarbon leakage. Detailed analyses of these three scenarios are demonstrated as sub-networks in Figures 3-3, 3-4, and 3-5. Among various influencing factors, some events can cause more than one failure scenario to occur, which is known as common cause failure (CCF). In the current study, corrosion, equipment displacement, and external damage are considered and analyzed as CCF, contributing to each leakage scenario. The nodes with a dotted border represent the CCFs that are considered in each scenario. In addition, arrows from CCF nodes to each scenario indicate their causal relationship. To reduce the complexity of the whole network, detailed CCF analysis is represented as individual sub-networks, which are shown in Figures 3-6, 3-7, and 3-8.

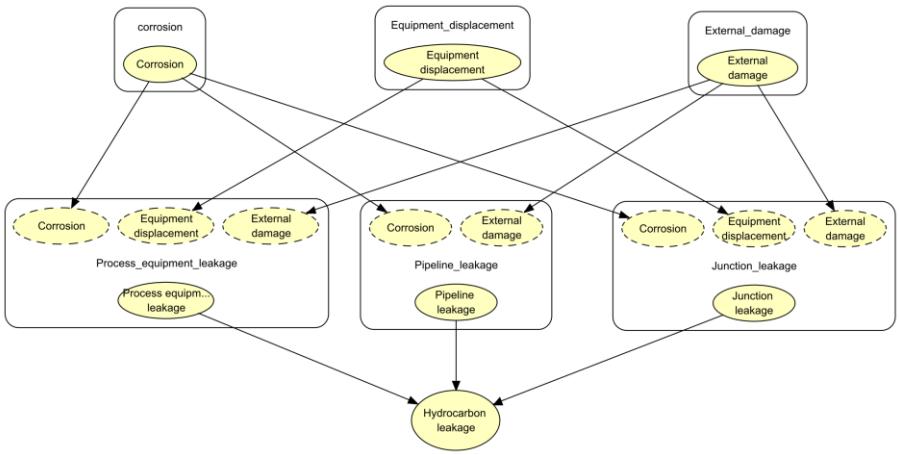

Figure 3-2 The overall OOBN of the hydrocarbon leakage in the studied area.

Figure 3-3 depicts the sub-network of the process equipment leakage in the studied area. In this model, overpressure inside the equipment as well as three CCFs,

including corrosion, equipment displacement, and external damage, are considered to be the critical influencing factors, and detailed analysis of CCFs are presented subsequently. In process equipment, overpressure can be caused by uncontrolled liquid flow or high-pressure gas. Uncontrolled flow occurs when the control valve fails and excessive flow occurs, and both LSV and FCV may cause the failure of the flow control. In addition, extremely high pressure of the gas is caused by the simultaneous occurrence of high pressure and pressure control failure, where the failure of the PCV and the pressure relief valve are two main issues leading to the pressure control failure. Figure 3-4 and Figure 3-5 outline the sub-networks of the pipeline leakage and the junction leakage. As shown in the network, two CCFs, including external damage and corrosion, are considered in the pipeline leakage in this study. For the junction leakage, as well as the three CCFs, faulty installation is considered to be another factor causing the failure.

To connect each sub-network to the overall OOBN, three leakage scenarios in the sub-networks, which are marked by a gray solid border, are set as output nodes affecting the overall OOBN of the hydrocarbon leakage.

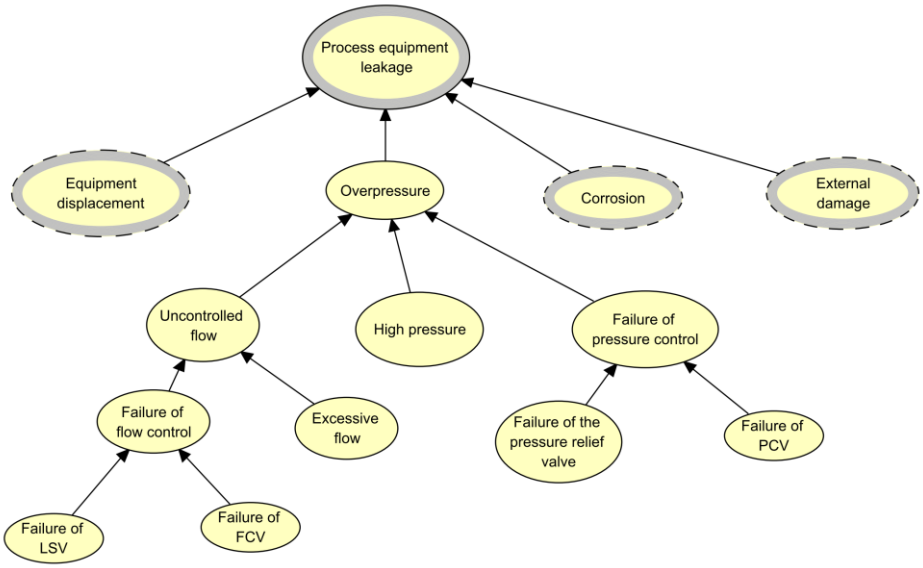

Figure 3-3 OOBN sub-network of the process equipment leakage.

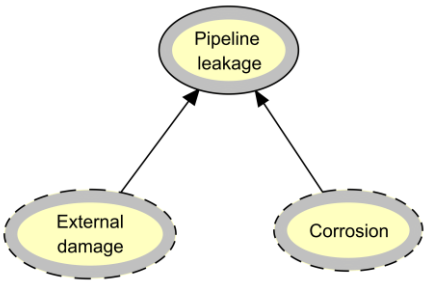

Figure 3-4 OOBN sub-network of the pipeline leakage

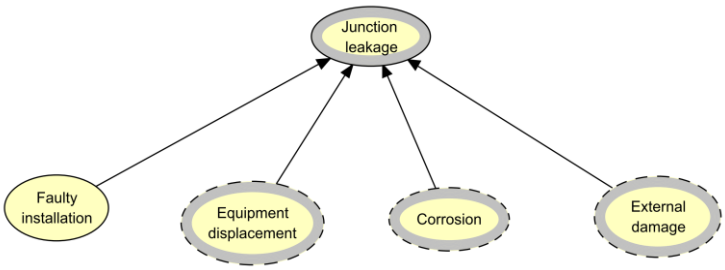

Figure 3-5 OOBN sub-network of the junction leakage

As CCFs, corrosion, equipment displacement and external damage are modeled and demonstrated separately in the current study, as shown in Figure 3-6 to Figure 3-8. In the corrosion sub-network, three principal causal factors, including fluid factors, surface factors, and asset integrity factors, are considered, as shown in Figure 3-6. Most of the principal causal factors of corrosion are listed and analyzed in this section. In the sub-network of external damage, the combination of third-party damage and poor maintenance practices contributes to the external damage of each leakage scenario. In addition, equipment displacement is another CCF contributing to each leakage scenario, as shown in Figure 3-8. Similarly, gray solid borders are marked as output nodes contributing to higher level nodes.

Given the networks shown in Figure 3-2 to Figure 3-8 and the probability of each node, shown in Table 3-1, the results of the OOBN model can be calculated using Hugin Software. The results of CCFs, each leakage scenario, and hydrocarbon leakage are presented in Table 3-2. According to the simulation result, the probability of the hydrocarbon leakage in the studied area, P_L, is estimated to be 0.1101. In addition, among three leakage scenarios, the probability of pipeline leakage is lowest while the probability of junction leakage is highest. Since any of three scenarios' occurrence can cause a hydrocarbon leakage, it can be concluded from the results that junction leakage contributes the most to the hydrocarbon leakage, while process equipment contributes the least.

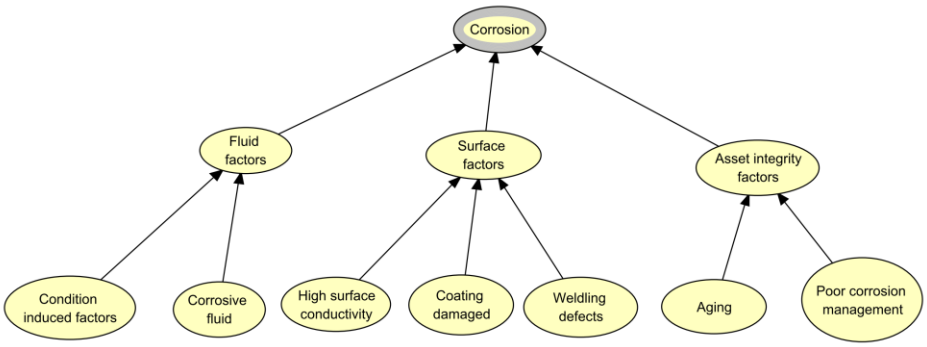

Figure 3-6 OOBN sub-network of the corrosion

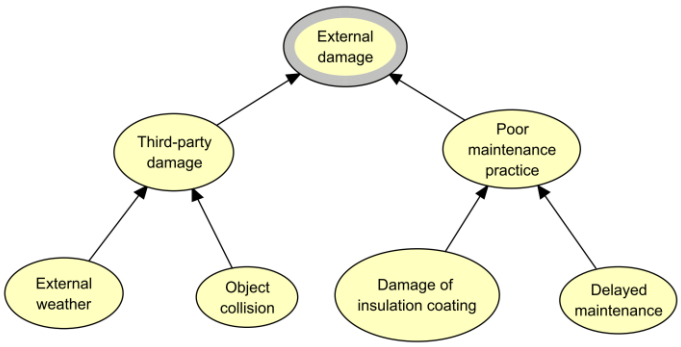

Figure 3-7 OOBN sub-network of the external damage

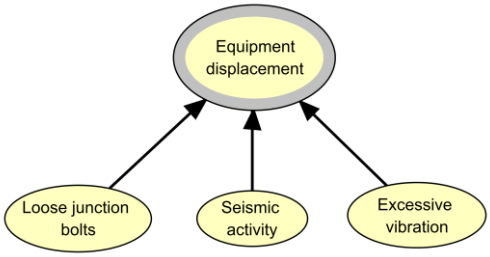

Figure 3-8 OOBN sub-network of the equipment displacement

Table 3-2 Results of the BN

Parameter	Probability
Process equipment leakage	0.0468
Pipeline leakage	0.0348
Junction leakage	0.059
Corrosion	0.0644
External damage	0.0183
Equipment displacement	0.0584
Hydrocarbon leakage	0.1101

3.3.2 Assessment of ignition probability

In this step, the SPN model is used to model the leakage control and extract the leakage duration for release modeling. Figure 3-9 presents the SPN model of the leakage duration, which is developed using GRIF software. As described in the methodology section, the leakage is assumed to have stopped before the inventory depletion, and the duration is analyzed by considering several leak inspection and maintenance parameters in the case study. After leakage occurs, the release detector system in the FLNG can detect the fuel vapour within a period of time. The total response time of a detector system depends not only on the time taken for the dispersed gas to reach the detector, but also the time for a sensor to respond and the response time of the processing signal [93]. In this study, the total response

time of the gas detector system is assumed to follow a lognormal distribution with an average time of 10 seconds and an error factor of 3. To entirely control the hydrocarbon leakage, the leak point needs to be determined for further application of the safety measure. It is assumed that the duration of each diagnosis of leak point identification follows a lognormal distribution with an average time of 20 seconds and an error factor of 3. In addition, the probability of each diagnosis can successfully identify the leak point, which is assumed to be 0.9. If the previous diagnosis fails to determine the leak point, another diagnosis is needed. Once the leak point is determined, some actions such as shutting down the sub-system would be applied to stop the leakage. The lognormal distribution with an average time of 20 seconds and an error factor of 3 is used to model the leakage control after successful leak point identification in this study.

Table 3-3 shows the parameters in the PN and their values.

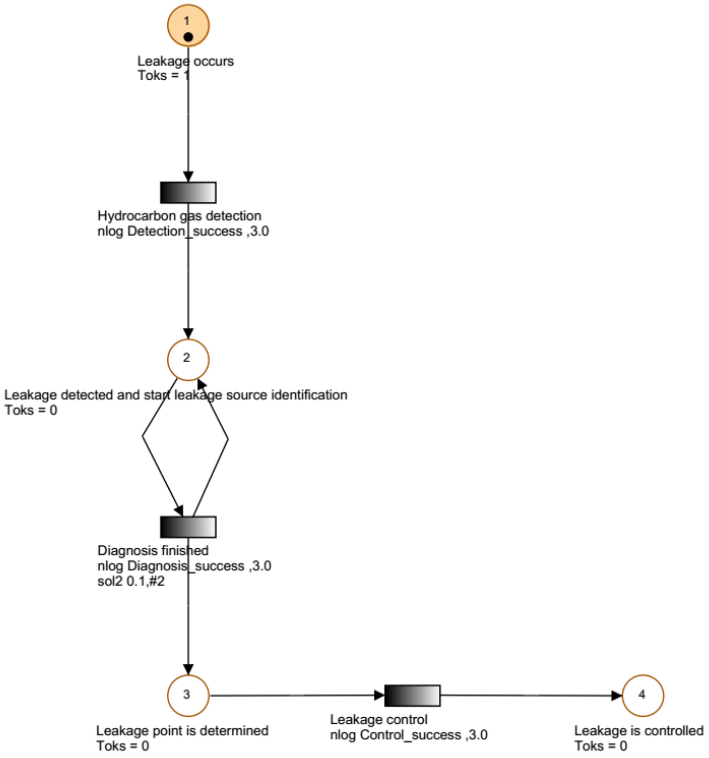

Figure 3-9 SPN model of the hydrocarbon leakage duration

Table 3-3 Parameters of the SPN model

Parameter	Values		
	Distribution	Average	Error factor
Detection success	Lognormal	10	3
Diagnosis success	Lognormal	20	3
Control success	Lognormal	20	3

Leakage duration can be obtained through applying Monte Carlo simulation with GRIF software. In this study, the total simulation time is 150 seconds, with steps of 0.036 seconds. The cumulative probability distribution (CDF) of the hydrocarbon leakage duration is presented in Figure 3-10. Given a specific leak duration, the maximum probability of the fuel being ignited can be determined. With an assumption that an ignition source always exists, the ignition probability

given a hydrocarbon leakage as well as the concentration being within the flammable limit, $P(I|L, C)$, is low for a lower leakage duration, while the ignition probability is high for a higher leakage duration.

As shown in Figure 3-10, the results demonstrate that the leakage duration typically varies between 20 and 120 seconds. The probability of a leakage duration of less than 50 seconds is 55 percent, and after 100 seconds, the probability is 0.95, which is high enough to conclude that most hydrocarbon leakages can be controlled within this time. Probability growth rate, which can be measured by the slope of the curve, increases from 20 seconds and peaks at approximately 40 to 60 seconds, and then decreases until the probability reaches 1.

Considering the leakage duration probability and the growth rate of probability obtained from the result, leakage durations of 50 seconds, 75 seconds and 100 seconds are selected and used as examples in the fuel release and dispersion simulation. The probabilities corresponding to these leakage durations are 0.55, 0.85, and 0.95, respectively.

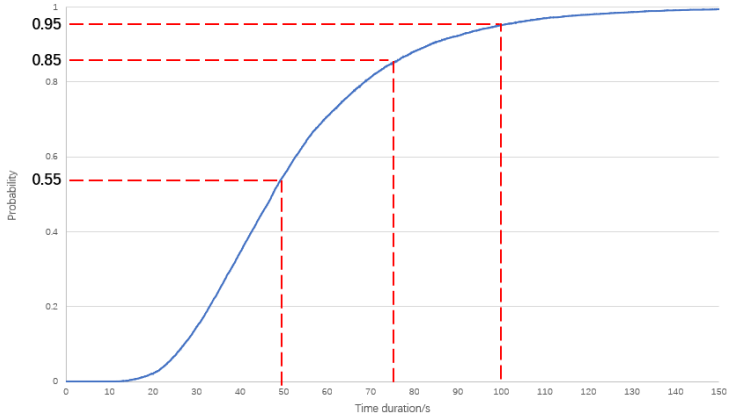

Figure 3-10 Probability of the leakage duration obtained in SPN.

3.3.3 Assessment of flammable vapour cloud probability

In this study, FLACS is used to simulate the result of the hydrocarbon release and dispersion, considering a specific leak rate and leak duration. The geometry of the target structure, as shown in Figure 3-11, is constructed using Auto CAD software. The detailed information is extracted from a typical FLNG processing facility. Considering the high risk, the fuel release and dispersion simulation in this study only focuses on the processing unit of the FLNG, as shown in Figure 3-12. Walls with holes around the processing unit are used to model the confinement around the studied area.

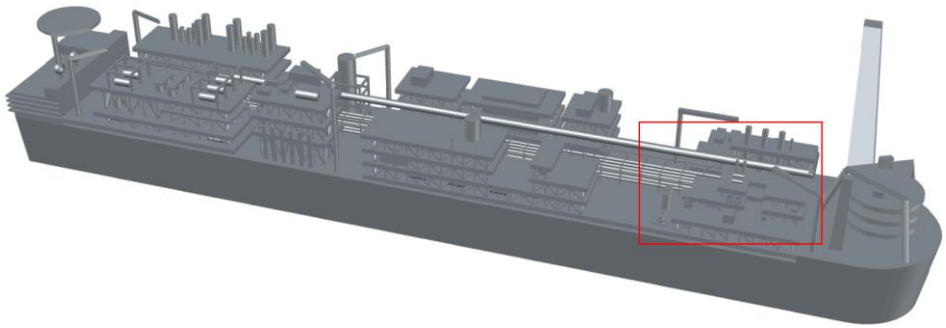

Figure 3-11 3D model of the FLNG structure highlighting the processing unit.

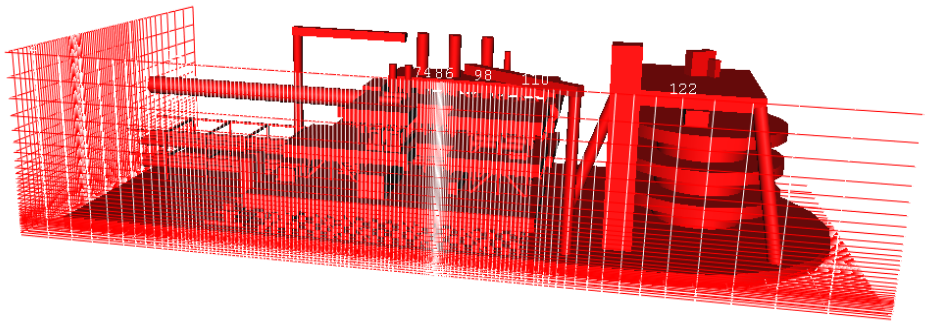

Figure 3-12 The simulation area and the mesh used in the numerical simulation

Considering the dilution process of the remaining fuel cloud after the leakage stops, the computation domain is set wide enough to cover the whole area that the vapour can reach. There are 324324 grid cells in total used in the computational domain. The mesh around the leak point is refined to prevent it from strong dilution [88], while the mesh outside the processing unit is stretched to balance the calculation time and the accuracy of the result, as shown in Figure 3-12. To guarantee that the simulation result is independent of the mesh size, a finer mesh as well as a coarse mesh have been used in sensitivity studies. In this study, a coarse mesh with 258048 cells and a fine mesh with 360960 cells are selected. Figure 3-13 shows good correspondence between the simulation results of flammable cloud volume over time with different meshes, which proves that the current mesh is reliable for simulation.

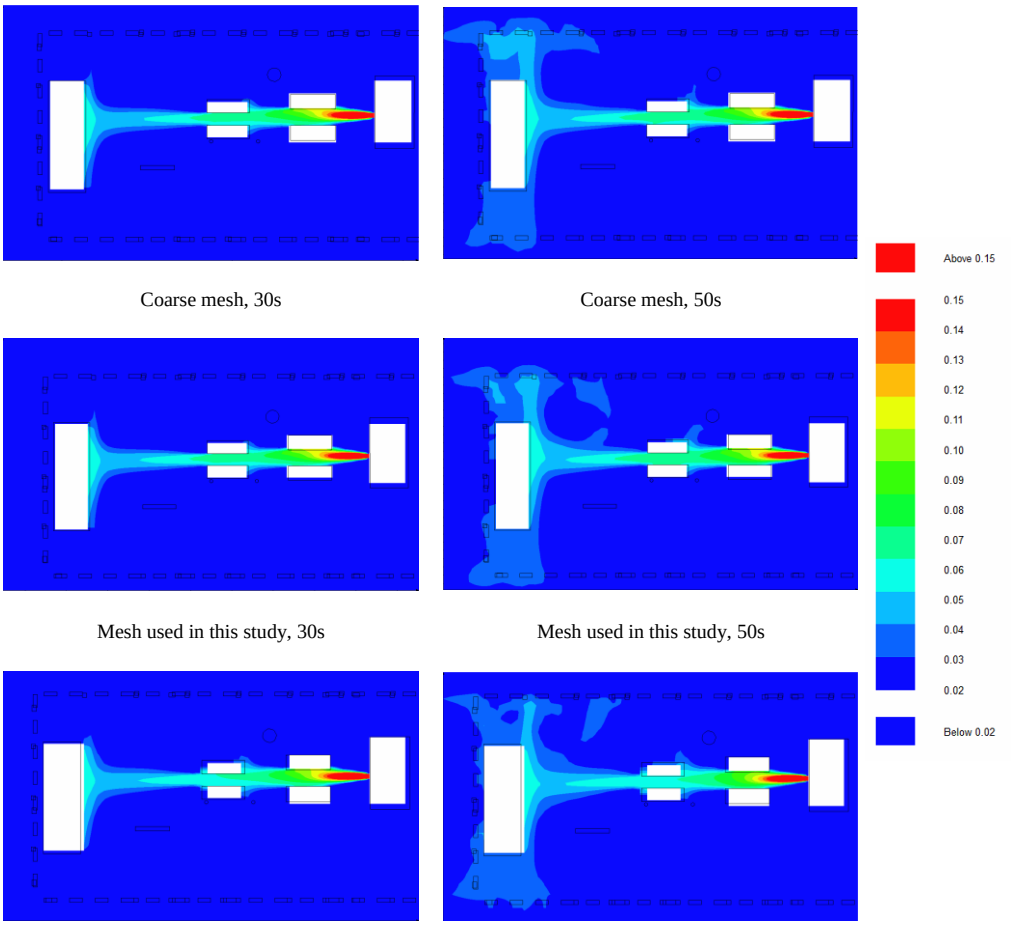

Coarse mesh, 30s | Coarse mesh, 50s

Mesh used in this study, 30s | Mesh used in this study, 50s

Fine mesh, 30s | Fine mesh, 50s

Figure 3-13 Mesh sensitivity analysis result

In the current study, the ambient pressure is set to be the atmospheric pressure, and the ambient temperature is set to be 20 degrees Celsius. The wind's influence on fuel dispersion is also considered in this study. The speed of the wind is assumed to be 2m/s and the wind direction is assumed to be from +X direction. Considering the wind speed and the topography in the sea, the stability class is defined to be D, the ground roughness condition is assumed to be rural, and the ground roughness is defined to be 0.2, according to the works by Ekerold and Piblada et al. [11, 94]. A hydrocarbon leakage with a leak rate of 4kg/s and an outlet area of $0.02\mathrm{m}^2$

occurs in the processing unit. The leakage direction is set from +X direction. The leakage starts at 20s after a steady wind field forms. As mentioned in the previous section, different leakage durations of 50 seconds, 75 seconds and 100 seconds are selected in this section.

Figure 3-14 shows an example of the simulation result of the hydrocarbon release and dispersion. The areas in different colours in this figure represent the fuel concentration in volumes from 0.05 to 0.15, which is defined to be the approximate flammable limit of the LNG in this section, to demonstrate the flammable cloud area after hydrocarbon leakage.

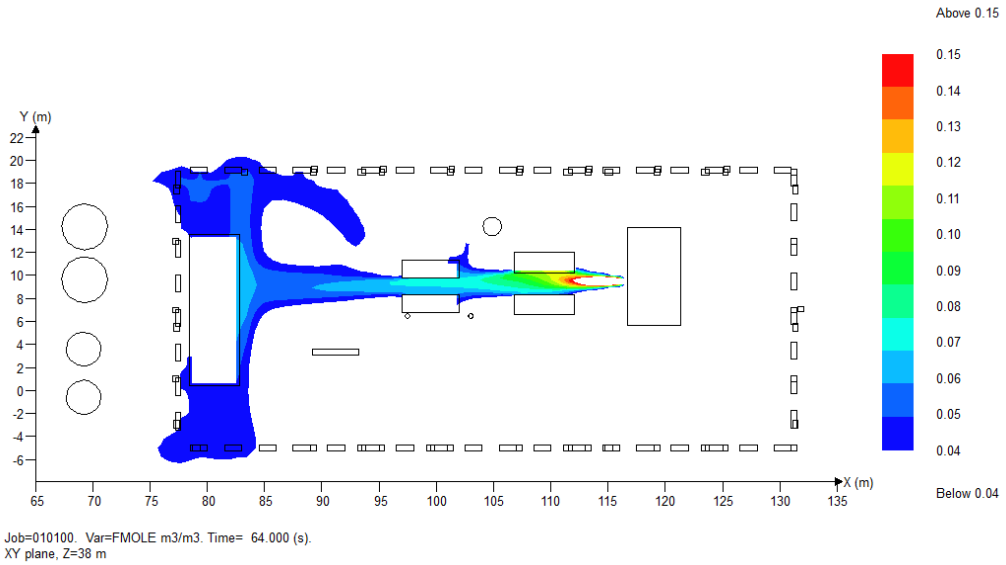

Figure 3-14 Illustration of the flammable cloud caused by the hydrocarbon leakage

To capture the volume of the flammable cloud, a gas monitor region, with a size of 60m × 61m × 26.5m, is defined around the studied area in the current study.

The 3D illustration of the gas monitor region is demonstrated in Figure 3-15. The total net area inside the gas monitor region, V_w, is $8,8597\ m^3$. The volume of the fuel cloud at the flammable limit, calculated by the equivalence ratio (ER) between the lower flammable limit (LFL) and upper flammable limit (UFL), V_i, for different leakage durations is shown in Figure 3-16. The flammable cloud volume increases rapidly after the leakage starts and then stabilizes at around $1,480\ m^3$. As the leakage continues, the volume of the flammable cloud continues to rise to approximately 46 seconds. This can be caused by the dilution process under the influence of the wind and the confinement of the studied area. The volume peaks at the time after the leakage is controlled, and then it returns to zero gradually under the influence of dilution. For hydrocarbon leaks with different leakage durations, the maximum volume of flammable cloud then reach and the time for the cloud to dilute back to a normal level varies widely. As the results show, longer leakage duration results in longer dilution time as well as greater flammable volumes. Both of these variables can lead to a much higher fire risk.

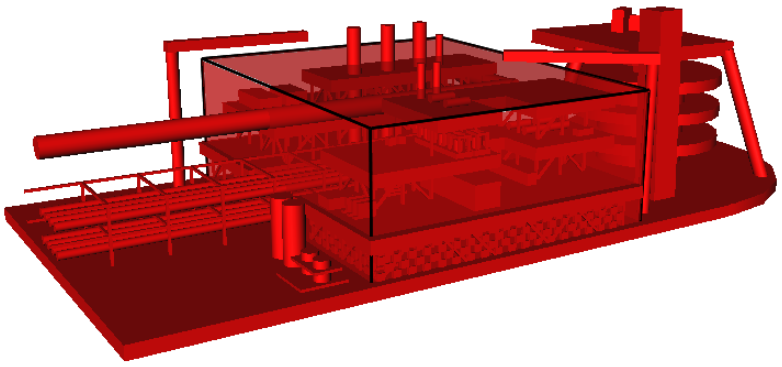

Figure 3-15 3D illustration of the gas monitor region in the FLNG

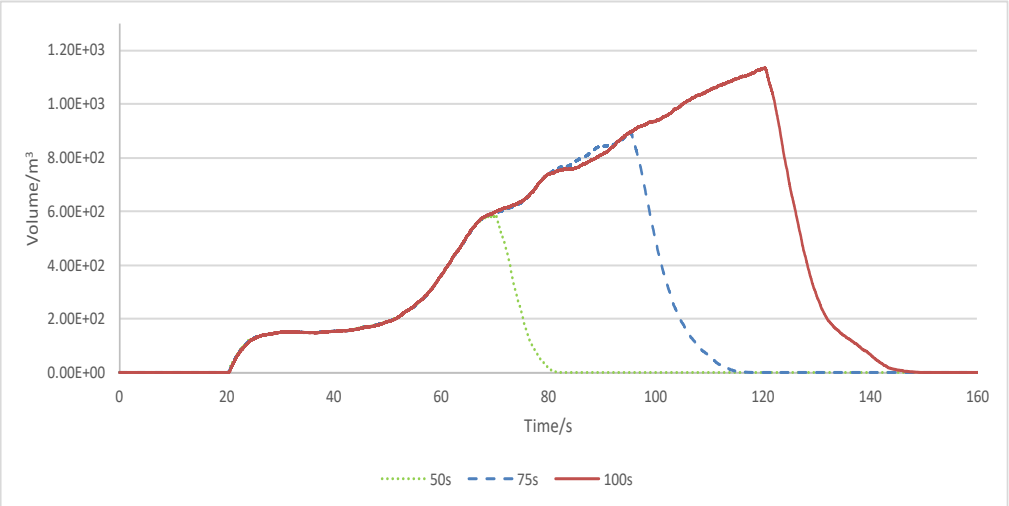

Figure 3-16 The volume of the flammable cloud with different leak durations obtained by the numerical simulation

3.3.4 Probability assessment of a fire accident using an integrated method

The probability of a fire accident in the processing unit of an FLNG is calculated according to Equation (3.6) in the proposed methodology. Equation (3.6) can be further expanded to Equation (3.8) assuming that the probability of the concentration being within flammable limits given a leakage is represented by the flammable cloud volume and the net volume of the studied area.

$$P(f) = P(I, L, C) = P(L) \times P(C|L) \times P(I|L, C) = P(L) \times \frac{V_i}{V_w} \times P(I|L, C) \quad (3.8)$$

The results obtained by applying Equation (3.8) are shown in Figure 3-17. In summary, the results show that the fire probability, given a specific leak duration and leak rate, varies greatly over time. With different leakage durations, the probability of a fire accident differs greatly. It can also be concluded that a high leakage duration leads to a significantly higher probability of fire than low leakage duration at a given time as well as a longer fire risk period. Therefore, trying to

decrease the leakage duration can be a very powerful approach to reduce the fire probability

In addition, applying safety measures at different times may have different effects. With the help of this model, the best time for workers to apply safety measures after hydrocarbon leakage can be studied. The result demonstrates the necessity to identify the temporal dependency of the fire probability. Therefore, it is essential to assess the change of the fire probability over time and identify the dangerous period. System optimization can be applied based on the results of the assessment to reduce the fire probability in the event of a hydrocarbon leakage.

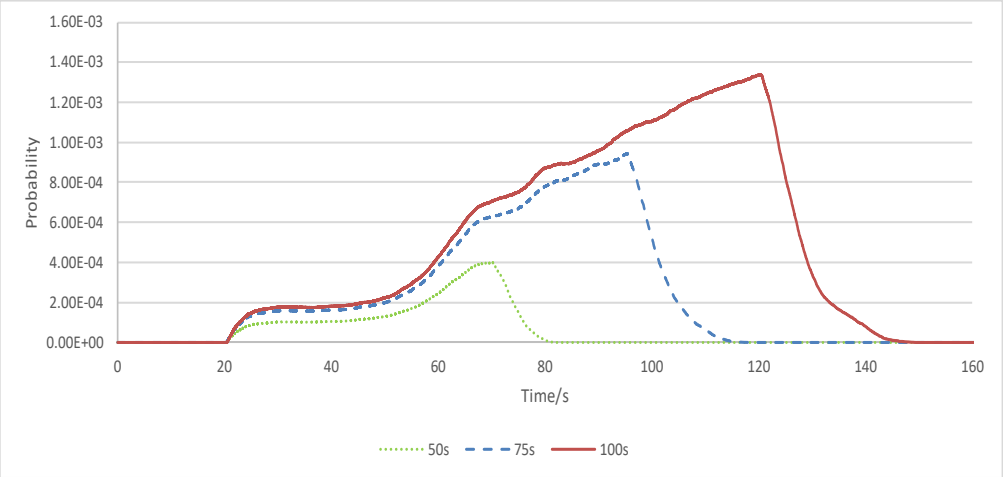

Figure 3-17 The probability of a fire in the processing unit of an FLNG given a specific leak rate and duration

3.3.5 System configuration optimization to minimize fire probability

Once the fire probability profile is obtained, system optimization can be performed if the probability of fire is unacceptably high. Configuration and layout optimization provide a preventive approach and can inherently improve safety in terms of fire accidents [41]. In this case study, the system configuration optimization is applied as an example of system optimization to reduce the

probability of fire accidents.

Dispersion and ignition are sensitive to the confinement and congestion levels. Confinement is defined by the presence of physical surfaces which can limit the expansion of the flame [95]. Under the same leak conditions, systems with different confinement and congestion levels have different risks of fire accidents. Previous experiments show that confinement is needed for flame acceleration, which can cause a further explosion [95].

In this study, four simplified configuration models considering different confinement and congestion levels are tested, as shown in Figure 3-18. In terms of confinement, the worst case of a hydrocarbon leakage is that the system is completely confined, with solid walls around the leak area, as shown in configuration 1 of Figure 3-18. In this case, leaking gas cannot be ventilated from the system. Thus, it is possible that the flammable cloud continues growing over time even if the leakage stops. In configuration 2, the walls around the structure are removed, and the system is completely open to the air. This configuration model is ideal for the chemical industry; however, this model cannot be practical for some facilities such as the FLNG where space is limited. Configurations 1 and 2 are modeled in this study as benchmarks for current configuration and optimized configuration. Configuration 3 is the model that was formerly used as a case study. In this model, a semi-confined area is generated by the blocks around the system, which is used to simulate the complex layout of equipment and pipelines inside the FLNG processing unit. In this step, configuration model 4 is proposed to optimize the configuration used in the previous steps to decrease the probability of fire accidents. According to the definition of confinement mentioned above,

configuration 4 has the same confinement as configuration 3, but with a different layout. This layout accounts for the optimization of the configuration without reducing the number and size of components inside the unit, when the confinement level caused by the existing equipment is not decreased. However, the equipment in configuration 4 is not placed as decentralized as that in the layout in configuration 3. As shown in configuration 4, equipment in the unit is properly grouped together to some extent, which can provide leaking fuel a more reasonable escape space than in configuration 3.

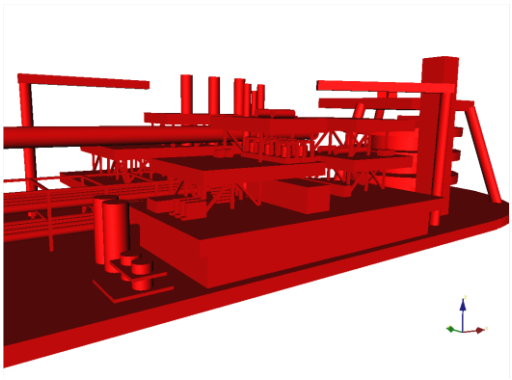

Configuration 1: Completely confined

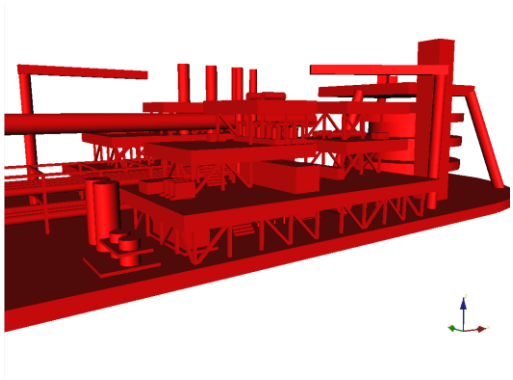

Configuration 2: Open to the air

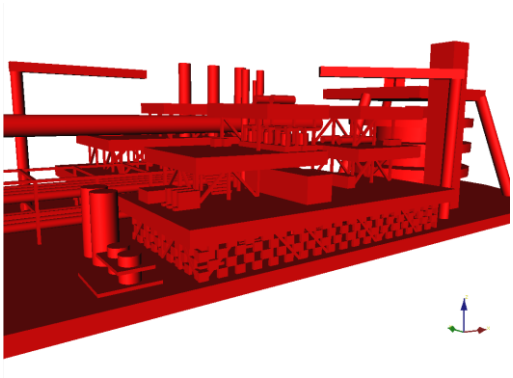

Configuration 3: Semi-confined A

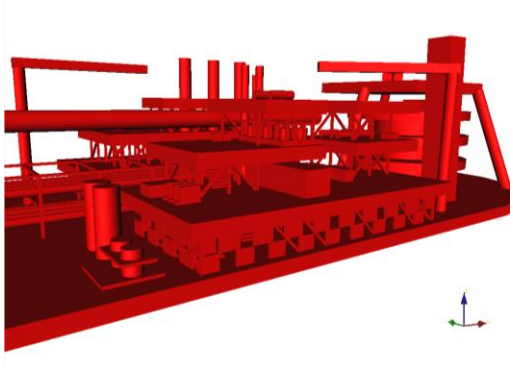

Configuration 4: Semi-confined B

Figure 3-18 Models with different configurations

In this study, the analysis has identified configuration 1 to be the worst case, with

100s hydrocarbon leakage being simulated to demonstrate the influence of the high confinement. As shown in Figure 3-19, the volume of the flammable cloud increases quickly once the leak starts. Unlike the result shown in configuration 3, where the volume begins to decrease after the leak is stopped, the flammable volume in the system with configuration 1 continues to increase, even if the leak stops under the influence of the solid walls around the leak area and the dispersion process of the fuel. At approximately 280 seconds, the volume stops increasing and is maintained at a constant level, which is $6,370\ \mathrm{m}^3$, till the end of the simulation. Regarding the duration of the fire risk, which can be roughly estimated by the duration of the existence of the flammable cloud, the totally confined system prevents the ventilation of leaking gas, resulting in a long-term existence of the flammable cloud, and thus a long-term risk of fire. Furthermore, the comparison between the system with configuration 1 (the worst case) and configuration 3 shows that in the worst case, the volume of the flammable cloud can be nearly ten times that in configuration 3,which is the normal case. This fact further increases the fire risk in configuration 1.

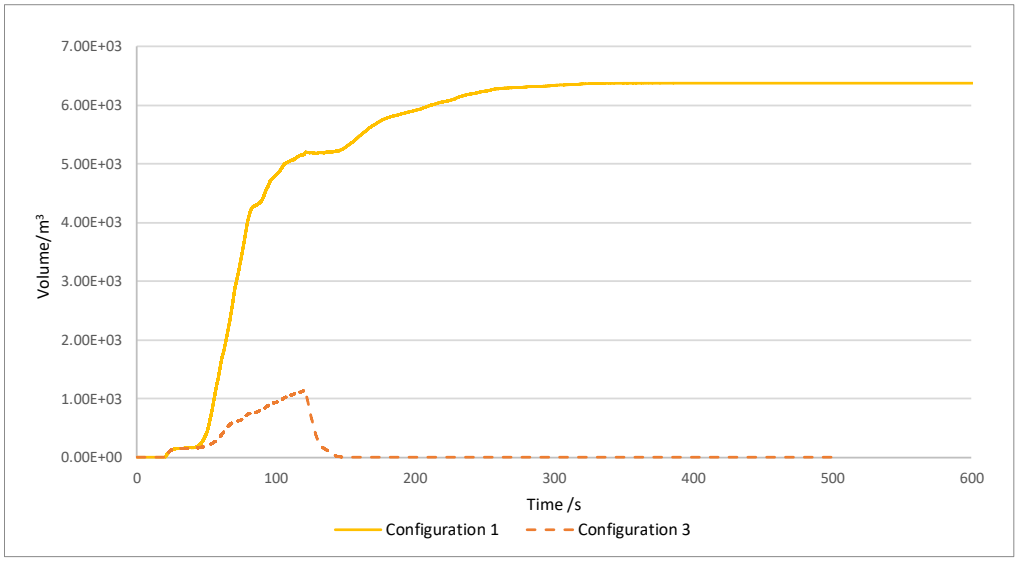

Figure 3-19 The flammable cloud volume of systems with configurations 1 and 3

To reduce the fire probability, an optimized configuration (configuration 4) is proposed in this study. Simulations of different configurations are conducted under the same leakage conditions to demonstrate a reduction in fire probability by applying an optimized configuration. As shown in Figure 3-20, the leakage occurs in the system with configuration 4, creating a much lower flammable volume compared with configuration 3. Without reducing the number and size of components inside the unit, the new design can greatly improve the ventilation of leaking gas. In addition, in terms of flammable cloud volume and the duration of the fire risk, the system with configuration 4 has almost the same value as the system applying configuration 2, which is an ideal configuration for the chemical industry, as described above. It can be concluded that through configuration optimization, it is possible to decrease the flammable cloud volume to the greatest extent. Calculating the fire probability using the simulation result, Figure 3-21 shows that with the application of configuration 4, the fire probability can be reduced to nearly one-tenth of the value caused by configuration 3. Also, due to the new design, the leaking gas is more easily ventilated from the system, reducing the fire risk duration by 20 seconds, which provides workers more time to take further safety measures. Regarding the fire probability and its risk duration, it can be concluded that the configuration in this case study is optimized by applying configuration 4. The improvement in fire safety caused by the difference between the configurations indicates the importance of a sufficient escape space for the leaked gas.

This case study demonstrates that the proposed methodology is a robust and practical model for analyzing the fire probability in a congested and complex processing area and is also a reliable tool for optimizing systems in terms of fire risk.

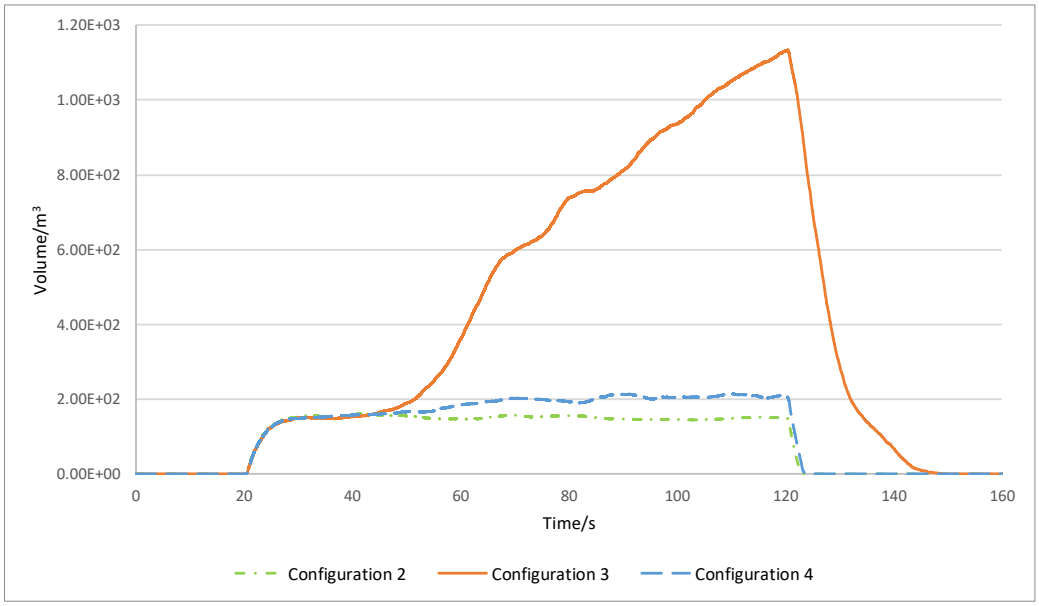

Figure 3-20 The flammable cloud volume of systems with configurations 2, 3, and 4

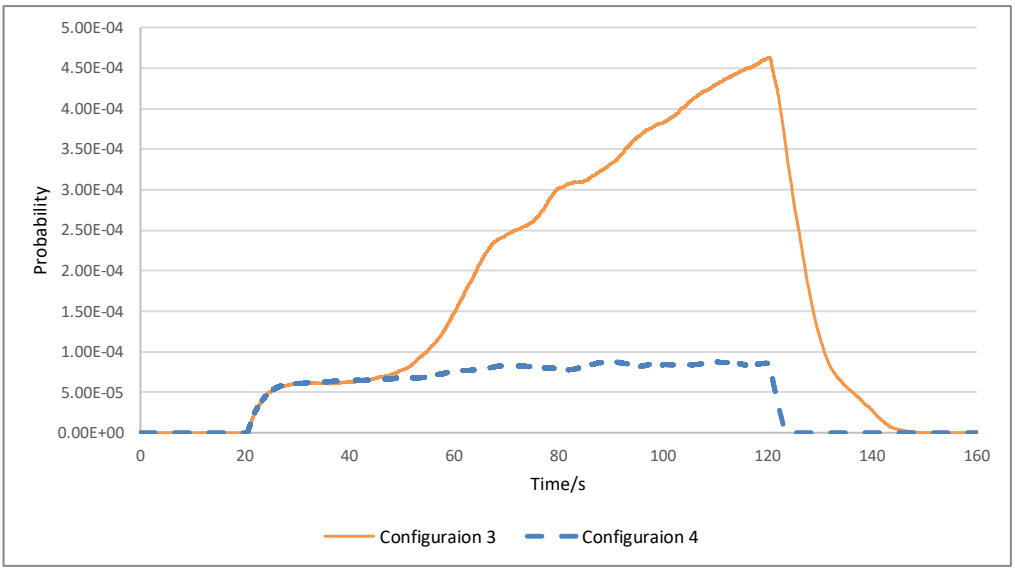

Figure 3-21 The fire probability caused by configurations 3 and 4

3.4 Conclusion

Considering the temporal dependency of the fire accident scenario, a robust and practical model to analyze the fire probability in a congested and complex processing area is presented in this study, combining the BN, the SPN, and the CFD models. In the proposed methodology, the BN is applied to analyze the leakage source and calculate the probability of hydrocarbon leakage. The SPN model, coupled with Monte-Carlo simulation, is used to analyze the fuel leakage duration, which determines the ignition probability. The simulation result of SPN is also an essential parameter used in the numerical simulation. FLACS is used to conduct the fuel release and dispersion modeling, which determine the probability of a flammable vapour cloud.

Applying the proposed approach to a case study of an FLNG, the probability of a fire accident in the processing unit is analyzed. According to the results, as the volume of the flammable cloud changes, the fire probability changes accordingly over time. With a different leakage duration, the probability of a fire accident as well as fire risk duration differs greatly. It can be concluded that a time-dependent fire probability analysis model is necessary. In addition, with the help of this model, it is possible to determine when workers should apply safety measures after a hydrocarbon leak.

Through applying the proposed approach, a system optimization for fire accident probability can be conducted if the probability of fire is unacceptably high. In this study, a configuration optimization is applied as an example. Through measuring

the maximum fire probability and the fire risk duration, systems with different confinement and congestion levels are analyzed and an optimized configuration is proposed. The results show the importance of a sufficient escape space for the leaked gas. A system configuration is necessary when the probability of fire is unacceptably high.

Possible improvements to the current work can be considered, including (1) implementing uncertainty propagation in the source data while simulating the hydrocarbon leakage probability; (2) consideration of interdependence of the parameters in modelling leakage probability; (3) analyzing the impact of safety strategies in preventing and controlling the leakage and fire accidents; (4) consideration of loss modelling in analyzing the leakage and fire accident scenarios and also the effectiveness of safety strategies.

Acknowledgements
The authors thankfully acknowledge the financial support provided by the Natural Science and Engineering Council of Canada and the Canada Research Chair (CRC) Tier I Program on offshore safety and risk engineering

Chapter 4. Could pool fire alone cause a domino effect?

Co-authorship statement

A version of this manuscript has been submitted for publication in the Journal of Reliability Engineering & System Safety on September 2019. Ruochen Yang is the primary author of this manuscript, along with co-authors Faisal Khan, Eugenio Turco Neto and Jie Ji. Ruochen Yang conducted this study under the direct supervision of Faisal Khan. The framework concept was proposed by co-author Faisal Khan, and Ruochen Yang developed the model and conducted the analysis under the guidance of author Faisal Khan. Faisal Khan helped test the model results and verified the developed model. Eugenio Turco Neto helped with the CFD modeling and reviewed the simulation result. Author Jie Ji helped conduct the application. All co-authors reviewed and provided feedback on the manuscript. Ruochen Yang revised the manuscript based on the co-authors' feedback.

Abstract

A chain of accidents, also known as the domino effect, is responsible for a number of severe accidents in the chemical and process industries. As frequent and dangerous accidents occur in the chemical industry, the pool fire is often blamed as one of the primary accidents triggering a domino event. The present study is

devoted to analyzing whether the pool fire alone can cause a domino event in the current industry. Two models, including a solid flame model and numerical model, are applied to simulate the escalation vector caused by a pool fire, while the escalation probability of a domino effect is calculated using a probit model. This study collectively explores the potential factors that can cause a domino effect and determine credible accident scenarios. In addition, the case studies based on real accidents are conducted using the developed models to explore the possibility that pool fires cause a domino effect in the current industry.

4.1 Introduction

A chain of accidents, also known as the domino effect, is responsible for a number of severe accidents in the chemical and process industries [21-23]. Such accident scenarios are very much more likely to cause huge damage to people, assets, and the environment than stand-alone accidents. Also, previous studies indicate that the frequency of the domino effect has increased in the chemical and process industries in recent decades [24, 25]. Disasters caused by the domino effect such as the BP Deepwater Horizon explosion[20], Buncefield oil depot fire[4], Puerto Rico's CAPECO explosion and fire accident [5], and the Jaipur fire accident [26] have demonstrated the domino effect's huge damage to society, which urgently claims researchers' attention to this area.

The term "domino effect" is used to describe a chain of accidents in which a primary accident escalates into higher-order accidents [27].As this type of frequent and dangerous accident occurs in the chemical industry, the pool fire is often blamed as one of the primary accidents triggering a domino event [27-32]. According to the study by Reniers et al. [32], the pool fire accounts for 44 percent of all accident scenarios that escalate into a domino effect. A pool fire is defined as a turbulent diffusion fire that occurs in a horizontal pool of flammable liquid fuel, such as liquefied natural gas (LNG), gasoline, etc. [6, 28]. This accident scenario usually occurs when the liquid fuel pool is ignited followed by the liquid fuel's leakage, or the tank fire occurs in a fuel tank after it is damaged by other

accidents such as a vapour cloud explosion (VCE). A pool fire's effect on adjacent equipment or human beings depends on many factors, including fuel properties, pool size, the distance between the fire and target equipment, and meteorological conditions. Under different conditions, the possibility that a pool fire will cause a domino event can vary.

Several previous studies have been conducted on the domino effect caused by pool fires. In the study by Jujuly et al., a computational fluid dynamics (CFD) model is used to simulate an LNG pool fire and analyze its effect on the adjacent equipment. In this study, the wind speed is found to have a significant effect on the pool fire and its possibility of being causing a domino effect [28]. Khan and Abbasi conducted a series of studies on the domino effect, in which the pool fire is believed to be one of the principal accident scenarios that can escalate into a domino effect [24, 25, 33-35]. In a study by Khan and Abbasi, two failure modes, failure of the nearby equipment due to high-pressure buildup and equipment rupture due to material failure are considered to be the main failure modes of a vessel exposed to fire. A series of analytical formulas are derived in their study to calculate the escalation probability of a domino effect in the case of fire accidents [25].The research by Landucci et al. mainly focuses on the damage probability of equipment in domino events triggered by the fire. A simplified model was proposed to estimate the vessel time to failure (ttf) in the case of thermal radiation [30]. In addition, the studies by Cozzani et al. proposed a series of probit models

to analyze the escalation probability of a domino effect caused by various accident scenarios. The proposed probit models serve as simplified and practical ways for the probabilistic assessment of the domino effect [21, 31]. In several studies by Khakzad et al., the propagation sequence of the domino effect is analyzed with the help of a dynamic Bayesian network (DBN) and the probit method proposed by Cozzani et al.. The time-dependent feature of the domino effect is also considered and explored in these studies [27, 29, 36].

In the previous studies on the domino effect mentioned above, the pool fire is usually studied as one of the main causes of the domino effect. However, the domino effect is a phenomenon that can be caused by complex factors and their relationships, and whether the pool fire alone can cause a domino effect need to be identified. The present study is devoted to analyzing whether the pool fire alone can cause a domino effect in the current industry. The escalation vector leading to a domino effect is determined using both an analytical method and numerical method, while the escalation probability of a domino effect is calculated using a probit model based on the value of the escalation vector obtained in the last step. The conditions under which a pool fire can cause a domino effect are determined using the developed model. To collectively analyze the pool fire and its possibility of escalating into a domino event, several influencing factors are considered and explored in this study. Two case studies based on real accidents are conducted using the developed method in this study to explore the domino effect possibility

caused by fire in the current industry.

The present paper is structured as follows. Section 2 recapitulates the developed methodology. Section 3 demonstrates the application of the methodology with an example, and then the influence of factors that affect pool fires is explored as a sensitivity analysis using the developed methodology. In Section 4, two case studies based on real accidents are conducted. The conclusions of the present study are presented in Section 5.

4.2 Escalation Modeling of Domino Effect

4.2.1 Escalation Vector Modeling

A primary accident triggers a domino event by the effect of escalation vectors, which are physical effects, including fire impingement, fire engulfment, heat radiation, overpressure, and fragment projection caused by explosions [36]. To determine whether adjacent equipment is affected by the fire accident and escalates to a domino event, the escalation vectors exerted by previous events need to be accurately simulated. In the domino event solely caused only by a pool fire, only heat load needs to be considered among all escalation vectors. Also, Hottel's research shows that in the case of the pool fire with a large diameter, the radiation dominates the heat transfer rather than convection [96]. Thus, in this section, the radiation caused by a pool fire accident is modeled as the only escalation vector. Table 4-1 presents the threshold criteria for the escalation vector caused by pool

fire accidents, according to the study by Cozzani et al. [31]. These values are based on the assumption that the heat load has an impact time of 15 minutes. The global National Fire Protection Association (NFPA) also suggested a threshold value of 30 kW/m^2 [97]. In this study, the solid flame model and the numerical model are applied to simulate the heat load caused by the pool fire accidents.

Table 4-1 Threshold values for escalation vectors related to pool fire [31]

Escalation vector	Target equipment	Threshold value
Radiation by pool fire and jet fire	Atmospheric	15kW/m^2 for more than 10min
	Pressurized	50kW/m^2 for more than 10min

4.2.1.1 Solid flame Model

The solid flame model is a classical semi-empirical model that is widely used due to its simple application and accurate results. The solid flame model assumes that the heat flux only originates from the surface of the flame with a specific solid shape such as a cylinder or a cone [6]. In the case of a pool fire accident, the flame shape is assumed to be cylindrical, and the emitting power is calculated based on this assumption. Taking the flame shape into consideration, the heat flux caused by a pool fire can be calculated as a function of the surface-emitting power, the view factor and the atmospheric transmissivity, as suggested by Assael et al. [6]. The detailed steps of the method are summarized and presented in Figure 4-1.

Based on the physical features of the pool and the environmental conditions, the

burning rate and the flame size can be determined based on the equations listed in this model. Then, the maximum surface-emitting power, which refers to the radiation from the flame's surface in cases when the soot is ignored, and the actual surface-emitting power, which takes the soot into consideration, can be determined. To calculate the flame's effect on the adjacent equipment, the view factor, which is defined as the fraction of the emitted radiation that reaches the receptor per unit area, is calculated assuming the flame is a cylindrical solid shape. In addition, atmospheric transmissivity is a factor that contributes to the heat flux. In summary, the heat flux, q, at a certain distance from the center of the fire, is calculated from the value of the actual surface-emitting power, SEP_{act}, the view factor, F_{view}, and the atmospheric transmissivity, τ_a, as shown in Equation (4.1).

$$q = SEP_{act} \times F_{view} \times \tau_a \quad (4.1)$$

When applying the solid flame model, more than one formula can be used to calculate a specific variable according to different conditions. The determination of formulas depends on the situation and the parameters' availability. In this study, the solid flame model is conducted to explore the escalation vector of the domino effect caused by pool fires, and can also serve as a benchmark study for the CFD model.

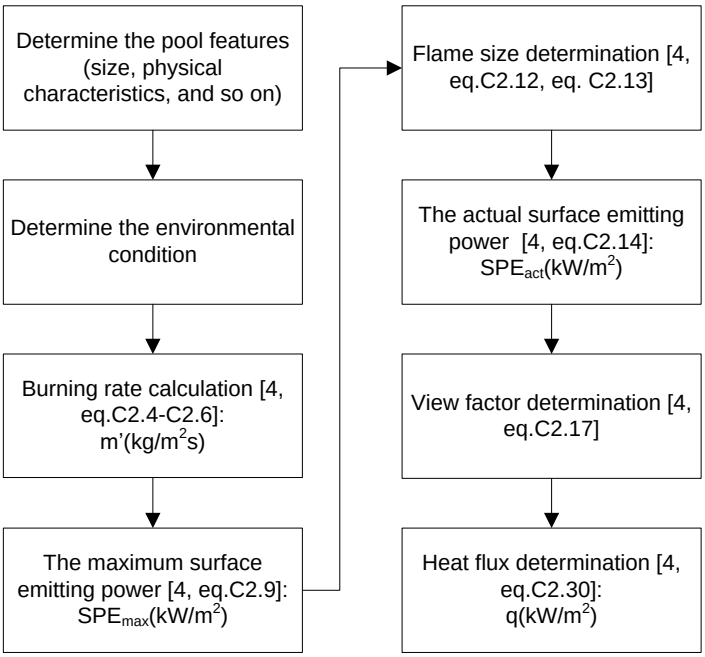

Figure 4-1 Flow chart of heat load calculation using the solid flame model

4.2.1.2 Numerical Model

Computational Fluid Dynamics (CFD) models, also known as field models, are based on the numerical solution of Reynolds-Average Navier-Stokes equations. Compared with other models such as the solid flame model, a CFD model can provide a more accurate result, though a large computation time may be required [6]. In this study, Fluent, a widely used CFD software, is applied to simulate the domino event caused by a pool fire. Yang et al. analyzed the main difference among several CFD models for fire modeling [8]. Among these softwares, Fluent is known for its extensive simulation areas and advantages in meshing and result post-processing. Currently, Fluent is selected for numerical simulation, considering its accuracy of the simulation and the ability of post-processing.

Figure 4-2 summarized the simulation steps using the numerical model

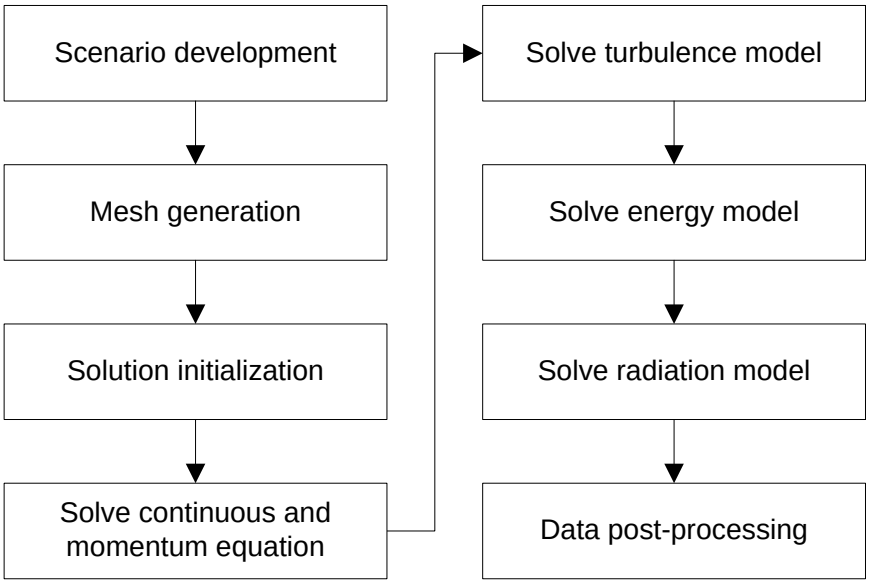

Figure 4-2 Flow chart of heat load calculation using the CFD model

As shown in Figure 4-2, several equations and models need to be solved in the numerical model. Principal conservation equations used in the simulation are shown below [98, 99]:

Continuity equation

$$\frac{\partial \rho}{\partial t} = \nabla \cdot (\rho \vec{v}) = 0 \tag{4.2}$$

Momentum equation

$$\frac{\partial}{\partial t}(\rho \vec{v}) + \nabla \cdot (\rho \vec{v} \vec{v}) = -\nabla \mathrm{p} + \nabla \cdot \bar{\bar{\tau}} + p\vec{g} + \vec{F} \tag{4.3}$$

where

p is the static pressure,

$\bar{\bar{\tau}}$ is the stress tensor (described below), which is given by Equation (4.4)

$p\vec{g}$ is the gravitational body force.

$\vec{F}$ contains other source terms that may arise from resistances, sources, etc.

$$\bar{\bar{\tau}} = \mu[(\nabla\vec{v} + \nabla\vec{v}^T) - \frac{2}{3}\nabla \cdot \vec{v}I] \quad (4.4)$$

where μ is the molecular viscosity, I is the unit tensor and the second term on the right-hand side is the effect of volume dilation.

Energy equation

$$\frac{\partial}{\partial t}(\rho h) + \nabla \cdot (\rho h\vec{v}) = \nabla \cdot [(k + k_t)\nabla \mathrm{T}] + S_h \quad (4.5)$$

Where k is the molecular conductivity, k_t is the conductivity due to turbulent transport, and the source term S_h includes any defined volumetric heat sources.

In order to set up the CFD simulation to describe the pool fire, appropriate physical models need to be selected. The physical models used in this study are shown in Table 4-2.

Table 4-2 Physical models used for fire simulation

Sub-models in Fluent	Physical models used for fire simulation
Turbulence model	k-omega, SST
Combustion model	Eddy-Dissipation
Radiation model	P1 radiation model

To simulate the turbulence in the domain, the k-omega SST model is applied. This

is a hybrid model that combines the k-epsilon model in the free stream and the k-omega model near the walls. Since the vessel needs to be considered in fire modeling, this feature can ensure the appropriate turbulent model is utilized in the computation domain. For combustion modeling, the Eddy-Dissipation model is applied in this study. This model assumes that chemical reactions occur much faster than turbulent mixing, so the average reaction rate is limited by the turbulent mixing rate. Once the turbulence occurs, the reaction will start. This assumption applies to most fuels, and it could provide a relatively accurate result. The P1 radiation model is selected to calculate the Radiative Transfer Equation (RTE), due to its accuracy and less time being demanded for computation. In the case of large optical thickness, such as combustion, the P1 model can work reasonably.

4.2.2 Escalation Probability

Once the heat load caused by the flame is determined, the probability that a pool fire will escalate into a domino event can be calculated.

In a fire accident scenario, the wall of the target vessel is heated due to the existence of a heat load, which may lead to the failure of the vessel. However, this heating process is a relatively slow process, since the equipment is resistant to fire and other disruptions. It is possible that the time is sufficient for applying mitigation and emergency actions before the escalation. Therefore, the escalation probability can be calculated based on the time that a heat load needs to cause the

failure of a vessel, which is called time to failure (ttf). This value is used to express the ability of the target equipment to resist a fire accident [30].

In this study, the escalation probability is estimated using the probit model. The probit method has been widely used to analyze the relationship between a stimulus and a quantal response. In the current research, a probit model is applied to calculate the escalation probability of a domino event caused solely by a pool fire. For the calculation of the escalation probability, as the consequence of an escalation vector, the following Equations (4.6) and (4.7) are employed:

$$P = \frac{1}{(2\pi)^{1/2}} \int_{-\infty}^{Pr-5} \exp\left(-\frac{u^2}{2}\right) du \tag{4.6}$$

and

$$Pr = a + b * \ln(D) \tag{4.7}$$

where Pr is the probit value, a and b are the coefficients of the probit function.

By determining different probit coefficients, the probit function can be used in various scenarios. Given the accident scenario of pool fire accidents, Cozzani et al. proposed a series of probit functions to relate the ttf to the probit value, as shown in Table 4-3 [31]. This model assumes that the radiation intensity and the time exposed to the heat are two principal factors contributing to an accident's escalation. In this study, this probit model is applied to determine the escalation probability of pool fire accidents.

Table 4-3 Probit model used for the estimation of escalation probability [31] (I: radiation intensity (kW/m^2); V: volume of the target unit (m^3))

Escalation vector	Target equipment	Probit model
Heat radiation	Atmospheric	$Pr = 12.54 - 1.847\ln(ttf)$ $\ln(ttf) = -1.128\ln(I) - 2.667 * 10^{-5}V + 9.877$
Heat radiation	Pressurized	$Pr = 12.54 - 1.847\ln(ttf)$ $\ln(ttf) = -0.95\ln(I) + 8.85V^{0.032}$

4.3 Domino Effect Modeling

For the sake of clarity, the application of the developed methodology is presented based on an example. In this section, the possibility that a single pool fire causes a domino effect on the adjacent tanks is analyzed using the developed methodology. In addition, the possible factors affecting the pool fire are also explored as a sensitivity analysis following the case study, and scenarios with different variables are taken into consideration in this section.

4.3.1 Accident Scenario

Figure 4-3 depicts the layout of the pool fire accident scenario studied in this section. The tank studied in this scenario is assumed to be an atmospheric storage tank filled with gasoline. It is assumed to be cylindrical, with a diameter of 30 meters and a height of 16 meters. Caused by other incidents, a gasoline pool forms next to the tank, and has the potential to cause a pool fire, considering its flammable characteristic. In this case, the diameter of the fuel pool is assumed to

be constant and has the same value as the gasoline tank. This is assumed to be caused by another tank of the same size. Assuming that the distance between the tanks is equal to the diameter value of a tank, the distance between the tank and the fuel pool is also set to 30 meters. This section also considers the effect of wind on pool fire accidents. Considering the worst case of the wind direction, it is assumed that the wind direction is directly from the fuel pool towards the tank, and the wind speed is assumed to be 3 m/s.

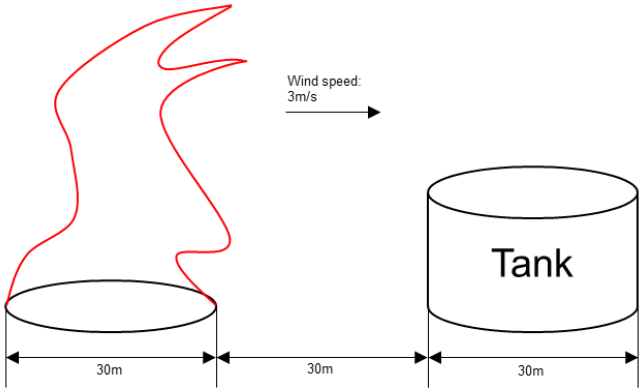

Figure 4-3 The layout of the accident scenario

4.3.2 Escalation Vector modeling

4.3.2.1 Solid flame Model

Following the steps summarized in Figure 4-1, the solid flame model is applied to simulate the escalation vector of the domino effect, which is mainly the heat load in this case. Table 4-4 presents the modeling result of the pool fire accident using the solid flame model.

In this modeling, the burning rate is calculated as 0.055 kg/m^{2}s, using the

Zabetakis-Burgess method [100]. This method takes the characteristics of the flammable fuel and the pool size into consideration, and the value increases with the increase of the pool size. Due to the existence of the wind, the flame is tilted in the same direction as the wind, and the length is also elongated. In this case, the mean flame length is estimated as 51.7756 meters according to the Thomas method [101], which is a method sensitive to the pool size and environmental conditions. Given the physical feature of the fuel and the flame size, the maximum surface emitting power is calculated as 66.5265 kW/m^2. Taking the soot into consideration, the actual surface emitting power is determined as 29.3053 kW/m^2 in this example.

To calculate the flame's impact on the adjacent equipment, the view factor is calculated assuming the flame to be a cylindrical solid shape in this case. In addition, atmospheric transmissivity is a factor that contributes to the heat flux, which is calculated as 0.7646 in this example. In summary, the heat flux is estimated as 8.2128 kg/m^2s, according to Equation (1).

Table 4-4 Modeling result of pool fire accident using solid flame model

Variables	Values
Burning rate (kg/m^2s)	0.055
Mean flame length (m)	51.7756
Angle of tilt (°)	43.49643
View factor (-)	0.3665
Maximum surface emitting power (kW/m^2)	66.5265
Actual surface emitting power (kW/m^2)	29.3053
Atmospheric transmissivity (-)	0.7646

Heat Flux (kW/m^2)	8.2128

4.3.2.2 Numerical Model

Figure 4-4 illustrates the geometry developed in the CFD simulation. The dimension of the whole computation domain is set as 325m×250m×150m. While the fuel pool and the tank are placed in the central part, other boundaries are placed far enough to reduce the effects of the boundary, ensuring that the pool fire can be fully developed. Boundaries in this simulation comprise wind inlet, outlets, fuel pool, tank surface and the ground. Detailed boundary conditions used in this section are presented in Table 4-5. The boundary condition of the wind inlet is defined as a velocity inlet for forming a stable wind field with a speed of 3m/s. The other four boundaries, including three side outlets and an upper outlet, are defined as pressure outlets that simulate the open area. In addition, the boundary condition of the fuel pool is defined as the mass flow rate inlet to simulate the vaporization rate. Since the burning rate of the flammable material is observed to be equal to its vaporization rate in a pool fire, [6], the burning rate of the flammable material is first calculated to determine the mass flow rate in this study. According to the Zabetakis-Burgess Method [100], the burning rate is calculated to be $0.055 kg/m^2 s$, and thus the mass flow rate is the same. The temperature at this boundary is set at 399.2K, which is believed to be the boiling point of gasoline.

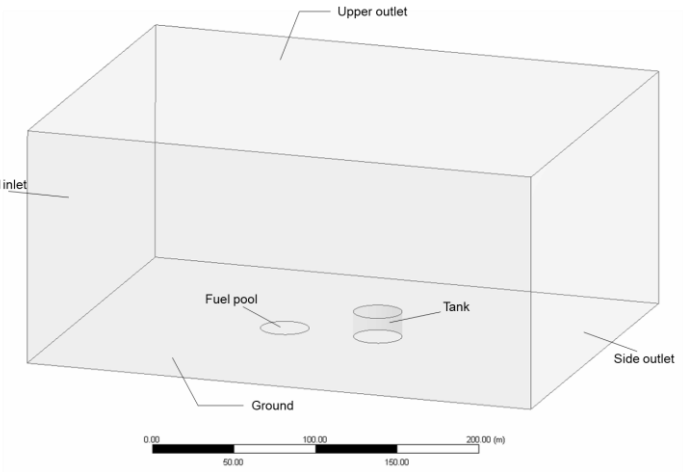

Figure 4-4 Illustration of the CFD geometry

Table 4-5 Boundary conditions applied in CFD simulation

Surfaces	Boundary condition
Fuel pool	Mass flow rate inlet
Wind inlet	Velocity inlet
Outlets (3 sides and upper)	Pressure outlet
Tank surface	Wall
Ground	Adiabatic wall

To obtain a satisfactory mesh, computation with different meshes is applied until the simulation result is independent of the mesh quality. As shown in Figure 4-5, a tetrahedral mesh with total elements of 2231800 is used in this section. The finer mesh is applied to the fuel pool and the potential areas where the fire may develop, to capture the physical characteristics of the pool fire. In addition, the mesh around the surfaces, including the tank surface and the ground, is also refined. Inflation layers are applied to resolve the boundary layer and ensure that the y+ satisfies that the applicability of the SST k-w model. In this case, a coupled solver is used

for a steady state simulation of the combustion model.

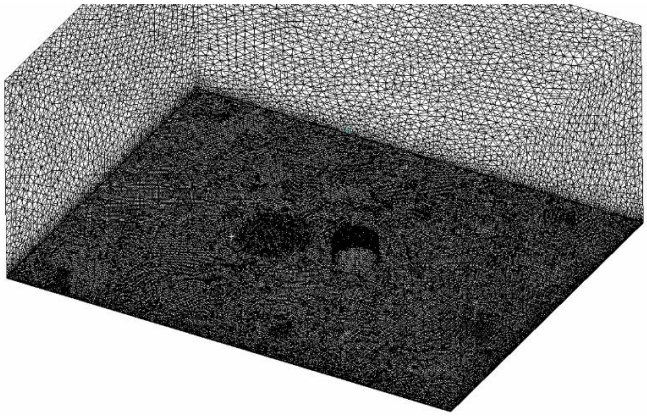

Figure 4-5 Mesh applied in the CFD simulation

The flame profile obtained in the CFD simulation is shown in Figure 4-6. Under the influence of the wind, the flame tilts directly toward the tank; however, the tank is placed far enough for the flame to reach. According to the result shown in Figure 4-6 (a), the length is around 60 meters while the angle of tilt is around 40 degrees, which is consistent with the result obtained from the solid flame model. Figure 4-6 (b) shows the radiation intensity profile of the flame. It generally ranges from 31.3 to 198 kW/m^2 As the distance between the fuel pool and the tank increases, the influence of the flame decreases rapidly.

Figure 4-7 shows the temperature and radiation intensity that reached the tank. As shown in Figure 4-7 (a), the tank surface is heated due to the existence of the fire nearby. The highest temperature is found to be 417.8 K. For most construction materials, the strength will dimish 40 percent when the temperature is higher than

670 K, while the material will not be affected drastically when the temperature is lower than 570 K [102]. Given the result in this example, the target tank is less likely to be drastically damaged in terms of the temperature threshold value. Figure 4-7 (b) shows the radiation intensity that the target tank received from the flame. The maximum heat load received from the pool fire is calculated as 9.82 kW/m^2, which is close to the simulation result from the solid flame model. Therefore, results from the two models show good consistency, which proves the validity of both models.

In summary, the two simulation methods show that the heat load is lower than the threshold value suggested by Cozzani et al. [31] and NFPA 59A [97]. This fact demonstrates that given the conditions in this example, the heat load caused by a fire is unlikely to drastically damage the target tank.

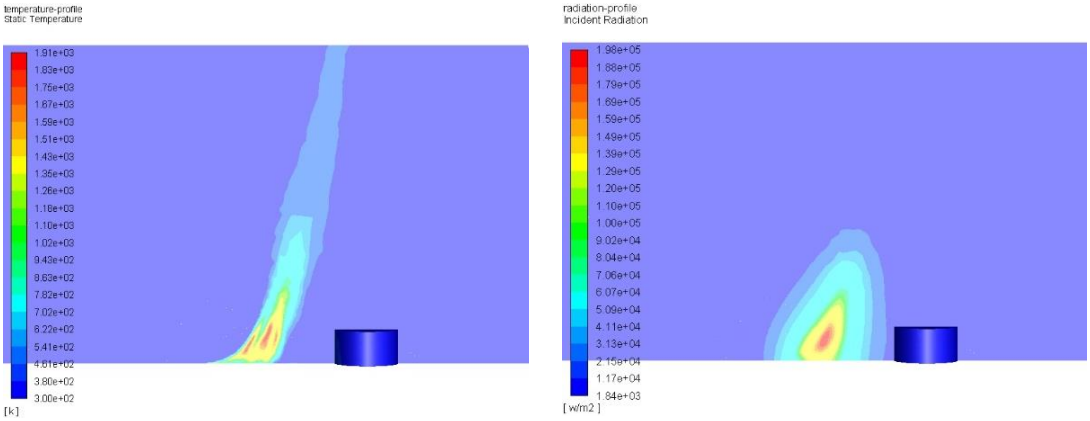

(a) Temperature profile (b) Radiation intensity profile

Figure 4-6 Flame profile obtained in the CFD simulation

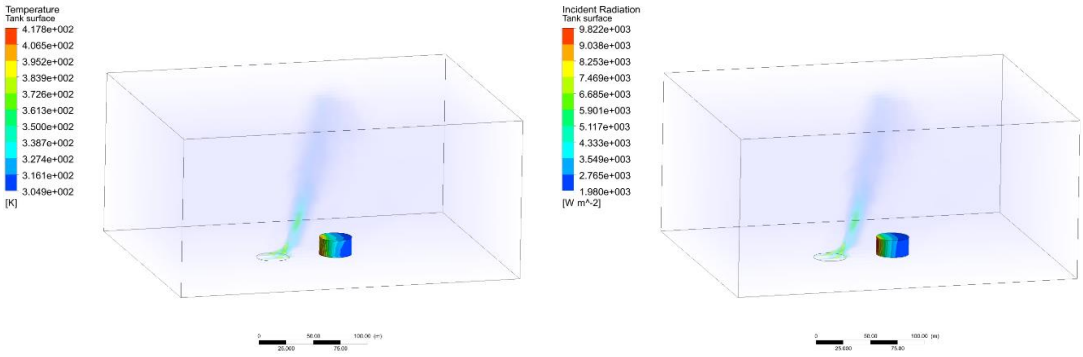

(a) Temperature profile (b) Radiation intensity profile

Figure 4-7 Temperature and radiation profile in the tank surface

4.3.3 Escalation Probability Modeling

Based on the results obtained in the previous sections, the escalation probability of the domino effect is calculated using the probit model proposed by Cozzani et al. [31]. Table 4-6 summarizes the result obtained from the probit model.

Table 4-6 Results of the probit model

	Solid flame model	CFD model
Heat flux (kW/m^2)	8.2128	9.8216
Time to failure (s)	1.3396e+03, 22.3mins	1.0948e+03, 18.2mins
Escalation probability	4.2389e-09	3.6028e-08

According to the result, the ttf calculated from both the solid flame model and the CFD model exceeds 18 mins. Given this value and the tank size, the escalation probability calculated by the probit model is relatively low, and unlikely to cause

a domino effect in this case.

4.3.4 Sensitivity Analysis

To comprehensively explore the factors affecting a pool fire, the study takes several essential factors into account, including pool size, the distance between fire and tank, and meteorological conditions such as wind speed. In this study, 18 scenarios with various parameters, including pool dimensions, the distance between fire and target tank, and wind speed, are selected to explore the effect of possible factors that affect a domino event caused by a pool fire. Table 4-7 shows the selected scenarios with detailed parameters. Two kinds of pool dimension, including 20m and 30m, are selected considering the potential tank size; distances between the fire and target tank are selected based on the diameter of the target tank, D, and three degrees, from 0.5D to 1D, are applied in this section, where D is set to be 30 meters. The wind's effect is also considered in this section, while the wind direction is assumed to be the worst case, which is from the pool fire directly to the target tank. Various wind speeds, from 1m/s to 5m/s, are selected and explored in this study considering from calm situation to gentle breeze according to the Beaufort wind scale.

Table 4-7 Scenarios with value parameters

	Pool diameter (m)	Distance between fuel pool and target tank (m)	Wind speed (m/s)

Scenario 1	20	0.5D	1
Scenario 2	20	0.75D	1
Scenario 3	20	1D	1
Scenario 4	20	0.5D	3
Scenario 5	20	0.75D	3
Scenario 6	20	1D	3
Scenario 7	20	0.5D	5
Scenario 8	20	0.75D	5
Scenario 9	20	1D	5
Scenario 10	30	0.5D	1
Scenario 11	30	0.75D	1
Scenario 12	30	1D	1
Scenario 13	30	0.5D	3
Scenario 14	30	0.75D	3
Scenario 15	30	1D	3
Scenario 16	30	0.5D	5
Scenario 17	30	0.75D	5
Scenario 18	30	1D	5

Table 4-8 demonstrates the simulation results for various scenarios using two heat load simulation models. In the solid flame model, it is assumed that the flame cannot reach the target equipment; therefore, the flame only affects the target equipment by thermal radiation, and other possible ways to affect the heat load value, including heat conduction and convection, are ignored in this model. Therefore, this model is not applicable in the case of an engulfed pool fire scenario, where the flame can reach the target equipment. In these cases, only the CFD model is applied to calculate the escalation vector caused by a pool fire, in this section.

As the results show, the CFD model and the solid flame model provide close results, given the same parameters. The solid flame model provides a slightly

lower value compared to the CFD model in most cases. Especially in the case when the flame is extremely close to the target equipment, the solid flame model provides a relatively lower value. This may be because many assumptions need to be made in the solid flame model, such as soot's effect, which are hard to accurately determine based on experience, but these assumptions have a significant effect on the result calculated by the solid flame model, which may lead to the underestimation of the final result in this section. In addition, while the CFD model can be applicable in most of the scenarios, several scenarios cannot be simulated using a solid flame model, due to its application limit. In general, the solid flame model can provide a reasonable estimation of radiation intensity with a relatively short calculation time; however, its application limit and its result's accuracy demonstrate that the CFD model is a more reliable model though sometimes the computation time can be long.

According to the results from different scenarios, it can be found that these three factors do have big effects on the heat load received by the target tank from a pool fire. Given the same pool dimensions and wind speed, the heat load increases rapidly with the decrease of the distance between the fuel pool and the target tank. In several scenarios, such as Scenarios 4 and 13, though the distance of 0.25 D is reduced, the decreased distance allows the flame to reach the target tank. In these cases, the heat loads from radiation and conduction work collectively on the tank and cause relatively high values. In addition, it can also be concluded that the heat

load caused by a pool fire depends, to a large degree on the wind speed. For example, in Scenarios 1, 4, and 7, and Scenarios 10, 13, and 16, the big difference among results from these scenarios demonstrates that the flame is easily affected by wind. Also, a small difference, for example, 2 m/s in this case, can lead to a much more inclined flame, and thus cause much more heat load to be received by the target tank. Results in this section show that the pool's dimensions have an effect on the heat load; however, varying pool dimensions do not cause such much change as the other two factors do.

Given the heat load calculated, the ttf of the target tank and the escalation probability of a domino effect is calculated and shown in Table 4-9. As shown in the results, the maximum escalation probability that a scenario in this section can cause a domino effect is 0.4013, which is caused by the scenario in which the pool diameter is 30 meters, and the distance between the fuel pool and the target tank is 0.5D , with a wind speed of 5m/s. In addition, it can be concluded that the small increase in the heat load can greatly decrease ttf and then increase the escalation probability.

In summary, most of the scenarios studied in this section have no capability to cause an escalation to a domino effect. Some accident scenarios such as Scenarios 7, 16, and 17, result in a high heat load being received by the target tank, which is likely to cause a domino effect, suggested by the simulation result. In these scenarios, due to the close distance between the fuel pool and tank or the

relatively high speed wind, the tank is engulfed by a pool fire, where not only thermal radiation but also heat conduction contribute to the heat load. Therefore, given a safe distance between the flame and the target tank, the pool fire alone is unlikely to case a domino effect.

Table 4-8 Heat load simulation results using solid-flame model and CFD model

	Pool diameter (m)	Distance between fuel pool and target tank (m)	Wind speed (m/s)	Heat load by solid-flame method (kW/m2)	Maximum Heat load by CFD method (kW/m2)
Scenario 1	20	0.5D	1	9.1995	12.5729
Scenario 2	20	0.75D	1	6.4264	7.804
Scenario 3	20	1D	1	4.61	4.235
Scenario 4	20	0.5D	3	-	40.5246
Scenario 5	20	0.75D	3	11.358	13.915
Scenario 6	20	1D	3	7.198	9.79
Scenario 7	20	0.5D	5	-	91.260
Scenario 8	20	0.75D	5	-	43.721
Scenario 9	20	1D	5	-	22.934
Scenario 10	30	0.5D	1	10.114	11.344
Scenario 11	30	0.75D	1	7.648	8.264
Scenario 12	30	1D	1	4.893	3.494
Scenario 13	30	0.5D	3	-	34.019
Scenario 14	30	0.75D	3	16.3015	17.1741
Scenario 15	30	1D	3	8.2	9.8216
Scenario 16	30	0.5D	5	-	115.55
Scenario 17	30	0.75D	5	-	98.970
Scenario 18	30	1D	5	-	52.233

Table 4-9 Time to failure and escalation probability calculated by probit method

	Heat load by solid-flame method (kW/m^2)		Maximum Heat load by CFD method (kW/m^2)	
	Time to failure (s)	Escalation probability	Time to failure (s)	Escalation probability
Scenario 1	1.179e+03	1.673e-08	828.642	5.539e-07
Scenario 2	1.767e+03	1.809e-10	1.419e+03	2.245e-09
Scenario 3	2.570e+03	1.680e-12	2.828e+03	4.716e-13
Scenario 4	-	-	221.321	0.0075
Scenario 5	929.286	1.856e-07	739.062	1.580e-06
Scenario 6	1.555e+03	8.025e-10	1.0990e+03	3.471e-08
Scenario 7	-	-	88.580	0.229
Scenario 8	-	-	203.157	0.012
Scenario 9	-	-	420.638	1.478e-04
Scenario 10	1.059e+03	5.052e-08	930.580	1.831e-07
Scenario 11	1.452e+03	1.741e-09	1.330e+03	4.577e-09
Scenario 12	2.403e+03	4.025e-12	3.513e+03	2.363e-14
Scenario 13	-	-	269.618	0.0026
Scenario 14	618.212	7.443e-06	582.898	1.212e-05
Scenario 15	1.340e+03	4.239e-09	1.095e+03	3.603e-08
Scenario 16	-	-	67.878	0.4013
Scenario 17	-	-	80.836	0.2834
Scenario 18	-	-	166.222	0.0284

4.4 Case study

4.4.1 Caribbean Explosion and Fire Accident

4.4.1.1 Accident Description

In October 2009, a large explosion occurred at the Caribbean Petroleum Corporation (CAPECO) oil refinery and oil depot in Bayamón, Puerto Rico [5]. Three people were injured in this accident, but fortunately, no fatalities were reported. The accident started with an overflowed gasoline storage tank at the tank farm; then, a 107-acre vapour cloud formed quickly over the facility after the fuel

aerosolized. The vapour cloud was ignited subsequently in the wastewater treatment area of the facility and led to a huge explosion. Multiple tank fires followed the explosion and burned for nearly 60 hours. Due to the subsequent explosions and fire, 17 of the 48 petroleum storage tanks were damaged significantly.

Figure 4-8 shows the layout of the tank farm at CAPECO. In the case study, Tank 407, which is assumed to have a height of 20m and a diameter of 30m, is selected as the target equipment, to explore its possibility of being affected by adjacent fires and escalating into a domino event. Three adjacent tanks, including Tank 405, Tank 408, and Tank 409, were damaged due to VCE, and then formed multiple tank fires. Considering their proximity, pool fires occurring in these tanks are simulated as the main sources of the heat load affecting the target tank in this study. The diameter of Tank 409 is 36.58 meters, according to the CSB accident investigation report [5], while the diameters of Tank 405 and Tank 408 are assumed to be 15 meters and 30 meters, respectively. In this study, the pool fire that occurs in each tank is assumed to have the same dimension as the corresponding tank. A light breeze of 3m/s is reported in the accident investigation [5], which is from the left side, as photographed in Figure 4-8.

Figure 4-8 Layout of the tank farm of CAPECO

4.4.1.2 Escalation Vector Modeling

Table 4-10 presents the heat load estimated by the solid flame model. In the case of multiple tank fires, the heat load caused by each tank fire (Q_1 to Q_3), is calculated separately using the solid flame model. As shown in the result, the fire occurring in Tank 409 contributes the most among the three tank fires, which is caused by its proximity to the target tank, having the largest pool size among the three tanks, with a relatively high view factor, due to its location and the wind direction. Tank 408 has a similar pool size as Tank 409; however, the distance to the target tank is relatively long compared to Tank 409, and the wind does not tilt the fire directly to the target tank. These reasons lead to a lower view factor compared to that of Tank 409, which causes the fire in Tank 408 to have a less thermal effect on the target tank. Though Tank 405 is the closest to the target tank among others, the wind tilts the flame in the direction away from the target tank,

and the small size of the fuel pool also explains its smaller effect on the target tank. The sum of the heat load caused by three tank fires, Q_{total1}, is calculated as 16.63 kW/m^2, which is believed to be the total radiation that the target equipment received from the adjacent multiple tank fires. Given the results from this model, the total heat load is slightly higher than the threshold value suggested by Cozzani et al. [31], but satisfies the requirement by NFPA 59A [97].

Table 4-10 Simulation result of Caribbean accident using the solid flame model

	Heat load (kW/m^2)
Q_1 (from Tank 405)	1.23
Q_2 (from Tank 408)	3.54
Q_3 (from Tank 409)	11.86
Q_{total1}	16.63

The results from the CFD model are shown in Figure 4-9. Under the influence of the wind, the flames tilt toward the tank, and affect approximately half of the targeted tank by varying degrees of heat load. Three tank fires affect the tank collectively and exert a heat load with the maximum value of 14.53 kW/m^2 on the tank surface, as shown in the results. This value is slightly lower than that of the solid flame model and the threshold value of radiation intensity, which is 15 kW/m^2.

Though the heat loads calculated from the two models are slightly different, both values are close to the threshold value for an atmospheric tank suggested by

Cozzani et al. [31], which indicates that the multiple tank fires in this case have the potential to cause damage to the target equipment once the exposure time is sufficient.

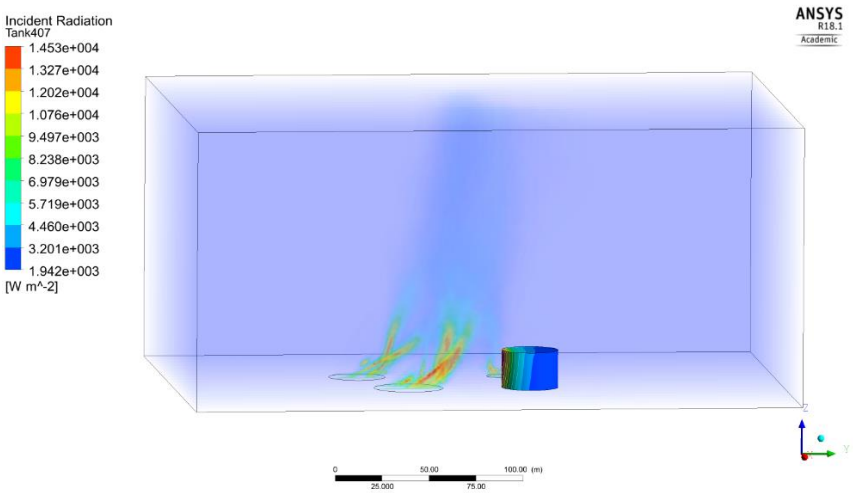

Figure 4-9 Simulation result of Caribbean accident using the CFD model

4.4.1.3 Escalation Probability Modeling

Table 4-11 Escalation probability results of the Caribbean accident

	Solid-flame model	CFD model
Heat flux (kW/m^2)	16.63	14.53
Time to failure (s)	560.5502	652.7477
Escalation probability	1.6659e-05	4.6951e-06

Given the heat load calculated in the previous section, the corresponding ttf and the probability of escalating to a domino event can be calculated. The results calculated using the probit method are presented in Table 4-11. The ttf calculated from the two models is approximately 10 mins, which means that the multiple fires

in this case need to last for at least 10 minutes to cause significant damage to the target tank. However, the escalation probability calculated using the corresponding ttf by the probit model is still low, which indicates that, given the conditions in this case, although the multiple pool fires have the potential to cause damage to the target equipment, they may not be significant, or have the ability to completely damage the equipment. Therefore, in this case study, the accident may not escalate into a domino event.

This conclusion is consistent with the result shown in the accident investigation report, that Tank 409 suffered a certain degree of damage during the accident, but did not catch fire and escalate into the next-level accident, even when multiple tank fires existed nearby [5].

4.4.2 Jaipur Fire Accident

4.4.2.1 Accident Description

The explosion and fire accident occurred on October 2009 at the Indian Oil Corporation (IOC) oil depot in Jaipur caused 12 deaths and over 300 injuries. The fires lasted for over one week and resulted in huge losses of people and assets, as well as harming the environment. To guarantee that residences were not affected by the accident, half a million people were evacuated from the affected area [26].

The accident started with a fuel leakage on the transfer line from the tank to the Motor Spirit (MS) pump. The leaked liquid fuel generated vapour rapidly and

formed a vapour cloud that covered the entire installation. A huge VCE occurred subsequently and destroyed the building and equipment within the depot. In addition, 9 of the 11 tanks were damaged in this explosion and soon caught fire. The multiple tank fires caused by the VCE spread subsequently to the remaining two MS tanks (Tank 409 A and B). Possible factors that caused the MS tanks 409 A/B to catch fire include explosion, nearby multiple tank fires and so on [26]. In this case study, Tank 409 A is selected as the target equipment, and the possibility of it being affected by the multiple tank fires nearby is explored.

As shown in Figure 4-10, nine tanks that caught fire due to the first VCE are located northwest of the MS tanks 409 A/B. Considering the worst case, the wind direction is set from MS tanks 401 to the target tank, MS tank 409 A, with a wind velocity of 3 m/s. In this study, fires in three MS tanks, Tanks 401 A/B/C, are selected and simulated as the main sources of the heat load affecting the target tank. According to the investigation report, Tanks 401 A/B/C have diameters of 24 meters and heights of 15 meters, while Tanks 409 A/B have diameters of 28 meters and heights of 15 meters [26].

Figure 4-10 Layout of the tank farm in IOC

4.4.2.2 Escalation Vector Modeling

The results obtained from the solid flame model are shown in Table 4-12. Due to the long distance between the tank fire and the target tank, the view factors calculated by the model are extremely low, which accounts for that most of the thermal radiation from the flames not being received by the target tank. As shown in the result, the radiation received from each tank fire is only around 0.2 kW/m^2, and the total heat load that the target tank received from the tank fires is calculated to be 0.598 kW/m^2, which is far below the threshold for heat load.

In the CFD modeling, as shown in Figure 4-11, the flames are tilted toward the target tank under the influence of the wind. However, given this layout, even if the wind direction is considered to be the worst case, which is directly from Tank 401 to Tank 409, the flame is still very far from the target tank and hardly affects it. The results from the CFD model present a bit higher heat load than that from the

solid flame model, and still much lower than the threshold value. By comparing the heat load simulated from the two models and the threshold value suggested by Cozzani et al. [31], it can be concluded that the pool fires are unlikely to cause any significant damage to the target equipment.

Table 4-12 Simulation result of Jaipur fire accident using the solid-flame model

	Heat load (kW/m^2)
Q1 (from Tank 401A)	0.135
Q2 (from Tank 401B)	0.193
Q3 (from Tank 401C)	0.270
Q (total heat load)	0.598

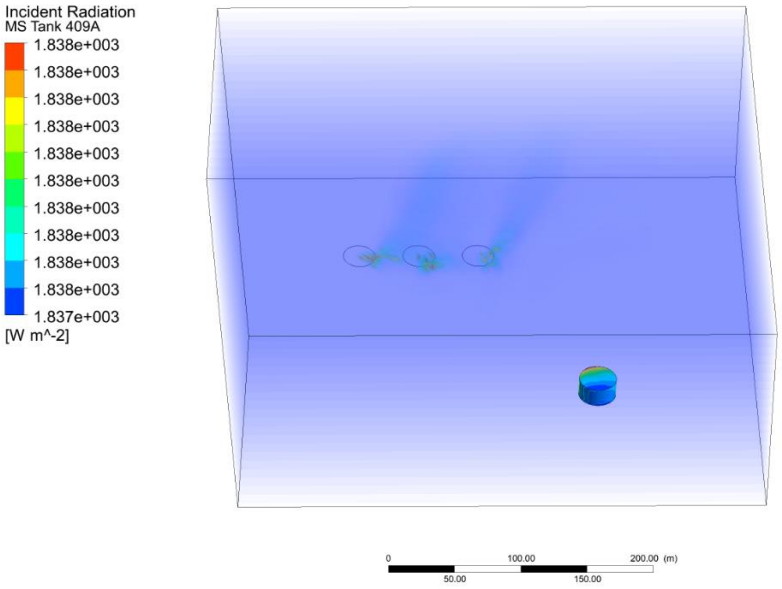

Figure 4-11 Simulation result of Jaipur fire accident using the CFD model

4.4.2.3 Escalation Probability Modeling

After the heat load is simulated, the ttf and the escalation probability are calculated,

as shown in Table 4-13. With a low value of the heat load, the ttf calculated from both models is very high, more than seven hours. Therefore, the escalation probability, which is calculated from ttf, is extremely low in the results derived from both models. In terms of the ttf and the escalation probability, the results prove again that in this case, the pool fires alone have almost no ability to cause significant damage to the target tank and escalate into a domino event. Instead of the pool fires, it is the other factors or the collective effect of several factors that cause the target tanks to be damaged and catch fire.

Table 4-13 Escalation probability results of Jaipur accident

	Solid-flame model	CFD model
Heat flux (kW/m^2)	0.598	1.838
Time to failure (s)	2.7191e+04	7.6624e+03
Escalation probability	5.2797e-30	1.3573e-19

In the accident investigation report by the Independent Inquiry Committee [26], which is constituted by the Ministry of Petroleum & Natural Gas (MoP&NG), the possible accident scenarios in this accident were analyzed and modelled, including flash fires, pool fires, jet fires and VCE. Each scenario was simulated considering various influencing factors to explore their effects in the accident. In the simulation result of the pool fires, since the distance is too far from the fuel pool, the heat load caused only by pool fires in the first 9 tanks is extremely low, which means there is no possibility to cause damage to the target tank. This result is consistent

with the result obtained in this study. In addition, the investigation report also shows that the overpressure caused by the VCE can affect the farther places, which has the ability to result in the failure of the target tank.

In summary, this case study as well as the result from the investigation report show that in this case, the pool fire alone cannot cause significant damage and escalate into a domino event. It is other factors' effect or the collective effect of several factors which contribute to the failure of the tank, resulting in a domino event.

4.5 Conclusion

This study explores the possibility that the pool fire alone causes a domino effect. By applying the developed method, three factors that have the potential to affect a pool fire's impact, including pool dimension, distance between fire and target tank, and wind speed, are determined and verified. According to the results in this study, it can be concluded that the pool fire does have the potential to cause damage to the adjacent equipment. As shown in the sensitivity analysis, in the case of fire engulfment, the heat load caused by the pool fire do has a significant possibility of causing a domino effect; however, as shown in other cases, as long as the layout guarantees a safe distance among tanks, the pool fire alone is unlikely to cause the failure of the target tank and thus the domino effect.

In addition, as shown in the two case studies, a pool fire alone sometimes may not cause a domino effect in the current industry. Other factors, such as explosion and

hydrocarbon leakage, work together with a pool fire to escalate into a domino event, for example, the results shown in the case study of the Jaipur fire accident.

Chapter 5. Summary, Conclusions and Recommendations

Fire is among the most dangerous accidents in chemical and hydrocarbon processing industries. This thesis analyzed several potential fire scenarios in the hydrocarbon production and processing industry and conducted risk assessments of fire risks.

Chapter 1 provides a brief introduction to the fire risks which threaten people in the current industry. Several current models for fire simulation are introduced, along with potential fire accident scenarios, such as their effects on offshore facilities and their likelihood of causing a domino effect.

Chapter 2 proposes a procedure to study potential fire accident scenarios in an offshore facility with different ignition source locations, and this procedure helps to design the safety measures. In this chapter, 14 credible scenarios with different ignition source locations are explored. The results are extracted to determine the most dangerous scenarios. In addition, the ranges of safety measures are also studied in this chapter to determine their effectiveness to prevent fires and mitigate their impact. Thus, this chapter provides a simple and efficient way to analyze the impact of key design parameters of safety measures. This work emphasizes that an FLNG layout must be considered with the utmost care since it is the most effective measure in limiting a potential LNG release and subsequent dispersion effect, and directly influences the fire dynamics and thus limits the potential damage.

In chapter 3, an integrated model is proposed to assess the probability of fire accidents considering their time-dependent features, by combining a conditional probability approach – the Bayesian network (BN) - with a time-dependent scenario evolution approach, Stochastic Petri Nets (SPN). The CFD tool is used to estimate the time-dependent scenario consequences. The outcome of the model is fire probability as a function of time and location caused by a specific leak rate and leak duration. Through applying the proposed approach, a system optimization for fire accident probability can be conducted if the probability of fire is unacceptably high. The results in this work show that a time-dependent probability analysis model is necessary for fire accidents. In addition, through measuring the maximum fire probability and the fire risk duration, systems with different confinement and congestion levels have different fire risk. The results show the importance of a sufficient escape space for the leaked gas, and also the necessity to conduct a system configuration when the probability of fire is unacceptably high. Chapter 4 explores the possibility that pool fires alone cause a domino effect. While two models, a solid flame model and numerical model, are applied to simulate the heat load caused by pool fires, a probit model is used to assess the escalation probability of a domino effect caused by pool fires. Several potential influencing factors that have effects on the pool fire results are explored in a sensitivity study. In addition, two case studies based on real accidents are conducted to analyze the pool fire's impact on the current industry. The results

demonstrate that a pool fire alone sometimes may not cause a domino effect in the current industry. It is other factors, such as explosion and hydrocarbon leakage, work together with a pool fire to escalate into a domino event, for example, the results shown in the case study of the Jaipur fire accident.

Finally, this chapter provides a summary of the work and highlights the achievements of this research. The following recommendations are provided for future work to improve the analysis of fire risk presented in this thesis.

First of all, since a fire accident in an offshore facility has a considerable potential to escalate into an explosion accident, the proposed numerical model for effective analysis of safety measures can be extended to take the transfer from fire to explosion accident into consideration. In addition, except for the location of the ignition sources, more factors can contribute to the result of the fire consequence, which could be the future's work. Besides, due to the complex relationship among factors causing a leakage, the interdependence of the parameters in modelling leakage probability need more attention, as well as more uncertainty, these factors can be considered in the time-dependent model in future work. For the study of the domino effect, a comprehensive study of previous accidents caused by the domino effect can be conducted to provide a clearer view. It would be better if the future work can focus on which combination of the accidents contribute most to the domino effect, and how to provide any preventative measures to avoid these combinations.

References

1. Cullen, L.W.D., *The public inquiry into the Piper Alpha disaster*. HMSO Publications Center, London, 1990.

2. Paté-Cornell, M.E., *Learning from the piper alpha accident: A postmortem analysis of technical and organizational factors.* Risk Analysis, 1993. **13**(2): p. 215-232.

3. Hopkins, A., *Failure to learn: the BP Texas City refinery disaster*. 2008: CCH Australia Ltd.

4. Ottemöller, L. and L. Evers, *Seismo-acoustic analysis of the Buncefield oil depot explosion in the UK, 2005 December 11*. Geophysical Journal International, 2008. **172**(3): p. 1123-1134.

5. CSB, *Caribbean Petroleum Tank Terminal Explosion and Multiple Tank Fires* 2009.

6. Assael, M.J. and K.E. Kakosimos, *Fires, explosions, and toxic gas dispersions: effects calculation and risk analysis*. 2010: CRC Press.

7. Paik, J.K., et al., *CFD simulations of gas explosion and fire actions.* Ships and Offshore Structures, 2010. **5**(1): p. 3-12.

8. Yang, R., et al., *A numerical fire simulation approach for effectiveness analysis of fire safety measures in floating liquefied natural gas facilities.* Ocean Engineering, 2018. **157**: p. 219-233.

9. Hansen, O.R., J.A. Melheim, and I.E. Storvik. *CFD-modeling of LNG*

dispersion experiments. in *AIChE Spring National Meeting, Houston, TX*. 2007.

10. Dadashzadeh, M., et al., *An integrated approach for fire and explosion consequence modelling.* Fire Safety Journal, 2013. **61**: p. 324-337.

11. Pitblado, R., et al., *Consequences of liquefied natural gas marine incidents.* Process safety progress, 2005. **24**(2): p. 108-114.

12. Baalisampang, T., et al., *Modelling the Impacts of Fire in a Typical FLNG Processing Facility,* in *International Conference on Safety and Fire Engineering-SAFE'17*. 2017: Cochin University of Science and Technology.

13. Baalisampang, T., et al., *Fire impact assessment in FLNG processing facilities using Computational Fluid Dynamics (CFD).* Fire Safety Journal, 2017. **92**: p. 42-52.

14. Baalisampang, T., et al., *An inherently safer layout design for the liquefaction process of an FLNG plant.* International Journal of Maritime Engineering (Transactions of the Royal Institution of Naval Architects: Part A), 2016. **158**(Part A2): p. 91-102.

15. Van Hees, P., *Validation and verification of fire models for fire safety engineering.* Procedia Engineering, 2013. **62**: p. 154-168.

16. Berg, J., et al. *A CFD layout sensitivity study to identify optimum safe design of a FPSO*. in *Offshore Technology Conference*. 2000. Houston, Texas: Offshore Technology Conference.

17. Binbin, W., *Comparative Research on FLUENT and FDS's Numerical*

Simulation of Smoke Spread in Subway Platform Fire. Procedia Engineering, 2011. **26**: p. 1065-1075.

18. Bunnag, M., et al. *FLNG Development: Strategic Approaches to New Growth Challenges*. in *International Petroleum Technology Conference*. 2011. International Petroleum Technology Conference.

19. Yeo, C., et al., *Dynamic risk analysis of offloading process in floating liquefied natural gas (FLNG) platform using Bayesian Network.* Journal of Loss Prevention in the Process Industries, 2016. **41**: p. 259-269.

20. Sammarco, P.W., et al., *Distribution and concentrations of petroleum hydrocarbons associated with the BP/Deepwater Horizon Oil Spill, Gulf of Mexico.* Marine pollution bulletin, 2013. **73**(1): p. 129-143.

21.Landucci, G., et al., *Probabilistic assessment of domino effect triggered by fire: implementation in quantitative risk assessment.* Chemical Engineering, 2012. **26**.

22.Lees, F., *Lees' Loss prevention in the process industries: Hazard identification, assessment and control*. 2012: Butterworth-Heinemann.

23. Khan, F.I. and S. Abbasi, *The world's worst industrial accident of the 1990s what happened and what might have been: A quantitative study.* Process Safety Progress, 1999. **18**(3): p. 135-145.

24. Khan, F.I. and S. Abbasi, *Estimation of probabilities and likely consequences of a chain of accidents (domino effect) in Manali Industrial Complex.* Journal of Cleaner Production, 2001. **9**(6): p. 493-508.

25. Khan, F.I. and S. Abbasi, *Models for domino effect analysis in chemical process industries.* Process Safety Progress, 1998. **17**(2): p. 107-123.

26. Committee, I.I., *IOC Fire Accident Investigation Report.* Ministry of Petroleum & Natural Gas, Government of India, 2010.

27. Khakzad, N., et al., *Risk management of domino effects considering dynamic consequence analysis.* Risk Analysis, 2014. **34**(6): p. 1128-1138.

28. Jujuly, M.M., et al., *LNG pool fire simulation for domino effect analysis.* Reliability Engineering & System Safety, 2015. **143**: p. 19-29.

29. Khakzad, N., *Application of dynamic Bayesian network to risk analysis of domino effects in chemical infrastructures.* Reliability Engineering & System Safety, 2015. **138**: p. 263-272.

30. Landucci, G., et al., *The assessment of the damage probability of storage tanks in domino events triggered by fire.* Accident Analysis & Prevention, 2009. **41**(6): p. 1206-1215.

31. Cozzani, V., et al., *The assessment of risk caused by domino effect in quantitative area risk analysis.* Journal of hazardous Materials, 2005. **127**(1-3): p. 14-30.

32. Reniers, G. and V. Cozzani, *Features of escalation scenarios,* in *Domino Effects in the Process Industries*. 2013, Elsevier. p. 30-42.

33. Khan, F.I. and S. Abbasi, *An assessment of the likelihood of occurrence, and the damage potential of domino effect (chain of accidents) in a typical cluster of*

industries. Journal of Loss Prevention in the Process Industries, 2001. **14**(4): p. 283-306.

34. Khan, F.I. and S. Abbasi, *DOMIFFECT (DOMIno eFFECT): user-friendly software for domino effect analysis.* Environmental modelling & software, 1998. **13**(2): p. 163-177.

35. Khan, F.I. and S. Abbasi, *Studies on the probabilities and likely impacts of chains of accident (domino effect) in a fertilizer industry.* Process Safety Progress, 2000. **19**(1): p. 40-56.

36. Khakzad, N., et al., *Domino effect analysis using Bayesian networks.* Risk Analysis: An International Journal, 2013. **33**(2): p. 292-306.

37. Xie, B., et al. *The Floating Liquefied Natural Gas Production, Storage and Offloading Technology Research*. in *Offshore Technology Conference-Asia*. 2014. Offshore Technology Conference.

38. Aronsson, E., *FLNG compared to LNG carriers-Requirements and recommendations for LNG production facilities and re-gas units*, in *Department of Shipping and Marine Technology, Division of Marine Design*. 2012, Chalmers University of Technology: Gothenburg, Sweden.

39. De Angelis, S., et al., *Detecting hidden volcanic explosions from Mt. Cleveland Volcano, Alaska with infrasound and ground‐coupled airwaves.* Geophysical Research Letters, 2012. **39**(21).

40. Lee, D.-H., et al., *Research of design challenges and new technologies for*

floating LNG. International Journal of Naval Architecture and Ocean Engineering, 2014. **6**(2): p. 307-322.

41. Xin, P., S. Ahmed, and F. Khan. *Inherent safety aspects for layout design of a floating LNG facility*. in *ASME 2015 34th International Conference on Ocean, Offshore and Arctic Engineering*. 2015. American Society of Mechanical Engineers.

42. Pitblado, R.M., et al., *Consequences of liquefied natural gas marine incidents.* Process Safety Progress, 2005. **24**(2): p. 108-114.

43. Johnson, D.W. and J.B. Cornwell, *Modeling the release, spreading, and burning of LNG, LPG, and gasoline on water*. J Hazard Mater, 2007. **140**(3): p. 535-40.

44. Yun-sheng, Q., F.q.Z., and H. Hua-gang, *The Consequence Analysis of LPG Storage Tank Fire and Explosion [J]*. Industrial Safety and Environmental Protection, 2008. **1**: p. 012.

45. Darbra, R.M., A. Palacios, and J. Casal, *Domino effect in chemical accidents: Main features and accident sequences.* Journal of Hazardous Materials, 2010. **183**(1): p. 565-573.

46. Luketa-Hanlin, A., *A review of large-scale LNG spills: experiments and modeling.* J Hazard Mater, 2006. **132**(2-3): p. 119-40.

47. Fay, J.A., *Model of spills and fires from LNG and oil tankers.* Journal of Hazardous Materials, 2003. **96**(2): p. 171-188.

48. Dan, S., et al., *Quantitative risk analysis of fire and explosion on the top-side LNG-liquefaction process of LNG-FPSO.* Process Safety and Environmental Protection, 2014. **92**(5): p. 430-441.

49. Sun, B., K. Guo, and V.K. Pareek, *Computational fluid dynamics simulation of LNG pool fire radiation for hazard analysis.* Journal of Loss Prevention in the Process Industries, 2014. **29**: p. 92-102.

50. Hissong, D.W., *Keys to modeling LNG spills on water*. J Hazard Mater, 2007. **140**(3): p. 465-77.

51. Ichard, M., O.R. Hansen, and J. Melheim. *Releases of pressurized liquefied gases: simulations of the Desert Tortoise test series with the CFD model FLACS*. in *the 91st American Meteorological Society's Annual Meeting*. 2010. Atlanta, GA, USA: American Meteorological Society.

52. Jin, Y. and B.-S. Jang, *Probabilistic fire risk analysis and structural safety assessment of FPSO topside module.* Ocean Engineering, 2015. **104**: p. 725-737.

53. Crowl, D.A. and J.F. Louvar, *Chemical process safety.* 2011.

54. Mokhatab, S., et al., *Handbook of liquefied natural gas*. 2013: Gulf Professional Publishing.

55. McGrattan, K., et al., *Fire dynamics simulator, user's guide.* NIST special publication, 2013. **1019**: p. 6th Edition.

56. McGrattan, K., et al., *Fire Dynamics Simulator Technical Reference Guide Volume 1: Mathematical Model.* NIST special publication, 2013. **1018**.

57. Rinne, T., J. Hietaniemi, and S. Hostikka, *Experimental validation of the FDS simulations of smoke and toxic gas concentrations.* VTT: Finlan, 2007.

58. Wen, J.X., et al., *Validation of FDS for the prediction of medium-scale pool fires.* Fire Safety Journal, 2007. **42**(2): p. 127-138.

59. McGrattan, K.B., et al., *Fire dynamics simulator--Technical reference guide*. 2000: National Institute of Standards and Technology, Building and Fire Research Laboratory.

60. Milke, J.A., *Analytical methods for determining fire resistance of steel members*, in *SFPE handbook of fire protection engineering*. 2016, Springer. p. 1909-1948.

61. AISC, C., *Specifications for the Design, Fabrication and Erection of Structural Steel for Buildings*. 1978.

62. Stouffer, K., J. Falco, and K. Scarfone, *Guide to industrial control systems (ICS) security.* NIST special publication, 2011. **800**(82): p. 16-16.

63. Association, N.F.P., *NFPA 2001 Clean Agent Fire Extinguishing Systems.* 2001. **14**: p. 2001-1.

64. NFPA, B., *13-Standard for the Installation of Sprinkler Systems.* National Fire Protection Association, 2013.

65. Crowl, D.A. and J.F. Louvar, *Chemical process safety: fundamentals with applications*. 2001: Pearson Education.

66. Ramsay, C.G., et al., *Quantitative risk assessment applied to offshore process*

installations. Challenges after the piper alpha disaster. Journal of loss prevention in the process industries, 1994. **7**(4): p. 317-330.

67. Aven, T., S. Sklet, and J.E. Vinnem, *Barrier and operational risk analysis of hydrocarbon releases (BORA-Release): Part I. Method description.* Journal of Hazardous Materials, 2006. **137**(2): p. 681-691.

68. Zhu, C., J. Jiang, and X. Yuan, *Study on ignition probability of flammable materials after leakage accidents.* Procedia Engineering, 2012. **45**: p. 435-441.

69. Paik, J.K., et al., *Quantitative assessment of hydrocarbon explosion and fire risks in offshore installations.* Marine Structures, 2011. **24**(2): p. 73-96.

70. Lee, S., S. Seo, and D. Chang, *Fire risk comparison of fuel gas supply systems for LNG fuelled ships.* Journal of Natural Gas Science and Engineering, 2015. **27**: p. 1788-1795.

71. Rew, P., H. Spencer, and A. Franks. *A framework for ignition probability of flammable gas clouds*. in *Institution of Chemical Engineers Symposium Series*. 1997. Hemspere Publishing Corporation.

72. Cavanagh, J., R. Cox, and G. Olson, *Computer modeling of cool flames and ignition of acetaldehyde.* Combustion and Flame, 1990. **82**(1): p. 15-39.

73. China Petroleum & Chemical Corporation, Q.I.o.S.E., *A guidance for quantitative risk assessment in the petrochemical plant*. 2007: Beijing.

74. Wang, Y.F., et al., *Fire probability prediction of offshore platform based on Dynamic Bayesian Network.* Ocean Engineering, 2017. **145**: p. 112-123.

75. Bilal, Z., K. Mohammed, and H. Brahim, *Bayesian network and bow tie to analyze the risk of fire and explosion of pipelines.* Process safety progress, 2017. **36**(2): p. 202-212.

76. Li, X., G. Chen, and H. Zhu, *Quantitative risk analysis on leakage failure of submarine oil and gas pipelines using Bayesian network.* Process Safety and Environmental Protection, 2016. **103**: p. 163-173.

77. Li, X., et al., *Dynamic risk assessment of subsea pipelines leak using precursor data.* Ocean Engineering, 2019. **178**: p. 156-169.

78. Weber, P., et al., *Overview on Bayesian networks applications for dependability, risk analysis and maintenance areas.* Engineering Applications of Artificial Intelligence, 2012. **25**(4): p. 671-682.

79. Kamil, M.Z., et al., *Dynamic domino effect risk assessment using Petri-nets.* Process Safety and Environmental Protection, 2019. **124**: p. 308-316.

80. Haldar, A. and S. Mahadevan, *Probability, reliability, and statistical methods in engineering design*. Vol. 1. 2000: Wiley New York.

81. Deyab, S.M., et al., *Failure analysis of the offshore process component considering causation dependence.* Process Safety and Environmental Protection, 2018. **113**: p. 220-232.

82. Nielsen, T.D. and F.V. Jensen, *Bayesian networks and decision graphs*. 2009: Springer Science & Business Media.

83. Taleb-Berrouane, M., et al., *Model for microbiologically influenced corrosion*

potential assessment for the oil and gas industry. Corrosion Engineering, Science and Technology, 2018: p. 1-15.

84. Weidl, G., G. Vollmar, and E. Dahlquist, *Adaptive Root Cause Analysis under uncertainties in industrial process operation.* Structure, 2005. **1**(S2): p. S3.

85. Talebberrouane, M., F. Khan, and Z. Lounis, *Availability analysis of safety critical systems using advanced fault tree and stochastic Petri net formalisms.* Journal of Loss Prevention in the Process Industries, 2016. **44**: p. 193-203.

86. Hansen, O.R., et al., *Validation of FLACS against experimental data sets from the model evaluation database for LNG vapor dispersion.* Journal of Loss Prevention in the Process Industries, 2010. **23**(6): p. 857-877.

87. Hanna, S.R., O.R. Hansen, and S. Dharmavaram, *FLACS CFD air quality model performance evaluation with Kit Fox, MUST, Prairie Grass, and EMU observations.* Atmospheric Environment, 2004. **38**(28): p. 4675-4687.

88. GexCon, A., *FLACS v10.0 User's Manual*. 2013, Norway.

89. Oreda, *Offshore reliability data handbook*. 2002: OREDA.

90. Yang, Y., et al., *Corrosion induced failure analysis of subsea pipelines.* Reliability Engineering & System Safety, 2017. **159**: p. 214-222.

91. Wang, Y.F., et al., *Probability analysis of offshore fire by incorporating human and organizational factor.* Ocean Engineering, 2011. **38**(17–18): p. 2042-2055.

92. *HUGIN Expert software version 8.6.* 2018.

93. Kelsey, A., et al., *Evaluation of flammable gas detector networks based on experimental simulations of offshore, high pressure gas releases.* Process Safety and Environmental Protection, 2002. **80**(2): p. 78-86.

94. Ekerold, E.N., *Interpretation of geometrical effects in consequence modelling. Comparison study between the commercial consequence assessment tools FLACS and PHAST for flammable gas dispersion*. 2014, The University of Bergen.

95. Woodward, J.L., *Estimating the flammable mass of a vapor cloud*. Vol. 21. 2010: John Wiley & Sons.

96. Hottel, H.C., *Certain laws governing the diffusive burning of liquids-A review*. Fire Res. Abs., Rev., 1959. **1**: p. 41-44.

97. Raj, P.K. and T. Lemoff, *Risk analysis based LNG facility siting standard in NFPA 59A.* Journal of Loss Prevention in the Process Industries, 2009. **22**(6): p. 820-829.

98. Vela, I., *CFD prediction of thermal radiation of large, sooty, hydrocarbon pool fires*. 2009: Citeseer.

99. Fluent, A., *Ansys fluent theory guide.* ANSYS Inc., USA, 2011. **15317**: p. 724-746.

100. Zabetakis, M.G. and D.S. Burgess, *Research on hazards associated with production and handling of liquid hydrogen.[Fire hazards and formation of shock-sensitive condensed mixtures]*. 1961, Bureau of Mines, Washington, DC (USA).

101. Thomas, P., *The size of flames from natural fires.* Fire Safety Science,

1962. **497**: p. 844-859.

102. Landucci, G., V. Cozzani, and M. Birk, *Domino Effects in the Process Industries: 5. Heat Radiation Effects*. 2013: Elsevier Inc. Chapters.